CHAPTER 4

FINITE ELEMENT MODELING OF COMPOSITE FLOORS FOR VIBRATION SERVICEABILITY

4.1 Finite Element Modeling of Composite Floors for Vibration Serviceability

The objective of this chapter is to present general finite element (FE) modeling techniques for composite floor systems. Methods of creating valid computational models of composite floors subjected to dynamic loads provide a tool for designers, consultants, and researchers to evaluate proposed and existing composite floor systems for serviceability. The actual method of evaluation using the computed parameters and response values is still a subject of debate, even amongst the various simplified methods for evaluating serviceability. However, without question, the ability to adequately represent the dynamic behavior of a floor system with a computational model provides many options for the development of serviceability evaluation methods because iterations of analyses on a suite of computational models is much easier than testing even a small sample size of in-situ floors.

This chapter discusses the fundamental techniques used in development of FE models of the tested in-situ floors. Although three floors were tested, only the NOC VII-18 and VTK2 floors were modeled. Only one model was developed for NOC VII, as the two different tested floors (NOC VII-24 and NOC VII-18) shared identical framing with only slightly different interior partition configurations. NOC VII-18 was the basis for comparison for the NOC VII model, as this was the most extensively tested of the two floors in the NOC VII building. The intent of the investigation was not to independently create ideal models for each individual floor using automated finite element modeling algorithms, but rather to model both floors using broad, fundamental, logical, and most importantly common/shared techniques that resulted in FE models that adequately represented the dynamic behavior of the floors. The two modeled floors were different, both in geometry and boundary conditions, thus identifying common modeling techniques that applied to both floor models builds confidence that the techniques are applicable to a variety of configurations of composite floor systems. Although three tested in-situ floors may seem to be a low number of test specimens for identification of fundamental modeling techniques, additional “samples” are intrinsic from bays of variable geometry and boundary

conditions within each floor's own assemblage. Each tested bay demonstrated unique dynamic behavior, including different dominant frequencies. Thus, the measurements from the in-situ floors presented in Chapter 3 provide an adequate sample of stiffness, geometry, and boundary conditions for identification of the FE modeling trends required to bring experimental and analytical results into agreement

Dynamic FE models of composite floor systems require adequately representing mass, stiffness, and boundaries within the model to analytically compute frequencies and mode shapes. Damping in a structure is not computed by FE analysis. For forced response computations, damping must be specified within the model, either from assumed values or based on measured estimates. Theoretically, if all of the above listed parameters are adequately represented, a forced response analysis should result in computed accelerations similar to measured acceleration response. Previous FE modeling research has had success in matching frequencies of composite floors but struggled to adequately predict the acceleration response, the most important value for vibration serviceability (Sladki 1999; Alvis 2001; Perry 2003).

The process of developing the modeling techniques described in this chapter involved creating FE models of the NOC VII and VTK2 floors and manually updating the models to bring the computed dynamic properties and acceleration response into agreement with the experimentally measured values presented in Chapter 3. In the most basic terms, floor models were created in the XY-plane with the Z-plane representing the direction of vibration. The models consisted of frame and rectangular plate area elements located in the same plane (with stiffness adjustments to represent composite behavior) and analyzed as a plane grid structure, using only UZ, RX, and RY as available degrees of freedom (DOF). UZ is the out-of-plane translational DOF, and RX and RY are the rotational DOFs about the X and Y axes, respectively. Creating an FE model of a floor system for evaluation of vibration serviceability can be summarized in six general steps:

1) Lay out the floor geometry using the design specified steel framing members for the beams and girders and vertical restraints at the locations of the columns.
2) Define area elements and materials to represent the composite slab and apply the slab area elements to the model.
3) Adjust model to adequately reflect mass and stiffness (mesh size and subdivision of members, additional restraints or releases, application of stiffness property modifiers to

represent composite stiffness, etc.).

4) Perform modal analysis on the FE model to compute the frequencies and mode shapes.
5) Specify damping in the model.
6) Apply dynamic loads and perform forced response analysis for use in evaluation of vibration serviceability.

The recommended techniques used for the above listed steps are presented first in Sections 4.1.1 and 4.1.2 using an example 8-bay floor model, followed by the application of these techniques to generate and analyze FE models for the two tested floors presented in Section 4.2.

The commercially available finite element analysis software used in the presented research was SAP2000 Nonlinear version 9.1.4 (CSI 2004). SAP2000 was used for its availability to the researcher, its dynamic finite element capability including transient time history analysis and steady-state analysis, and its popularity with practicing design engineers. The latter broadens the applicability of the presented research, as more practicing design engineers are likely familiar with performing analysis using commercial software like SAP2000 than with other FE analysis programs such as ANSYS, ABACUS, or ADINA, which are more oriented towards research. The practicing engineer's familiarity with the software is likely limited to static analysis rather than dynamic analysis, but the basic menus and commands for modeling structures for dynamic analysis are very similar.

Many of the basic techniques used for modeling composite floors in SAP2000 were based on those used by others for floor vibration research (Kitterman 1994; Rottman 1996; Beavers 1998; Sladki 1999; Alvis 2001; Perry 2003). These basic techniques were either used as-is, improved upon, disproved, or new techniques developed through comparison of the modeling results with measured in-situ floor behavior, which was generally not available when the basic techniques were originally developed. The initial discussion and application of the modeling techniques are presented in a fair amount of detail, thus Section 4.3 is a concise summary of the recommended modeling techniques. Section 4.4 presents a proposed method of evaluation for vibration serviceability using the forced response analysis results of composite floor FE models. The method combines the forced response analysis presented in this chapter with present design guidance for representing forces due to walking and the threshold of human tolerance.

4.1.1 Representing Mass, Stiffness, and Boundary Conditions

Mass & Materials

Within SAP2000, the mass of an individual element is computed from its volume and the mass density of the material, which is lumped at its joints and assigned to the translational degrees of freedom (UZ for the modeled floors analyzed as plane grid structures). SAP2000 does not compute or assign mass moments of inertia for the rotational degrees of freedom (CSI 2004). The mass of the floor in the FE model, or more accurately the distribution of mass of the floor, is represented by the mass of the assembled elements. The beams and girders of the floor framing were modeled using the predefined wide flange sections available within SAP2000. These predefined frame elements included all the geometric section properties necessary for analysis, including cross-section area, torsional constant, moments of inertia, and shear areas. Additionally, these frame elements are assigned SAP2000's default STEEL material, which contains necessary constitutive properties such as mass density, modulus of elasticity, and Poisson's ratio. An example of the first general step of creating an FE model, laying out the floor geometry with the specified framing members, is shown for an example 8-bay floor model in Figure 4.1.

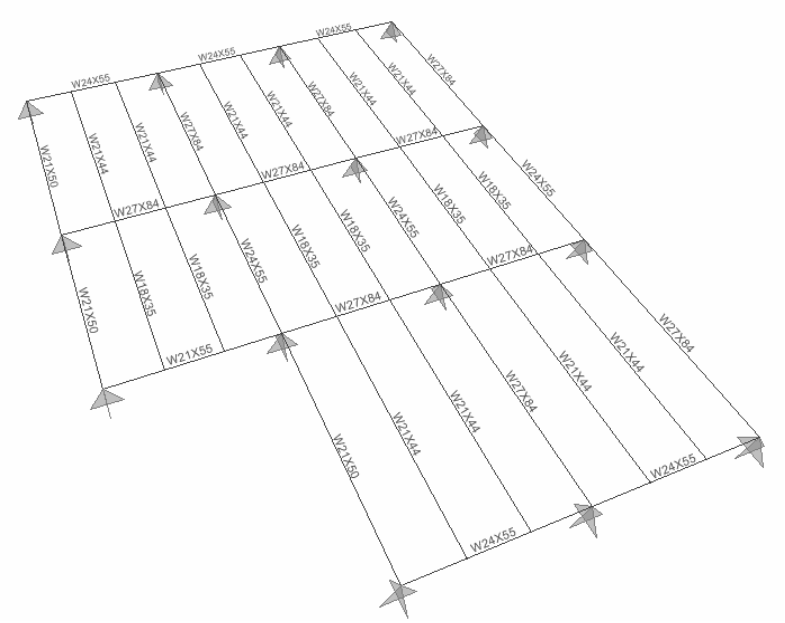

Figure 4.1: 8-Bay Floor Model Example – Framing Member Layout

The concrete slab on steel deck was represented by user-defined rectangular plate area elements assigned a user-defined material. It should be noted that plate elements were used to

represent the composite floor slab in lieu of shell elements. The in-plane forces from membrane behavior are not a factor for vibrations of composite floors. Several iterations of analysis were performed using full space frame analysis (all six available DOF) and shell area elements. The results indicated there was no significant effect on the computed frequencies, mode shapes, and response, only a significant increase in computation time. Rather than using a predefined material of concrete or steel, a user-defined material named *VIBCON* was created and assigned to the plate area elements to represent the dynamic properties of the concrete slab and metal deck. These properties included the composite slab's mass, the mass of any superimposed loads, and the dynamic stiffness of concrete ($1.35*E_c$). For both the tested/modeled floors, the same composite slab system was used, a 5.25-in. total depth slab with 18-gage 2-in. LOK-Floor steel deck. The thickness of the user-defined plate element named *SLAB* was specified as 3.25 in., equal to the depth of the concrete above the corrugated steel deck ribs. It should be noted that this method is purely a convenience to ensure adequate mass distribution using the assigned material weight and mass densities; the ramifications of this approach on representing stiffness of an orthotropic deck must be dealt with in a manner discussed in the following sections. The weight density and mass density of the user-defined material were computed using Equations (4.1) and (4.2), respectively (Beavers 1998; Sladki 1999; Perry 2003).

$$w_{material} = \left[\left(\frac{d + d_r/2}{12} \right) w_c + w_{deck} + w_d + w_l + w_{coll} \right] \left(\frac{12}{d} \right) \left(\frac{1}{1,728,000} \right) \; kips/in^3 \tag{4.1}$$

$$m_{material} = \frac{w_{material}}{g} = \frac{w_{material}}{386 \; \text{in}/\text{s}^2} \quad kips \cdot s^2/in^4 \tag{4.2}$$

where

$d =$ depth of concrete above the ribs (*in.*)
$d_r =$ depth of steel deck ribs (*in.*)
$w_c =$ unit weight of concrete (lbs/ft^3)
$w_{deck} =$ area weight of steel decking (lbs/ft^2)
$w_d =$ superimposed dead load (lbs/ft^2)
$w_l =$ superimposed live load (lbs/ft^2)
$w_{coll} =$ superimposed collateral load (lbs/ft^2)

The advantage of using this method for assigning weight and mass density is that it allows any desired superimposed dead or live load (furniture, lighting, utilities, etc.) to be included as additional mass in the computation of frequencies and mode shapes, although no superimposed loads were used in the models of the presented research due to the bare conditions of the tested floors. Because the tested floor systems had no superimposed load, only the unit weight of the concrete slab, w_c = 115 lb/ft^3, and area weight of the steel deck, w_{deck} = 2.4 lb/ft^2, was included in the specified mass density of the material. For the 5.25-in. composite slab of both modeled floors, the depth of the concrete above the ribs, d, is 3.25 in. and the depth of the steel deck, d_r, is 2 in.

Besides specifying weight and mass density, the constitutive properties of the user-defined material were defined per DG11 recommendations previously described in Section 1.1.2. The modulus of elasticity of the user-defined material representing the concrete slab was taken as 1.35 times the modulus of elasticity of the concrete as "specified in current structural standards" to account for a greater stiffness of the floor slab system under dynamic loads (Murray et al. 1997). The modulus of elasticity of concrete used was based on the unit weight and compressive strength and was computed using Equation (1.6). Poisson's ratio for the user-defined material was taken as 0.2, a typical value for concrete.

Because the FE analysis program apportions the mass of an element at each of its joints, it was important to use enough elements to properly represent the uniform distribution of mass across the slab areas and along the framing member lengths. To adequately distribute the mass of the floor, the *SLAB* area elements were appropriately meshed across their areas and the beam/girder framing members were similarly subdivided along their lengths at each mesh joint. An overly fine meshed model is computationally expensive, thus the frequencies and mode shapes of a single-bay FE model were computed at various mesh subdivisions until the first four frequencies of the model converged to within 0.01 Hz. It was found that *SLAB* area element sizes of 26 in. to 30 in. along each side gave convergent results, which corresponded to a mesh with 12 to 20 elements along a bay's width or length, depending on the floor model and bay's configuration. SAP2000 recommends an element aspect ratio close to unity for best results (CSI 2004), which was factored into determining the mesh and element sizes. The plate area elements representing the composite slab and the corresponding area mesh for the example 8-bay floor model are shown in Figure 4.2.

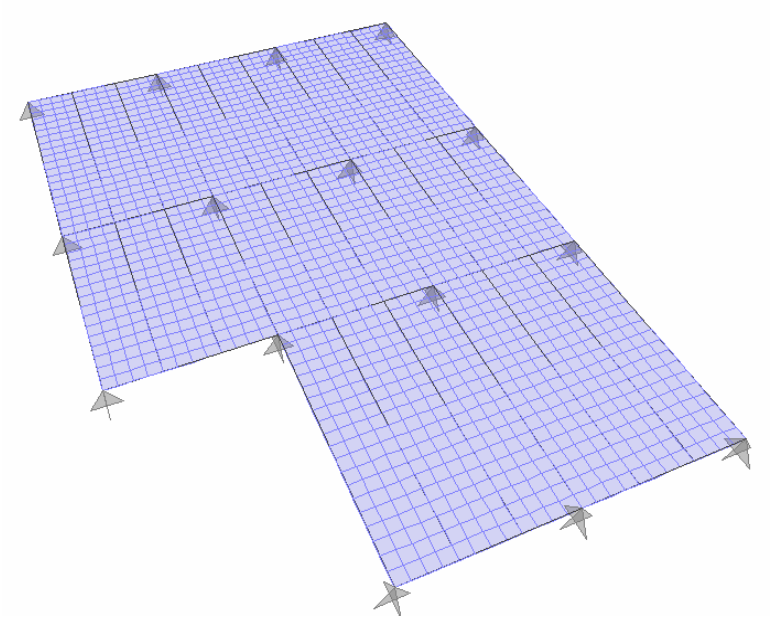

Figure 4.2: 8-Bay Floor Model Example – Plate Area Element Layout and Mesh

To ensure connectivity of the slab and framing elements and to provide the same distribution of mass along their lengths, the frame elements representing the girders and beams were auto-subdivided along their lengths corresponding with the slab mesh size. Experimental measurements were taken at quarter points of the bays of the tested floors. For convenience, the number of elements used along the length/width of a bay in the model was kept to a multiple of four to ensure a joint existed where the mode shape or response value was desired.

Stiffness

As previously stated in Section 1.1.2, if a slab/deck system is in continuous contact with the beams and girders, the floor system is assumed to act compositely, regardless of whether or not the floor was designed with shear connectors (Murray et al. 1997). The assumption did not have to be made for the two modeled floors, as they were both designed with composite shear studs on all beams and girders. By modeling both the area elements and the framing elements in the same plane to take advantage of the plane grid analysis, an adjustment must be made to the stiffness properties to account for the composite bending stiffness. As the first step in this adjustment, the composite transformed moment of inertia for each beam/slab and girder/slab element was computed using traditional engineering mechanics and the recommended dynamic modulus of elasticity and concrete effective width guidelines of DG11. The effective width guidelines include limitations based on beam/girder span as well as considerations for spandrel

members. Because the steel deck is oriented perpendicular to the beam framing members, the transformed moments of inertia were based on only the 3.25-in. thickness of concrete raised above the steel member, as shown in Figure 4.3(a). For girder members, where the deck is parallel to the girder span, the transformed moments of inertia were based on a T-beam approximation of the slab, as shown in Figure 4.3(b).

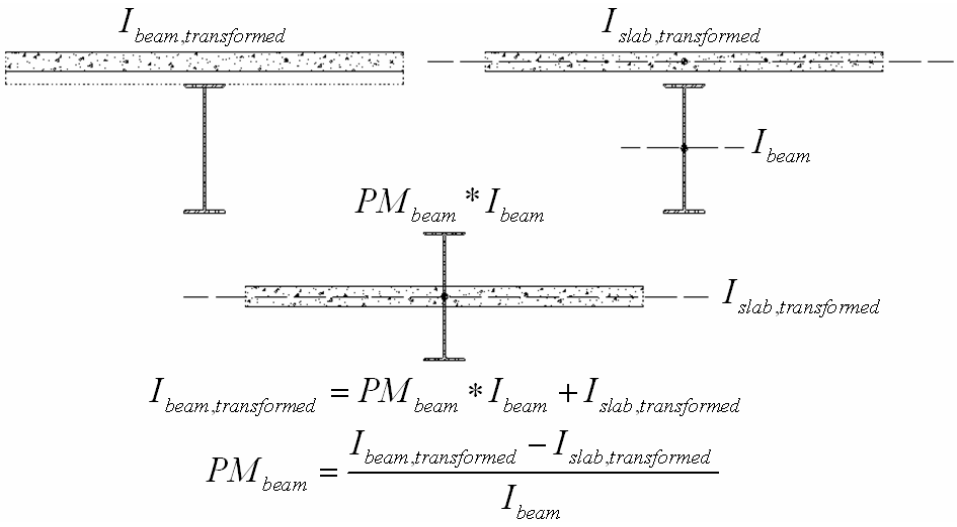

(a) Composite Slab on Beam (Deck Ribs Perpendicular to Member)

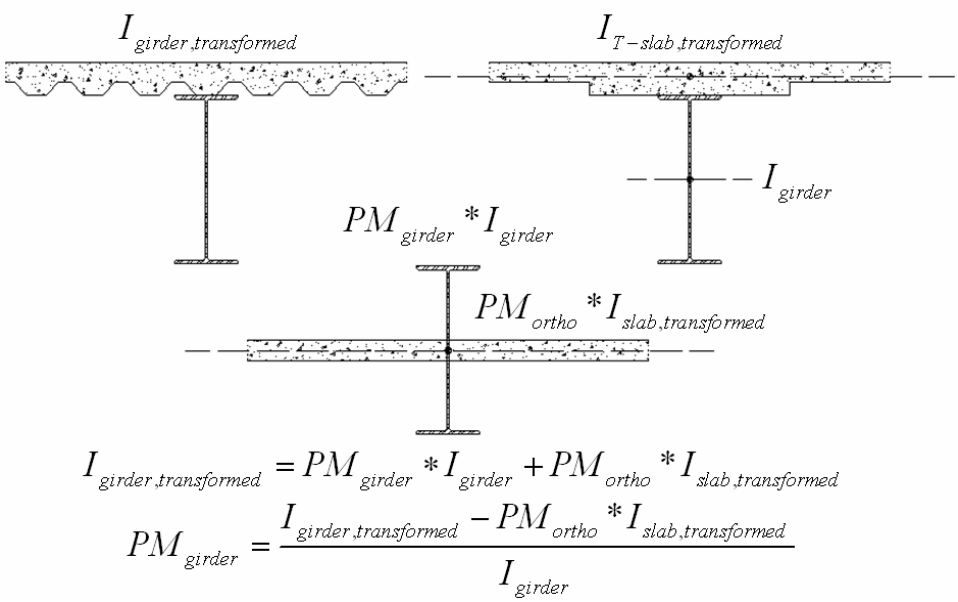

(b) Composite Slab on Girder (Deck Ribs Parallel to Member)

Figure 4.3: Representations of Composite Slab and Framing Members

Because the slab and framing members were modeled as separate elements, each has its own assigned moment of inertia about its own centroid, and from the plane grid modeling

choice, the centroids are located in the same XY-plane as shown in Figure 4.3(a) and (b). Thus, because the individual moments of inertia for the frame and slab elements about their own centroids are known, and the target transformed moment of inertia is also known, then a stiffness property modifier (PM) can be assigned to the strong axis moment of inertia of the frame members to represent a composite stiffness. Within SAP2000, property modifiers are multiplication factors that are applied to the desired geometric or material property of an element to increase or decrease its value. Using this approach, the sum of the transformed moment of inertia of the slab about its own neutral axis and the "modified" moment of inertia of the framing member will equal any desired target transformed moment of inertia for the composite beam/slab or girder/slab members. Identifying the strong axis stiffness property modifier to be applied to the framing member involved several steps, including computing the transformed moment of inertia for the beam/slab or girder/slab, subtracting out the computed transformed moment of inertia of the 3.25-in. slab area element about its own neutral axis, and then dividing through by the default strong axis moment of inertia of the predefined wide flange framing member. For girders, which include the deck ribs in calculations, the orthotropic stiffness property modifier on the slab must also be subtracted out so that it is not accounted for twice. An example of the computation of a transformed moment of inertia and baseline stiffness property modifier for a beam and a girder member can be found in Appendix K. It should be noted that property modifiers were computed using this method for all framing members of the modeled floors. These represent the "baseline" PM values computed and applied to the framing members. Adjustments to the stiffness PMs was the primary method for representing a different stiffness that was not considered in the composite calculations, such as spandrel or interior boundary members that may have greater stiffness due to attached exterior cladding or partition walls. The stiffness PMs used on these stiffer boundary elements are expressed as a multiple of the baseline values (e.g. 2.5 times baseline) in the presented research. The baseline computed composite stiffness property modifiers typically ranged from approximately 2.5 to 3.8 for the primary framing members of the modeled floors.

The user-defined *VIBCON* material was specified as an isotropic material, which assumes the same constitutive properties (modulus of elasticity, Poisson's ratio) in all directions. While not an orthotropic material, the slab has an orthotropic stiffness due to the corrugated ribs. Assigning a property modifier to the girder members accounts for the composite action, however

using area elements with a constant 3.25-in. thickness (the portion of the slab above the deck ribs) does not account for the additional bending stiffness of the corrugated slab spanning the direction between beams. The strong direction moment of inertia of the 5.25-in. corrugated slab (i.e. bending includes deck ribs) is approximately three times larger than the moment of inertia of just the 3.25-in slab above the ribs, which is the effective portion resisting bending in the weak direction. To account for this, a bending stiffness property modifier of 2.88 was assigned to the *SLAB* plate area elements, which is the computed ratio of strong direction-to-weak direction moment of inertia of the concrete. As expected, applying this bending stiffness property modifier to the slab had the effect of increasing computed frequencies by 5-10%. More importantly, the effect was quite evident on the computed mode shapes, which included much more participation in bays adjacent in the direction of the deck ribs. This follows the behavior observed during experimental testing. The 2.88 ratio assigned to the slab element was also used to compute the PM for the girders, so as not to double count the orthotropic stiffness (although the bending stiffness of the slab is much smaller than the composite stiffness of the girder, so not subtracting out the 2.88 modifier has negligible effect).

As previously mentioned, the wide flange beams and girders were modeled explicitly using SAP2000's predefined steel sections rather than creating user-defined frame elements. An obvious advantage to this approach is that it more easily accommodates adjusting an existing floor model created by a design engineer for other analysis. Creating user-defined sections for a large number of framing members would be tedious, requiring the input of a wide variety of cross section properties that may or may not apply to the floor model. Although property modifiers were assigned to the strong axis moment of inertia to increase the section's bending stiffness to represent composite action, using the specified steel section kept all of the other member section properties intact and ensured the mass of the frame member was captured correctly. This approach also allows, if desired, shear deformations to be included in the computed frequencies and mode shapes. Shear deformations could be neglected simply by setting the framing members' shear area property modifiers to zero. Neglecting shear deformations essentially neglects flexibility, resulting in stiffer framing members and a 3-5% increase in computed frequencies for the floor models used in this study but no notable effect on mode shapes.

The plate elements used in the floor models of this research were the program default thin-plate elements, based on the Kirchhoff (thin-plate) formulation, which neglects transverse shear deformations. The alternative plate elements (not used) available in SAP2000 are based on the Mindlin/Reissner (thick-plate) formulation, which includes the effects of transverse shearing deformation but tends to be somewhat stiffer than the thin-plate formulation (CSI 2004). Iterations of models comparing the two plate formulations showed this to be true; however the computed frequencies were less than 1% higher for the stiffer thick-plate elements.

End Releases, Partial Fixity, and Boundary Conditions

Although modeling end and boundary conditions is a subset of representing the stiffness in a floor structure, they deserve a separate section to stress their importance as the greatest unknowns in modeling floors for evaluation of serviceability. One of the most significant modeling parameters that affected the computed frequencies and mode shapes was the stiffness of connections between beam, girders, and columns. The stiffness of beam and girder connections was handled using moment end releases and restrained DOFs in SAP2000. Moment end releases specify a pinned connection, allowing rotation between the end of the member and whatever it is connected to. When the end moment is not released, rotation between connected members is not allowed, however the joint itself is still free to rotate. Moment end releases differ from rotationally restrained DOF in that the assigned joint is not allowed to rotate when the DOF is restrained.

Intuition would suggest using a rotationally restrained DOF for members connected to columns with moment connections, however several model iterations demonstrated that this modeling technique over-restrained the models and did not allow certain mode shapes (and response in the members framing between columns) that were clearly measured during testing. Intuition may also suggest releasing the end moment of all members that are connected to columns with simple shear connections; however this provided too flexible of a system that also poorly represented mode shapes when the technique was applied to all locations with this connection type. From the presented research, the recommended configuration of beam/girder-to-column moment end releases that produced the best results for both frequency and mode shapes was releasing all end moments of members framing into column webs and *not* releasing end moments of members framing into column flanges, despite whether either connection was specified as a moment connection. It should be noted that this is a very simplified approach to

very complicated behavior of the column joint that is a function of several competing sources of stiffness, some of which are:

- Shear connections are not true pinned connections and provide rotational restraint.
- Centerline dimensions are used for the modeled geometry of all framing members and composite stiffness calculations, however members framing into column flanges can be 12-18-in. shorter (thus stiffer) based on actual clear distance.
- Although the framing members are assigned a composite moment of inertia over their full length, the actual stiffnesses at the ends are probably reduced by the perforation of the slab/deck system by the column and cracks that typically occur in the slabs over inter-column beams and girders, particularly if they are part of a moment frame (observed in the tested buildings).
- Shear connections into the webs of columns are rotationally more flexible compared to shear connections into the flange of a column. Moment end-plate weak axis connections (i.e. through the web of a column) are also rotationally flexible.
- The rotational contribution of the column will also affect the behavior of the joint for both moment and shear connected framing members.

Obviously the numerous contributions to the rotational stiffness of column joints, many of which remain unknown, are difficult and tedious to account for in a manner appropriate for the presented research. However, the competing inaccuracies of the proposed simplification resulted in models that adequately represented the behavior and response of the tested floors.

Most beams are connected to girder webs with simple shear connections, and it is generally assumed the continuity of the slab/deck over the joint provides enough continuity in the composite system that the slopes of the connecting beams on either side of girder are approximately the same. When moment end releases were applied to the ends of beams framing into girder webs, some of the computed mode shapes resulted in excessively discontinuous (i.e. kinked) mode shapes over the girder between adjacent panels due to differential rotation of the ends of the beams. Examining the experimentally measured mode shapes of the tested floors, there was often a noticeable discontinuity in the shape over the girder supports, although generally not nearly as excessive as in the full moment end-released models. It should also be noted that inspection of the tested floors showed cracks in the concrete slab over most girders and many beams spanning between columns, indicating a less-than-continuous floor slab over

these intermediate supports. The implication of this experimental observation on FE modeling is quite significant. Essentially, neither a continuous beam representation (i.e. no moment end releases for the beam members on either side of the girder web) or fully end-released beam representation may be adequate. When full moment end releases are specified, the only element providing continuity between adjacent bays across a girder is the thin 3.25-in. slab area element, which has a relatively weak bending stiffness resulting in the excessively discontinuous mode shapes. The measured behavior implies a rotational stiffness at this interface somewhere between the two representations. When specifying an end release in SAP2000, the option to include a partial fixity is available, which for moment end releases requires a value for the rotational spring in units of *kip-in/rad*. Figure 4.4 shows the example 8-bay floor model framing members with assigned releases and partial fixity designations. The columns in the example are oriented with their webs parallel to the direction of the beam framing, thus all girders have full moment end releases and the inter-column beams do not have any moment releases.

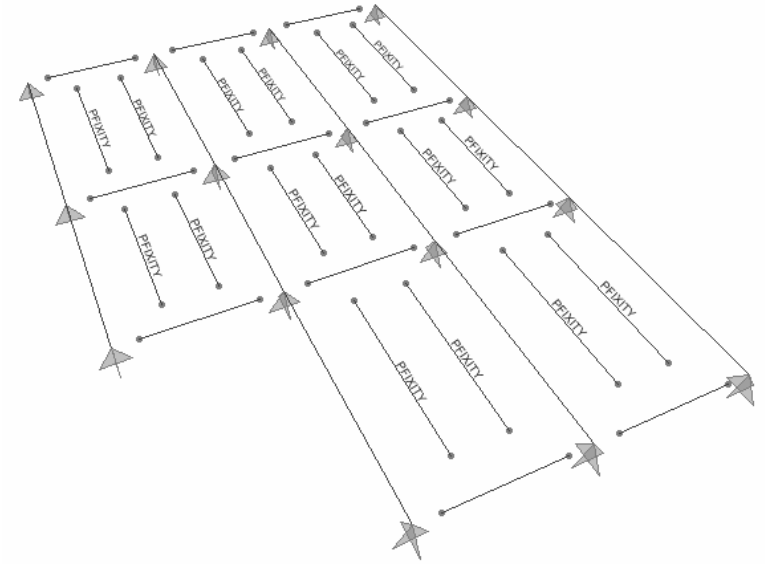

Figure 4.4: 8-Bay Floor Model Example – End-Release and Partial Fixity

Partial fixity spring values used were not based on experimental testing of the joints, instead they were determined from model iterations that produced frequencies and mode shapes that were in agreement with measured values. However, the values used *were* based on an assumed level of rotation at the end of the member that was translated into a fraction (or multiple) of *EI/L* for the framing member. This approach for specifying partial fixity was used for several reasons, but mainly so the rotational spring value used for any model would be based on properties of the actual framing member rather than arbitrary values. Additionally, by

specifying the rotational spring in terms of a coefficient to the frame member's baseline *EI/L* value, this coefficient can be used as an iteration parameter for model refinement. From iterations of the floor models in the presented research, it is recommended to use a moment end release partial fixity rotational spring value of 6*EI/L* at both ends for floor beam members that frame into girders. The 6*EI/L* value corresponds to a rotational spring at the ends of a simply supported beam under a static uniform load that responds with 25% of the rotation of a pinned-pinned supported member and 75% of the end moment of a fixed-fixed supported member under the same load. Ordered pairs of assumed moment and rotation can be used to solve for a value of the coefficient, such as 2*EI/L* for 50% end fixity or (2/3)*EI/L* for 25% end fixity, although 6*EI/L* was used in the models of the presented research. A derivation of this method for determining rotational spring values is found in Appendix L.

The only end releases used in the presented models were the strong axis moments. Perry (2003) suggested releasing the weak axis moments at both ends of the member as well as one end of the torsional moment. The weak axis moment end releases had no effect on the computed frequencies because the floor models were analyzed as plane grid structures and the RZ rotational DOF was not used in analysis. Model iterations investigating the effect of releasing the torsional moment showed that this practice had virtually no effect on results, only changing frequencies by less than 0.001 Hz.

Like the end releases and partial fixity values, the boundary conditions of the floor models arguably had a very significant effect on the computed frequencies and damping. Boundary conditions consist of interior boundaries such as columns, interior partition walls, and the exterior spandrel members of the floor. The building's columns were modeled as pinned supports that restrained translational movement but allowed rotation. The vertical response of the columns was considered negligible because experimentally measured values from driving sinusoidally at the dominant frequency indicated the response was less than 1% of the response at the center of the bay. This small response at other frequencies was also confirmed by experimental measurements. The minimal response that was measured at the columns was more likely a function of the accelerometer being located some distance from the column centroid than an actual vertical response. Interior braced frames, such as those in the end bays of NOC VII, were also represented by pinned supports.

Generally, spandrel beams and girders were modeled with an increased stiffness modifier to represent the stiffening effect of the exterior cladding. An "increased" stiffness modifier means that a larger PM was used on the spandrel member than the original baseline PM computed based on DG11 composite section transformed moment of inertia calculations. Perry suggested using a stiffness property modifier of 1000 on the strong axis moment of inertia for spandrel beams and girders because the exterior walls and cladding sufficiently stiffen these members for floor vibration purposes (Perry 2003). Assigning stiffness property modifiers this large, the exterior boundary members essentially act like rigid walls within the model, however the experimental behavior of the tested floors proved otherwise. The measured response at these boundaries was much greater than an assumed wall (9-26% the mid-bay response), thus the suggested PM of 1000 was not used for spandrel members in the presented floor models. From model iterations comparing the spandrel member response with the mid-bay response, it is recommended to use a stiffness property modifier of 2.5 times the computed baseline PM. Another method used to stiffen the interior bays enclosed by full height partition walls was placing pin supports within the bays, essentially restraining the interior of the bay from vibration. Figure 4.5 shows the final layout of the example 8-bay floor model, including pinned supports along an interior beam to simulate cross bracing and additional pinned restraints to the slab on the interior of an enclosed bay to simulate an increased stiffness within this bay due to small mechanical rooms or elevator cores.

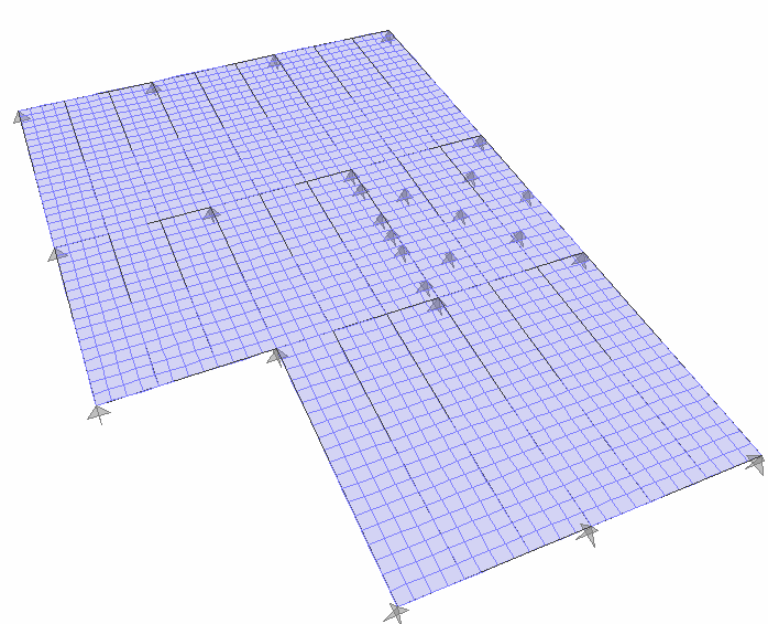

Figure 4.5: 8-Bay Floor Model Example – Pinned Supports Representing Interior Restraints

4.1.2 Dynamic Finite Element Analysis Techniques for Floor Systems

The previous section presented the first three general steps for creating an FE model of a floor system for evaluation of vibration serviceability, but the final three general steps described in this section outline the dynamic analysis of a floor's FE model for interpretation and evaluation. There are a variety of dynamic analysis case types available in SAP2000, including multi-step static, modal, response spectrum, time history, moving load, buckling, steady state, and power spectral density (CSI 2004). There are even more sub-options within each type of analysis case. Only three of these analysis case types were used and are discussed here: modal analysis, time history analysis, and steady state analysis (although modal analysis and steady state analysis are highlighted as the most important for the presented research). It should be noted that rather than describing all options and sub-options of each of the analysis cases in detail, only the relevant modeling choices (and justifications for each) are discussed. Beyond what is necessary to describe for the presented research, presentation of detailed background on the computational methods of SAP2000 is best left to the program's user manual. Additionally, the computational methods used in the research are described in as generic terms as possible so that the fundamental modeling and analysis techniques may be applied to other dynamic FE programs.

Modal Analysis

SAP2000's modal analysis of the floor's FE model computes the frequencies and mode shapes based on the assembled mass and stiffness matrices, without consideration of the presence or level of damping in the structure. The computed modes can be used as the basis for time history analysis; although the most important aspects of the modal analysis feature for evaluation of vibration serviceability are the computed dominant frequencies and the visual shapes of vibration for each of the modes. From experimental measurements, the lowest modes of a floor system generally have single curvature within bays, resulting in a concave up or concave down shape of the panel between columns. The same holds true for the FE model of a floor: the lowest computed modes are represented by single curvature within a bay, and double curvature within bays is not encountered until higher frequency modes. For a computed mode shape, just as in experimentally measured mode shapes, the response may be localized to just one bay or to several bays, generally located adjacent to one another. Again, this is a very important property for evaluation of serviceability because it links an area of the floor to a resonant frequency that

has the potential for excessive vibration due to human activities such as walking. In essence, visual inspection of the computed mode shapes highlights areas of vulnerability of a floor at their respective frequencies. The computed frequencies themselves are equally important, because the lower the frequencies of the floor, the more susceptible it is to lower harmonics of walking excitation. Using the 8-bay floor model as an example, the first six mode shapes and frequencies were computed using eigenvector modal analysis and are displayed in Figure 4.6.

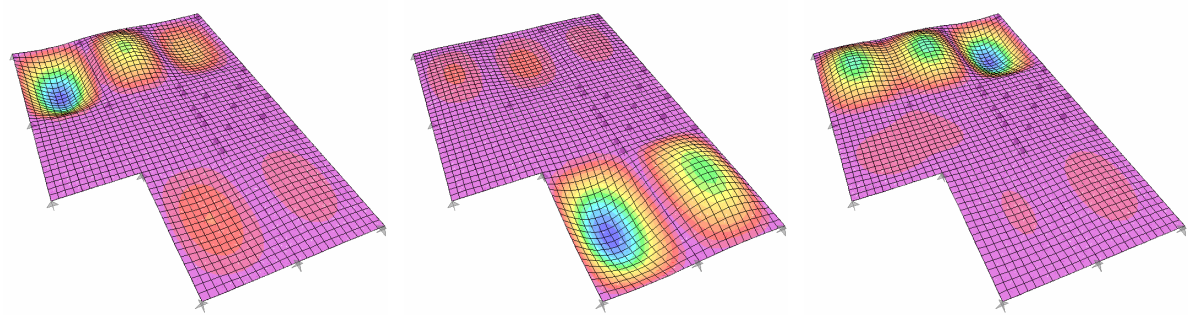

Mode 1: 5.119 Hz Mode 2: 5.149 Hz Mode 3: 5.327 Hz

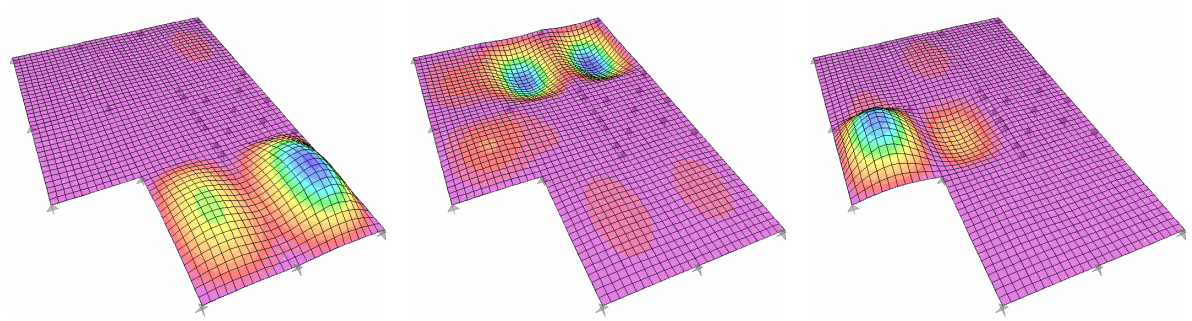

Mode 4: 5.622 Hz Mode 5: 5.692 Hz Mode 6: 6.051 Hz

Figure 4.6: 8-Bay Floor Example – Computed Frequencies and Mode Shapes

The term "dominant" frequency is just as applicable for discussing computed frequencies as for experimentally measured frequencies. As shown for the computed mode shapes in Figure 4.6, a single bay of the floor model generally has dominant participation (as defined as the bay with the greatest response for the mode shape) at one frequency, and perhaps significant response at one or more other frequencies. For example, the bottom left bay has a dominant response in Mode 2 (5.149 Hz) and a significant response in Mode 4 (5.622 Hz) as well. It is from this observation that it can be expected any forced response analysis for loads placed within this particular bay will be dominated by contributions from these participating mode shapes. This follows experimentally measured behavior indicated by the dominant peaks (and other significant peaks) of the mid-bay driving point accelerance FRFs.

SAP2000 offers two methods of modal analysis, eigenvector analysis and Ritz-vector analysis. Eigenvector analysis determines the undamped free-vibration natural frequencies and mode shapes using only the mass and stiffness matrices to solve the generalized eigenvalue problem, whereas Ritz-vector analysis looks to compute the modes that are excited by a particular applied loading pattern (CSI 2004). Theoretically, Ritz vectors yield excellent results in dynamic analysis because they account for the spatial distribution of the loading, whereas the natural mode shapes do not. Ritz-vector analysis requires at least one starting load vector, such as an acceleration load or any of the defined load cases for the model. Several analysis iterations for both types of modal analysis were applied to the 8-bay example floor model to investigate the effect on the computed frequencies and mode shapes. The starting load vectors used for Ritz-vector analysis included the dead load of the structure from its self-weight under gravity (a logical choice) and various mid-bay point loads applied to the bays for forced response analysis. To briefly summarize the investigation, it was found that using Ritz vectors did not offer any advantage over eigenvectors for computing the frequencies and mode shapes for plane grid floor models. Depending on the number of Ritz vectors specified to be computed, the lowest computed Ritz-vector modes gave reasonable frequencies and shapes; however the higher computed modes were largely illogical. In certain cases, some lower frequency modes were only computed when a higher number of Ritz-vector modes were specified in the analysis case. In contrast, eigenvector analysis always computed the same lower modes despite the number specified in the analysis, which was advantageous for identifying how many modes were needed to cover a frequency range of interest (such as 4-12 Hz). The inconsistency of the computed mode shapes indicates the use of Ritz vectors is likely better reserved for other structure types, such as those with multi-direction mode shapes where only one direction is of interest. For example, a joist-supported footbridge with each member explicitly modeled may have "flapping" modes of the joist members and only the vertical modes of vibration are of interest. In this situation, Ritz-vectors computed using gravity dead loads as the starting load vector may be advantageous in filtering out these unnecessary modes. For the plane grid floor models in the presented research, however, the direction of vibration was never in question. Eigenvector analysis consistently produced logical mode shapes and thus it was used exclusively for the floor models in the presented research. It is recommended that a large number of modes be computed during early iterations of modal analysis of the floor model to ensure that all modes including

single curvature within all bays of interest are represented. Once these modes (and frequencies) are determined, subsequent analyses involving the modal analysis case can be scaled back in the interest of computation effort to only include the relevant modes.

Damping

As previously mentioned, eigenvector modal analysis assumes all modes computed for the structure are non-complex, hence it solves the eigenvalue problem for frequencies and mode shapes without consideration of the presence or level of damping. For computation of forced response, however, SAP2000 requires damping to be specified. SAP2000 allows the option to specify damping in several different ways, generally in the form of modal damping ratios or as Rayleigh damping (i.e. using mass and stiffness proportional coefficients), depending on the type of dynamic analysis and the methods used to solve them. Brief descriptions of how damping was specified in the analysis methods used in this research are presented in this section. The user's manual for SAP2000 gives a more detailed description of the various ways the FE software incorporates damping in its analyses (CSI 2004).

For time history analysis using modal superposition (i.e. using the computed modes from the modal analysis), modal damping may be specified as constant for all modes, specified for each mode individually, interpolated by period or frequency, or even specified as a proportional level of damping based on the mass and stiffness matrices. For time history analysis using direct integration, where computed modes are not used in the computation of the response, Rayleigh damping is used and requires specification of mass and stiffness proportional coefficients. Additional damping may be included in the response if it is also included as an assigned property of the material.

For frequency-domain response calculations, such as the steady state analysis heavily used in this research, damping is specified in terms of hysteretic damping (also known as rate-independent damping) in the form of mass and stiffness proportional damping coefficients. These coefficients may be specified as either constant hysteretic damping for all frequencies or interpolated between specified frequencies and their respective damping values. As with time history analysis, stiffness and mass proportional coefficients may also be specified for individual materials to be included in frequency-domain computations. The steady state analysis solution is solved directly without computing the modes, thus specifying modal damping directly is not an option, only hysteretic damping. However, modal damping can be approximated by specifying

the mass proportional coefficient as zero and the stiffness proportional coefficient equal to twice the modal damping ratio (i.e. use 0.02 as a stiffness proportional coefficient for a target modal damping ratio of 1%). A full derivation of this property is presented in the text by Chopra (2000).

As previously stated, damping is not a value computed by FE analysis; it is specified from experimental measurements as estimated damping values. Unfortunately, the experimentally measured values of damping for the two modeled floors varied significantly with no discernable trend based on their corresponding frequencies. Measured modal damping values for NOC VII-18 were 0.60% to 2.4% of critical for frequencies between 4.85 Hz and 6.55 Hz. For VTK2, damping values were 0.50% to 1.3% of critical for frequencies between 6.58 Hz and 8.20 Hz. This wide range of damping values for the relatively narrow range of frequencies posed a significant challenge for specifying damping in the FE models and achieving forced response analysis results that were in agreement with measured response.

For simplicity, constant damping values for all frequencies were used in all steady state analyses in the presented research. The constant damping value used for each mid-bay analysis location was the estimated damping at the dominant frequency of the corresponding experimental driving point accelerance FRF measurement. This simplification was made for the benefit of using the recommended modeling and analysis techniques for evaluation of vibration serviceability. In the absence of any measured values, which is the case for a design engineer modeling a floor that has not yet been constructed, there is no other choice but to assume a level of damping for forced response analysis. DG11 recommends several damping ratios based on the structure type and fit out (Murray et al. 1997). For bare floors with no non-structural fit out components or furnishings, such as the tested floor, it recommends a damping ratio of 1% of critical (0.01). DG11 also recommends a damping ratio of 2% for floors with few non-structural components or furnishings and 3% for floors with non-structural components, furnishings, and small demountable partitions that are found in modular office spaces. To investigate the ability of the recommended modeling techniques to adequately represent the measured response assuming no prior knowledge of measured damping values, assumed values of damping were used in analysis for each investigated location on the floor models. This resulted in two steady state analyses for each mid-bay forcing location for comparison with measured values, one using a measured damping value and one using an assumed damping value. As expected from the

wide range of measured damping values, efforts using a single assumed value of 1% for all bays investigated did not give very good results. However, based on a few observations of the measured damping in different locations of the tested floor, there was much better agreement using the following recommended damping values:

- 1% damping for typical bays
- 1.5% damping for corner bays
- 2% damping for interior bays adjacent to interior framing

Although the higher levels of damping were not always observed for corner bays or interior bays, the trends were observed in some cases and are appropriate assumptions considering the most significant source of damping for a bare floor will likely be at its boundaries, such as the friction at exterior boundaries (a corner bay has two exterior boundaries) or semi-structural interior framing. Once a floor is occupied, the addition of fit out materials will likely become the dominant source of damping, and thus a constant value for all bays should be appropriate for modeling purposes.

Time-History Analysis and Steady State Analysis

For comparison of measured acceleration response to computed values, dynamic loads were applied to the FE models for forced response analysis. The two types of forced response analysis used were time-history analysis and frequency-domain steady state analysis, the latter being the most used type of analysis in the presented research for its direct comparison with measured response values in the frequency domain. Steady state analysis also serves as the cornerstone of the proposed method of vibration serviceability evaluation presented at the end of this chapter. Each of the two types of forced response analysis requires load(s) applied spatially to the structure. Because experimental measurements of the tested floors were only taken with one shaker at the center of a tested bay, the corresponding forced response analysis was performed with a single point load located at the mid-bay location. There are several opportunities when setting up the analysis cases in SAP2000 to scale the applied loads, therefore the magnitude of the mid-bay point load was set to 1 lb to allow flexibility in later analysis. The use of a unit load also proved advantageous for comparison with measured accelerance values because the computed steady state acceleration response to sinusoidal load in in/s^2 units would also be equivalent to accelerance units of in/s^2/lb of input force at the driving frequency. Figure 4.7 shows an example of the mid-bay location of the applied unit load for the 8-bay floor model.

Both the time-history analysis and frequency-domain steady state analysis examples that follow in this section refer to this driving point location as well as the computed mode shapes for the 8-bay floor model shown in Figure 4.6.

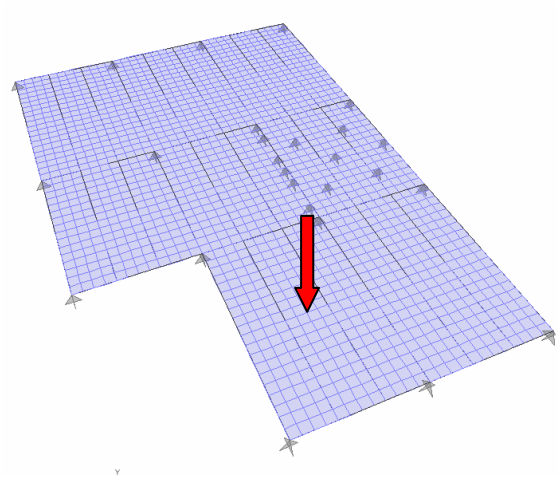

Figure 4.7: 8-Bay Floor Example – Applied Unit Load (1 lb) for Forced Response Analysis

Time-History Analysis – Time-history analysis, like its name, computes the time history response to a dynamic (time-varying) load. The dynamic equations of motion that are solved during the time-history analysis are shown in Equation (4.3) (CSI 2004):

$$\boldsymbol{M}\ \ddot{\boldsymbol{u}}(t)+\boldsymbol{C}\ \dot{\boldsymbol{u}}(t)+\boldsymbol{K}\ \boldsymbol{u}(t)=\boldsymbol{r}(t) \tag{4.3}$$

where

$\boldsymbol{M}$ = diagonal mass matrix
$\boldsymbol{C}$ = damping matrix
$\boldsymbol{K}$ = stiffness matrix
$\ddot{\boldsymbol{u}}(t)$, $\dot{\boldsymbol{u}}(t)$, $\boldsymbol{u}(t)$ = joint accelerations, velocities, and displacements, respectively
$\boldsymbol{r}(t)$ = arbitrary applied dynamic loading

There are several options for time-history analysis. For floor models, it is recommended that linear analysis is used rather than nonlinear. This is a safe assumption, as the small amplitude vibrations do not approach yielding conditions. Two different solution methods are available to perform the time-history analysis of the equations in Equation (4.3): modal superposition using the modes computed from the modal analysis, or direct integration of the coupled equations of motion. Ideally, both methods should yield the same results, however the modal method is recommended. Modal damping is generally used for the modal time-history analysis, and it is generally much faster than direct integration, which requires damping to be

specified using mass and stiffness proportional coefficients. It should be noted that modal time-history analysis uses all modes in the specified modal analysis case, thus any number of modes can be used for computation of the time-history response, depending on modes computed in the modal analysis case. Lastly, the time-history analysis may be performed considering the applied load is either transient or periodic. A transient solution considers the load as a one-time event, thus the solution is computed assuming the structure starts from rest when the applied loading begins and includes the transient response. The periodic solution considers the load to repeat indefinitely, with the transient response damped out (CSI 2004). The periodic option is only available if modal time-history analysis is used. For the purposes of any time-history analysis for floor models, it is recommended to use transient analysis.

SAP2000 offers several types of time history functions to attach to the applied load for dynamic analysis, such as sine, cosine, ramp, or triangular functions. The ability to apply a sinusoidal load to the model and compute the acceleration response is of immediate interest for several reasons. First, the accelerance frequency response function is simply a representation of the steady state sinusoidal response at various frequencies. More importantly, driving the model sinusoidally at its resonant frequency, by definition, will generate its greatest acceleration response. Additionally, the acceleration response at the mid-bay forcing location is the quantity most often computed by the various simplified design methods for comparison with some form of serviceability criterion. How to define a sinusoidal forcing function in SAP2000 is not presented here, but can be found in the thesis by Perry (2003) or the user's manual of the FE program (CSI 2004).

To demonstrate this application of time-history analysis, the example 8-bay floor model was driven sinusoidally by the mid-bay unit load shown in Figure 4.7 at 5.149 Hz, the dominant frequency of the bay of interest (as shown by the greatest response in this bay of any of the mode shapes in Figure 4.6). A linear modal-time history analysis was performed assuming a transient time history type. The analysis included all six modes shown in Figure 4.6 that were computed using eigenvector analysis, and modal damping was input as a constant 0.95% of critical for all modes. The computed time-history of the acceleration response at the mid-bay location is shown in Figure 4.8. The acceleration response is as expected, which includes the floor starting at rest followed by a build-up to resonance (note that there is a slight transient response at the beginning of the build-up) before reaching steady state response. The magnitude of the steady state portion

of the computed acceleration response is 0.8013 in/s^2. Because a unit load was used, it could be stated that the computed *accelerance* at the resonant frequency of 5.149 Hz was 0.8013 in/s^2/lb of input force. Response in the form of accelerance is a result that could be directly compared to experimentally measured values as the applied sinusoidal loads (and thus the corresponding acceleration responses) varied for different tests and different frequencies.

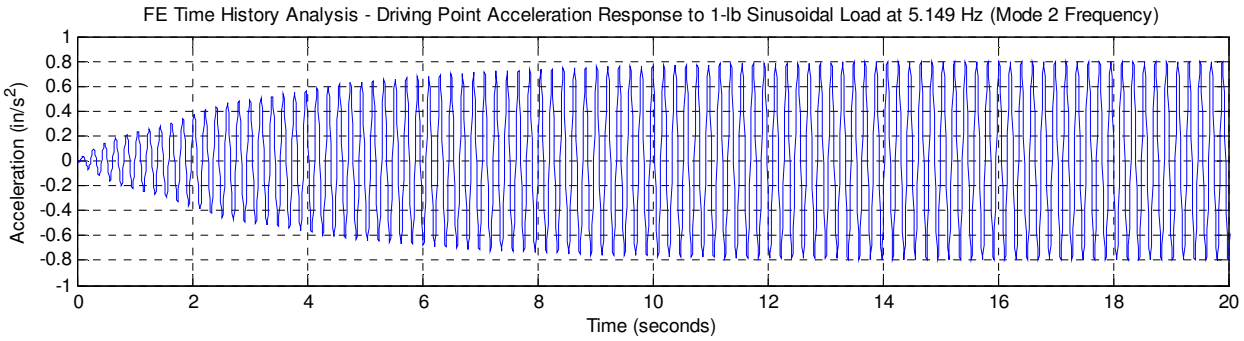

Figure 4.8: 8-Bay Floor Example – Time History Response to Sinusoidal Load

Note that the dynamic loading, ***r****(t)*, in Equation (4.3) is arbitrary. Besides the ability to define the above listed periodic time history functions, SAP2000 also allows the user to define any time varying load. Theoretically, the experimentally measured time-varying loads from the force time-histories of instrumented heel drops or burst chirp signals could be imported for analysis of the computed response and compared to measured response. Although a convenient feature that will likely prove useful in future research, the only dynamic functions analyzed using time-history analysis in the presented research were sinusoidal loads. While the computed acceleration response from an applied sinusoidal load is a convenient demonstration of mid-bay time-history analysis for comparison with measured values, it is a rather clumsy method for computing the accelerance because it is limited to the response at only a single frequency. Frequency-domain steady state analysis provides the most efficient method of comparison of response between measured and computed behavior.

Steady State Analysis – Frequency-domain steady state analysis computes the dynamic response to a set of harmonically varying loads (e.g. a sine and cosine function) at specified frequency increments. It seeks the steady state response, thus assuming the harmonic loading is indefinite and all transient response has damped out. Equation (4.4) shows the dynamic equations of motion that are solved in the frequency domain, for which the form of the solution is explained in greater detail in the user's manual for SAP2000 (CSI 2004):

$$\boldsymbol{M}\ \ddot{\boldsymbol{u}}(t)+\boldsymbol{C}\ \dot{\boldsymbol{u}}(t)+\boldsymbol{K}\ \boldsymbol{u}(t)=\boldsymbol{r}(t)=\boldsymbol{p0}\cos(\omega t)+\boldsymbol{p90}\sin(\omega t) \tag{4.4}$$

where $\boldsymbol{M, C, K,}\ \ddot{\boldsymbol{u}}(t),\ \dot{\boldsymbol{u}}(t),$ and $\boldsymbol{u}(t)$ are the same as previously defined and

$\boldsymbol{r}(t)$ = harmonic loading where $\boldsymbol{p0}$ is the in-phase (real) component
and $\boldsymbol{p90}$ is the 90° out-of-phase (imaginary) component
ω = the circular frequency of excitation (rad/sec)

The most important feature of Equation (4.4) is the harmonic loading that represents an in-phase and 90° out-of-phase component. This simplifies the equations to be solved in the frequency domain, but more importantly the resulting solution represents the real and imaginary components of response at each frequency increment. At each frequency increment, the real and imaginary component of response can be combined through a square root of the sum of the squares (SRSS) computation to give the magnitude of response. These quantities can also be used to determine the phase angle between the applied loading and the acceleration response. While any spatially distributed load can be used in steady state analysis (i.e. multiple point loads, distributed loads, acceleration loads, etc.), *the choice of using a unit point load at a single location for steady state analysis results in the computational equivalent of the accelerance frequency response and yields quantities directly comparable to measured accelerance FRFs*. Because steady state analysis computes the response for all degrees of freedom of the FE model, the results essentially represent a column of the accelerance FRF matrix just as a full set of experimentally measured accelerance FRFs would for a single location of excitation. This ability to compute the accelerance FRF of a floor's FE model is the most significant feature for validation of a model with respect to experimental measurements and also forms the basis for a proposed method of evaluation for vibration serviceability presented at the end of this chapter.

The application of steady state analysis is best demonstrated using the previously discussed example 8-bay floor model. For this example and comparison with the previous time-history analysis, the model was analyzed with the unit load located in the bay as shown in Figure 4.7. A target value of damping for the floor was 0.95% of critical for all modes. As previously stated, SAP2000 specifies hysteretic damping for frequency-domain calculations, thus damping must be specified as mass and stiffness proportional coefficients. It may be specified as constant hysteretic damping for all modes or interpolated hysteretic damping by frequency. For the presented example, an equivalent 0.95% modal damping for all modes was approximated by choosing constant hysteretic damping and specifying the mass proportional coefficient as 0 and

the stiffness proportional coefficient as 0.019 (see previous Damping section for details on this method). The range of frequencies to be solved was chosen to be 4 Hz to 8 Hz divided into 80 increments, resulting in a frequency resolution of the computed values of 0.05 Hz. It should be noted that the computed steady state solution is performed *directly* for all specified frequency increments, without use of the modes computed in the modal analysis case like the presented time-history analysis example. Consequently, computed values are just as susceptible to the effects of frequency resolution as experimental measurements because peak frequencies may lie between two computed/measured frequency increments. Although the modal analysis is not used directly in computing the solution, the frequencies from the modal analysis can be included as specified frequency increments to be solved during the analysis. Steady state analysis results may be presented in a variety of ways, although all are based on the computed real and imaginary components of response as shown in Figure 4.9 for the driving point location.

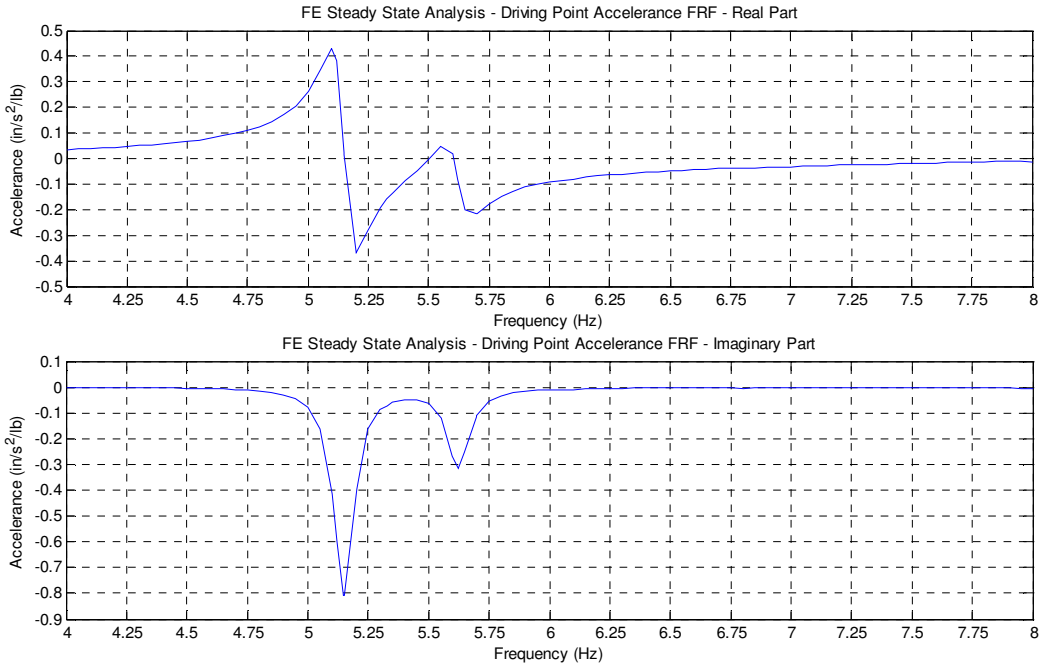

Figure 4.9: 8-Bay Floor Example – Driving Point Accelerance FRF (Real and Imaginary)

Although plotting the real and imaginary components gives valid representations of the accelerance FRFs, a more intuitive representation of the response for the presented research is given by the magnitude and phase as shown in Figure 4.10. From this representation, a few features are of immediate interest and provide valuable insight into the floor's behavior. First, there are clearly two significant peaks in the response, 5.149 Hz and 5.622 Hz, which correspond to the second and fourth modes of the 8-bay floor model as shown in Figure 4.6. Secondly, the

magnitudes of the computed response indicate both frequencies participate significantly, but the 5.149 Hz mode is clearly dominant. Lastly, the peak accelerance of the 5.149 Hz frequency was 0.8075 in/s^2/lb of input force, which is in excellent agreement with the 0.8013 in/s^2/lb accelerance estimated from the time-history analysis. Because steady state analysis directly solves the system of equations of motion, the results are likely to be more accurate than a modal time-history analysis that uses a finite number of modes and relies on the cumbersome method of identifying the peak amplitude of the time-history response once it achieves steady state.

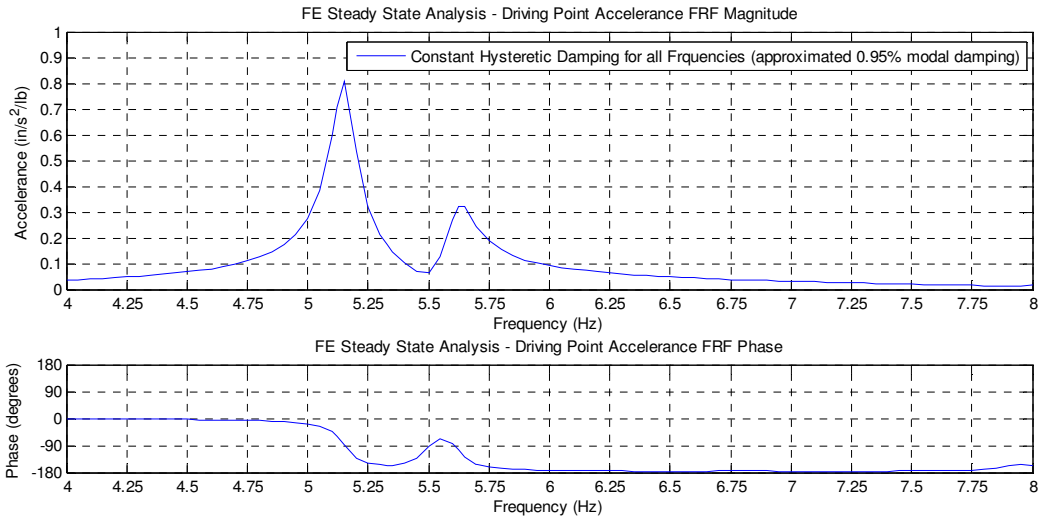

Figure 4.10: 8-Bay Floor Example – Driving Point Accelerance FRF and Phase

The computed real, imaginary, and magnitude components of response can be displayed in SAP2000 or exported for plotting in other programs, however the phase plot shown in Figure 4.10 is not internally computed by the program and was plotted by taking the inverse tangent of the imaginary component over the real. It should be noted that the computed accelerance trace shown in Figure 4.10 is only for one location on the floor, the driving point, and there are literally thousands of similar traces computed for all mass degrees of freedom in the floor model (1843 mass DOFs for the example 8-bay floor model). Like the experimental testing of in-situ floors, the driving point response is the most important computed response, however representing the response over the entire floor area is also of interest. SAP2000 allows animation of the computed response at any frequency increment (and any phase at that frequency increment). Figure 4.11 displays two animated representations of the response that are useful from a vibration serviceability standpoint. The first animated shape shown in Figure 4.11(a) is the floor response at its 5.149 Hz dominant frequency. Note that although this closely

approximates the mode shape, as a forced vibration response it is actually the computed equivalent of the operating deflection shape (ODS) at this frequency. It is plotted at a phase of 90°, as the response at resonance is almost purely defined by the imaginary component. Another useful form of the response is shown in Figure 4.11(b), which is the envelope of response that displays the absolute maximum response at any point on the floor model for any of the computed frequency increments between 4 Hz and 8 Hz. This is useful for displaying areas of the floor that are excited by the forcing location but are not readily apparent in the computed driving point accelerance FRF or the computed ODS at the dominant frequency.

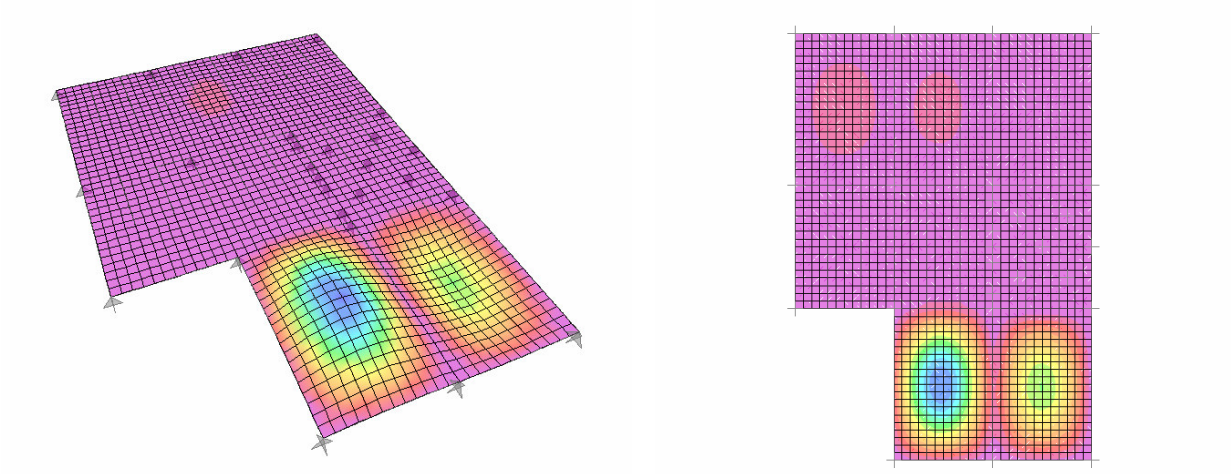

(a) Computed Forced Response ODS at 5.149 Hz (90° phase)

(b) Steady State Response Envelope (4-8 Hz)

Figure 4.11: 8-Bay Floor Example – Other Representations of Response

Although a unit load is used for steady state analysis to ensure the units of response are in/s^2/lb, the mid-bay unit load may be scaled to any value to effectively convert the computed accelerance values to the units of choice. For example, all accelerance FRF measurements in the presented research originated in units of volts/volts from the DSP spectrum analyzers. During post-processing, calibration values were used (240 lbs/volt for the force plate and 1 g/volt for the accelerometers) to convert to accelerance units of in/s^2/lb. For pre-test modeling of a floor system, the unit loading could be scaled to 0.622, effectively converting all computed response values from in/s^2/lb to volts/volt and allowing easy real-time comparison of measured accelerance magnitudes to pre-test FE values.

Constant hysteretic damping for all frequencies was used for the example presented above. The alternative method for specifying damping in steady state analysis is interpolated

hysteretic damping, which allows mass and stiffness proportional coefficients to be specified for any number of frequencies. To investigate the effect on the computed response using this interpolated hysteretic damping option, two analyses were run on the same 8-bay floor model. The first analysis specified 0.95% damping at the first peak (5.149 Hz) and twice as much damping, 1.80%, at the second peak (5.622 Hz). This effectively specified a linearly increasing level of damping that includes these two ordered pairs. For comparison with the constant hysteretic damping option, the second analysis specified 0.95% damping at both 4 Hz and 8 Hz, effectively specifying a constant level across the frequency range. The two computed driving point accelerance traces are plotted in Figure 4.12. As shown, nearly identical response was computed for the 5.149 Hz peak where 0.95% damping was specified for both cases. For the 5.622 Hz peak with twice as much specified damping, the response is obviously lower but not quite half the previous level of response, which would be expected. The analysis specifying constant damping using the interpolated option computed the exact same response as when constant hysteretic damping was specified. Although constant hysteretic damping was exclusively used in the presented research, the examples using the interpolated hysteretic damping option are presented for demonstration of alternative approaches to force response.

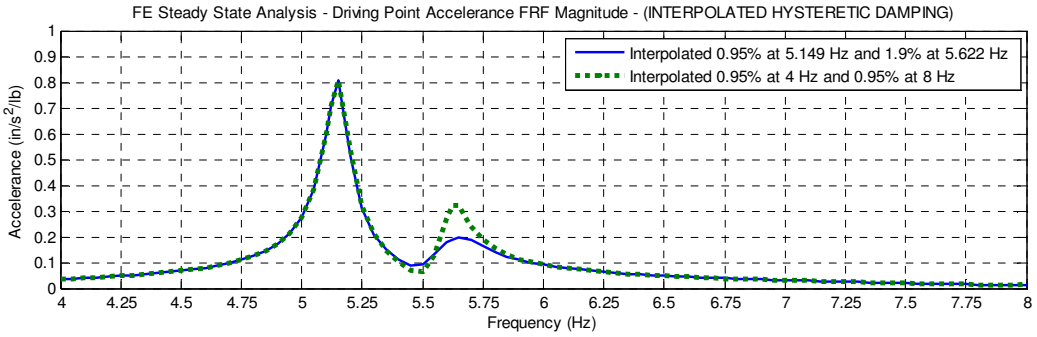

Figure 4.12: 8-Bay Floor Example – Examples Using Interpolated Hysteretic Damping

The implications of this application of FE frequency-domain steady state analysis is substantial for potential evaluation of vibration serviceability as well as experimental testing of in-situ floors. While the computed frequencies and mode shapes may provide insight into the areas of a floor that are potentially vulnerable to excitation at certain frequencies, this is only half of the information needed for evaluation of vibration serviceability, with the other half being the acceleration response in those areas at the vulnerable frequencies. The computed mid-bay driving point accelerance FRF provides all information in a single trace, with the magnitude and locations of the computed accelerance peaks representing the dominant and other significantly

participating frequencies (modes) of the bay as well as the estimated level of acceleration response. If an in-situ floor is modeled prior to experimental testing, the measured mid-bay driving point accelerance FRF can be directly compared to the computed accelerance FRF in the field for instant feedback of the validity of the pre-test FE floor model. This instant feedback may also alleviate the need for extensive modal measurements and post-processing to extract the experimentally derived mode shapes. Additionally, the experimental mid-bay floor evaluation approach described in Section 3.4 may be all that is required for validating and updating floor FE models. Using this approach, a set of experimental mid-bay driving point accelerance FRFs would indicate the participating frequencies of a bay, the accelerance at the peaks, the general mode shape if a set of mid-bay measurements were acquired, and measured estimates of damping that may differ from assumed values of the pre-test FE model.

4.2 Finite Element Analysis of Tested Floors

This section presents the finite element models of the tested floors that were generated using the techniques discussed in the previous section. It should be noted that the recommended techniques, particularly recommendations of spandrel member property modifiers, member end releases and partial fixity values, and damping used for analysis were developed during efforts to bring the results of the FE models into agreement with experimentally measured values. The FE models were developed *in parallel* so that the same techniques applied to each gave adequate results for both models. Although not presented here, certain model iterations were better at predicting frequencies and mode shapes, and other iterations were better at predicting acceleration response. This was achieved with different combinations of the above listed parameters; however the objective of the research was to identify a set of common/fundamental modeling techniques that yielded adequate results, not adjustments required to optimize an individual model unless those adjustments improved the results of both models. Thus, while the presented results may not represent the closest match of frequencies, mode shapes, and acceleration results achieved during the course of research, the promising results presented in this section demonstrate that an adequate representation of in-situ floor behavior is possible using a common set of basic modeling techniques. Although the two FE models of the tested floors were developed simultaneously, the FE model for NOC VII is presented first in Section 4.2.1, followed by the model for VTK2 in 4.2.2.

4.2.1 New Jersey Office Building, NOC VII

Two FE models are presented for the NOC VII floor. The first model represents the whole floor. A smaller model, representing a portion of the floor, was developed to address difficulties in achieving proper frequencies and mode shapes in bays along the long length of the building. Although not originally the intent of the research, the smaller model of a portion of the floor was generated using the same fundamental techniques and provided some encouraging results, highlighting an area for further research.

NOC VII Full Floor Model – Following the general steps previously discussed, the floor framing geometry was laid out for the full floor model with the steel framing members specified in the design drawings and pinned supports were applied at the column locations. A user-defined material (NOCVII-VIBCON) and area plate element (NOCVII-SLAB) were created to represent

the composite slab in the floor model. The input values of these user-defined parameters and the composite slab properties used in their development are presented in Table 4.1. The DG11 recommended dynamic modulus of elasticity was used ($1.35*E_c$) and the weight and mass densities of the material were computed using Equations (4.1) and (4.2). Slab details and the framing plan of the specified steel sections for NOC VII are presented in Appendix A. Plan and 3-D views of the floor model's slab and framing layout are in Figure 4.13, including the eleven locations of forced response analysis presented later in this section for comparison with experimental measurements.

Table 4.1: NOC VII – Composite Slab Parameters & Slab Area Element/Material Properties

Overall Slab/Deck Height:	5.25 in.	Unit weight of concrete, w_c:	115 pcf
Slab height above ribs, d:	3.25 in.	Concrete compressive strength, f'_c:	4000 psi
Deck rib height, d_r:	2.00 in.	Dynamic modulus of elasticity, $1.35*E_c$	3300 ksi
Area weight of steel deck, w_{deck}:	2.4 psf	Superimposed loads, $w_d + w_l + w_{coll}$:	0 psf

User-Defined Material Name:	**NOCVII-VIBCON**	User-Defined Area Section Name:	**NOCVII-SLAB**
Type of Material:	Isotropic	Type of Area Section:	Plate-Thin
Mass per unit Volume:	2.3869×10^{-7} k-s^2/in^4	Assigned Material:	NOCVII-VIBCON
Weight per unit Volume:	9.2156×10^{-5} k/in^3	Thickness (Membrane/Bending)	3.25 in.
Poisson's Ratio	0.2	Stiffness Modifiers:	Bending m11 = 2.88
Additional Material Damping:	None		

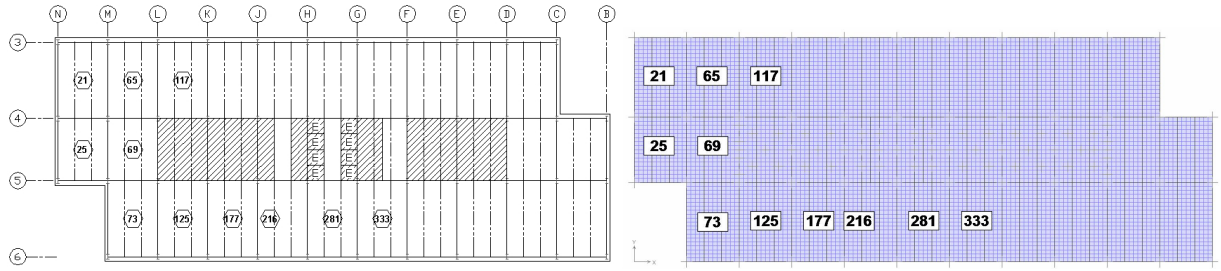

(a) NOC VII Floor Framing Layout (b) FE Model Plan View of Framing & Slab

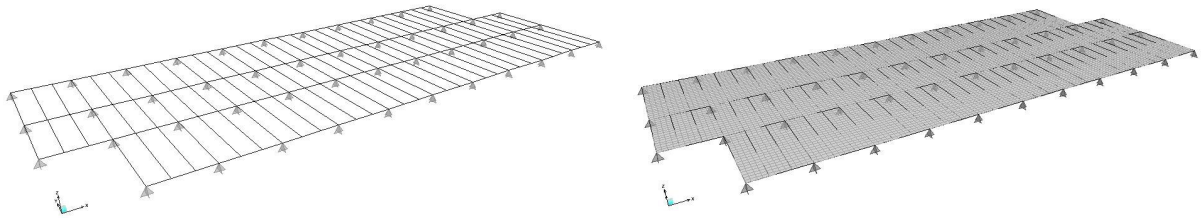

(b) 3-D View – Framing Only (c) 3-D View – Framing and Slab

Figure 4.13: NOC VII – Floor Layout and Full Floor FE Model

It was found that a slab area element size of 30 in. x 28 in., which corresponds to a mesh size of 12x16 elements for interior bays and 12x20 elements for exterior bays, gave convergent

results. With this configuration, the full floor model contains over 7,000 mass degrees of freedom (UZ). With the vast number of joint numbers to track, the joints were renumbered in a manner to ease analysis of the results. Initially, all joints were automatically numbered using the features available in SAP2000, starting from 1001. The joints on the model corresponding to a measured location were manually renumbered in the pattern of Figure 3.8. (Although not required, this practice is recommended as a convenience when models are to be used in comparison with floor testing. This method simplifies identifying points of interest for extracting accelerance response from steady state analysis. Additionally, this practice is also conducive for comparing measured/computed mode shapes because the DOFs of interest are the first in the list of tabulated joint numbers and the remaining values can be discarded.)

The transformed composite moments of inertia were computed for each framing member to determine the baseline stiffness property modifiers, which ranged from 2.6 to 3.6 for NOC VII. The modifiers were computed as described in Section 4.1, and an example of this computation is presented in Appendix K. A full listing of the calculated transformed moments of inertia and their respective baseline PMs for NOC VII is found in Appendix M. The baseline values were applied as PMs to the strong axis moment of inertia for all framing members, and 2.5 times the baseline values were applied as PMs to all spandrel beams, spandrel girders, and the interior girders adjacent to bays with full height partition walls to account for the increased stiffness along these interior boundaries. Final assigned PMs are also listed in Appendix M.

Strong axis bending moment releases without any partial fixity were applied to all members framing into the webs of columns, which were limited to all girders for NOC VII. No moment releases were applied to the beam members that framed into the flanges of columns. Strong axis moment releases were applied to all beams framing into the webs of girders, and partial fixity values of $6EI/L$ (EI/L computed using properties of the beam member) were applied at both ends. Again it should be noted that the release and/or partial fixity condition of the end of a beam member framing into a spandrel girder had a negligible effect on the frequencies and mode shapes of the floor because of the minute contribution of the torsional stiffness of the spandrel girders to the stiffness of the system. Because the effect is negligible, it is recommended to include the release and partial fixity at both ends for the convenience of not having to be concerned with the local axis of the member and whether or not the correct end is

released. Figure 4.14 shows the framing layout of NOC VII, the end releases, and members with assigned partial fixities.

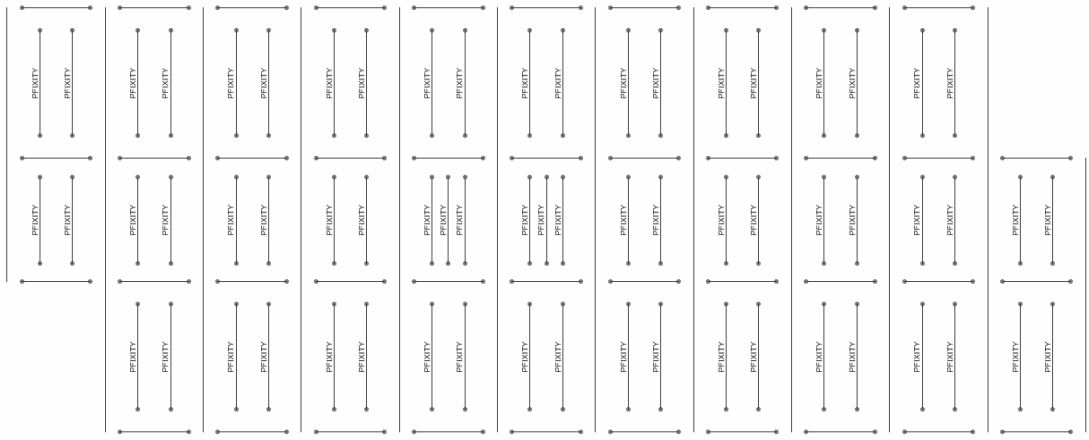

Figure 4.14: NOC VII – Full Floor Model Moment End Releases and Partial Fixities

Besides increasing the stiffness properties of the interior girders adjacent to the partition walls, additional pinned restraints were applied to the interior bays to represent elevator core framing, stairwells, restroom, mechanical room, electrical room partition walls, etc. The actual partition layout was not available, thus the layout of the pinned restraints was based on judgment. Along grid lines D and M, several pin restraints were added to represent the heavy concentrically braced frames attached to the beam members spanning between the columns. The locations of the interior pinned restraints are shown in Figure 4.15. It should be noted that the locations of these interior pins were based on judgment and may provide some degree of over-restraint that prevented the model from accurately predicting the mode shapes and frequencies of the exterior bays along the long side of the floor.

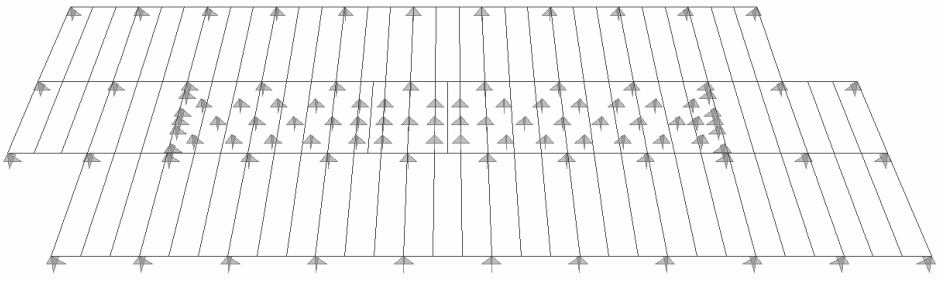

Figure 4.15: NOC VII – Full Floor Model Interior Restraints

An eigenvector modal analysis was performed on the floor model to compute the frequencies and mode shapes. The frequencies of the first 24 modes are presented in Table 4.2 and the corresponding mode shapes are presented in Figures 4.16 and 4.17.

Table 4.2: NOC VII – Computed Modes for Full Floor Model

Mode:	Frequency (Hz)	Mode:	Frequency (Hz)	Mode:	Frequency (Hz)
1	5.151	9	5.475	17	6.025
2	5.151	10	5.492	18	6.047
3	5.191	11	5.618	19	6.103
4	5.192	12	5.627	20	6.134
5	5.316	13	5.774	21	6.138
6	5.322	14	5.774	22	6.141
7	5.374	15	5.914	23	6.939
8	5.390	16	5.926	24	6.955

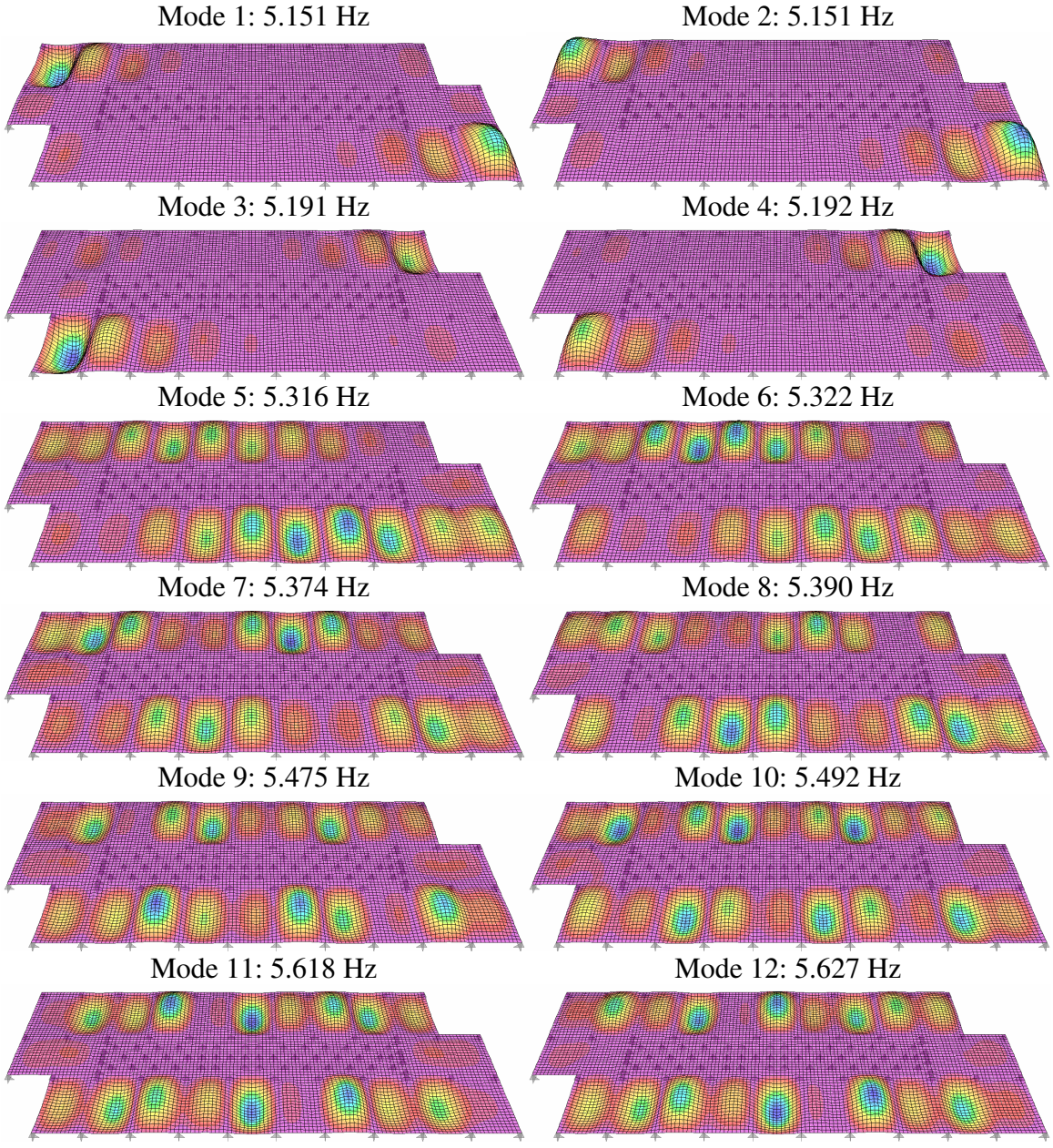

Figure 4.16: NOC VII – Full Floor Model Computed Mode Shapes (Modes 1-12)

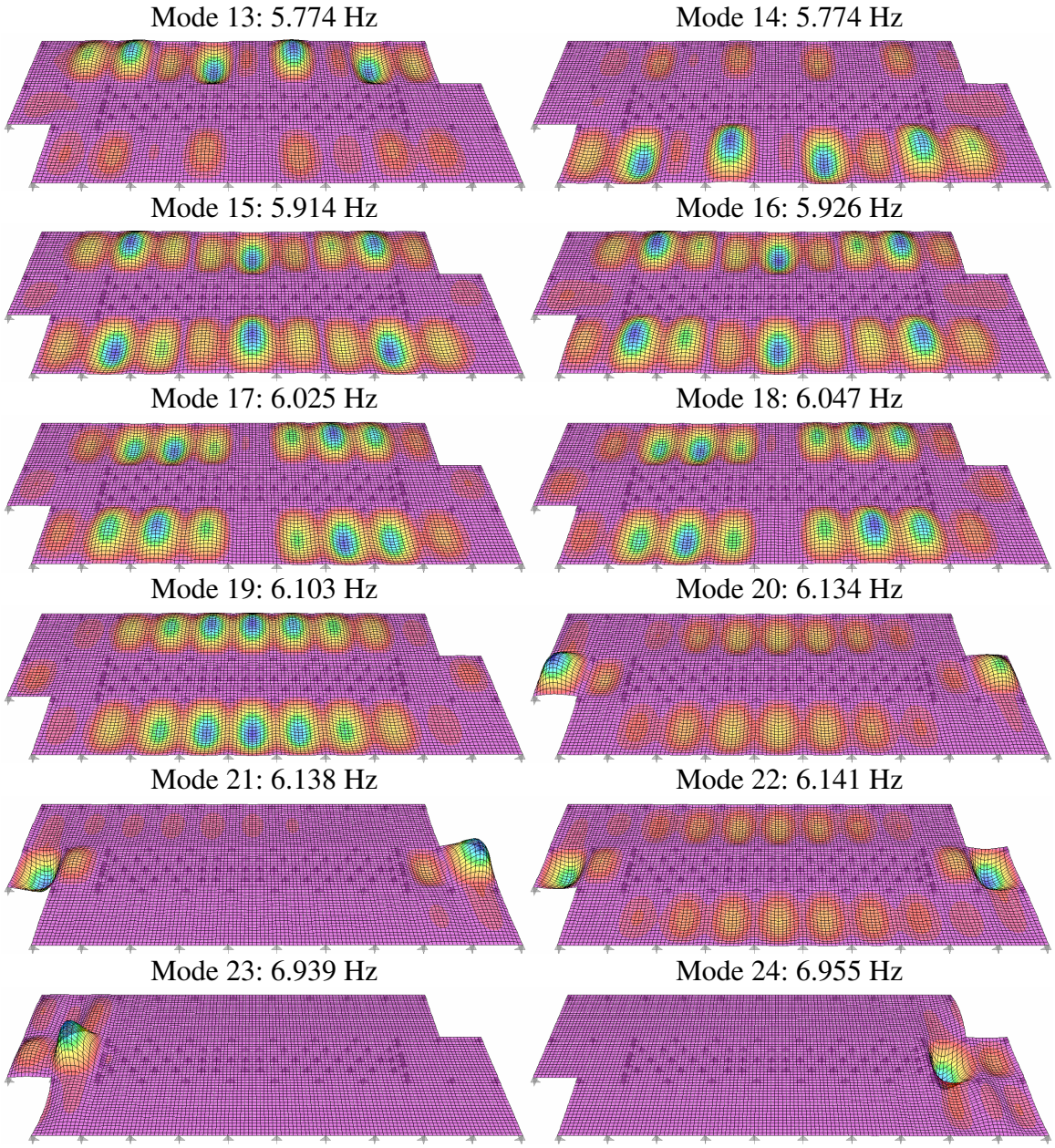

Figure 4.17: NOC VII – Full Floor Model Computed Mode Shapes (Modes 13-24)

Several iterations of the modal analysis were performed while varying the number of modes to be computed. This was accomplished to ensure that all mode shapes of interest were captured, namely the shapes that represented single curvature within a bay. It was determined that 24 modes were necessary to capture the dominant shapes of all bays; modes beyond this had double curvature within bays, which is not particularly of interest in the presented research due to comparison with mid-bay excitation locations that would likely not represent these modes well.

There are some interesting items to note in the computed mode shapes shown in Figures 4.16 and 4.17. First was the computation of "pairs" of point-symmetric mode shapes computed at nearly identical frequencies for the first 18 modes. Although not originally anticipated, this is a logical result due to the point symmetric nature of the floor framing with only slight differences in some of the interior restraints used toward the ends of the interior core of bays. Also because of this symmetry, it would be expected that the measured frequencies at the respective bays on either end of the floor will be the same or very similar, although this was not verified for the tested floor. The second observation is that certain mode shapes show a dominant response in a localized area, consistent with what was observed in experimental measurements. In particular, Modes 1, 3, 20, and 23 show clearly dominant response in the bays containing Points 21, 73, 25, and 69, respectively. These four mode shapes of the end portion of the floor that was tested are shown in Figure 4.18, along with the ODSs of the respective bay's dominant frequency. The frequencies for these modes and their respective shapes are in good agreement with the measured frequencies of the bays (less than 6% difference in frequency).

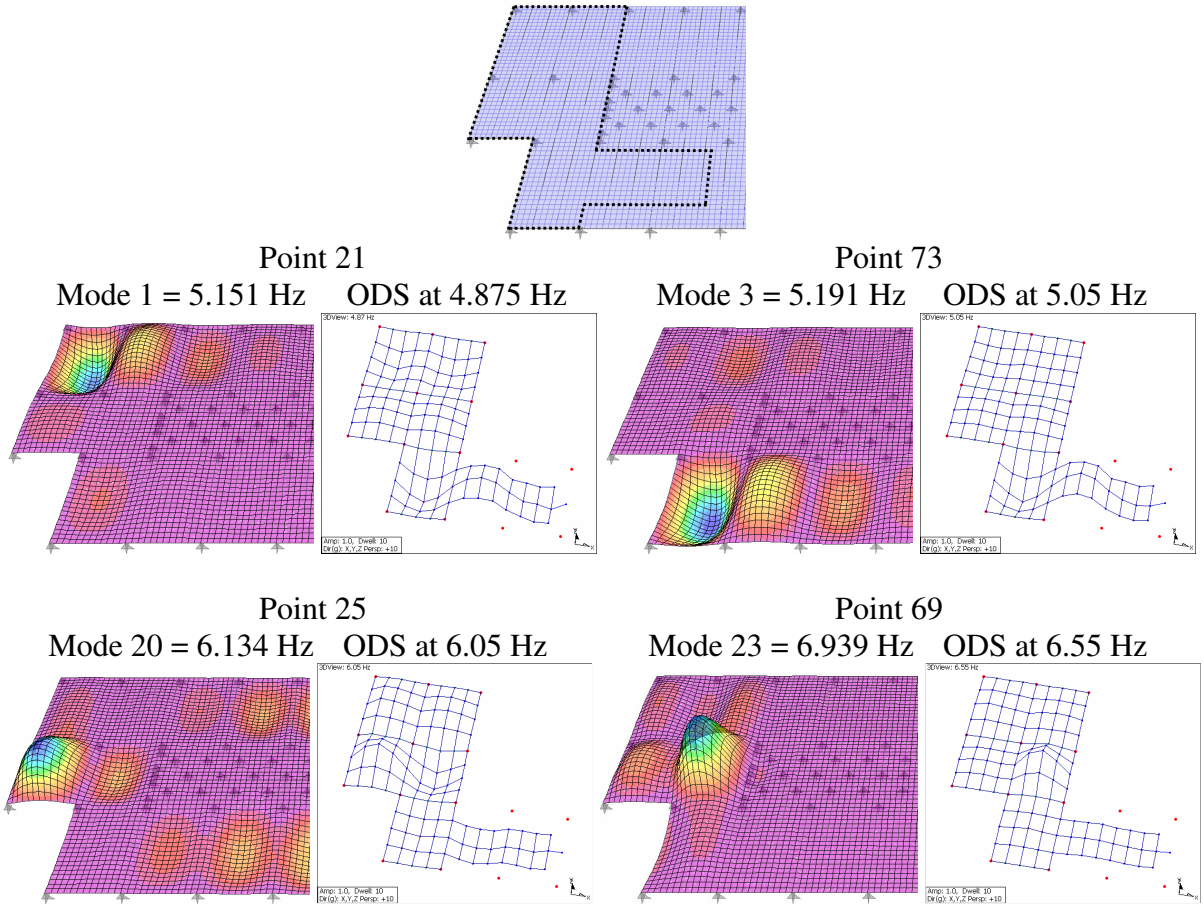

Figure 4.18: NOC VII – Full Floor Model Mode Shape and ODS Comparison

Unfortunately, there were several areas of the floor (the points of excitation other than the four listed above) that were not well represented with clearly dominant shapes, although they should be as indicated by dominant peaks in the experimentally measured driving point accelerance FRFs. Points 65 and 281 are the most notable locations with large accelerance values not well represented in the mode shapes of the model. Additionally, all excitation locations along the length of the building (Points 125, 177, 216, 281, and 333) had measured dominant frequencies of 5.025-5.05 Hz, indicating a dominant mode shape that was common to all bays along this strip. Extensive testing with the shaker located at Point 281 showed this shape to be a simple mode that alternated concavity at each bay (Figure 3.14). Examining the mode shapes for this strip of bays in Figure 4.16, Mode 5 at 5.316 Hz looks the most similar, however there are 13 other modes between 5.322 Hz and 6.103 Hz that show significant participation along this strip in various concave up or down configurations of the bays. As a result, it is likely that none of these modes will dominate the response, which is clearly not the case as indicated from experimental testing. A separate model representing this strip of bays was generated to try and isolate the response better than the full floor model and is discussed later in this section.

Although comparison of frequencies and mode shapes was a necessary step in the model validation process, the comparison of forced response analyses with experimental measurements was the final step in assessing the ability of the FE model to adequately represent the dynamic behavior of the floor system. Steady state analysis was performed on the modeled floor for the eleven different unit load locations shown in Figure 4.13(b), each corresponding to a driving point location on the floor during modal testing. These eleven locations were all at mid-bay with the exception of Point 216, which was at the quarter point of the bay along the centerline of the long direction of the floor. To correspond with the burst chirp frequency range of the experimental driving point accelerance FRFs, the steady state analyses evaluated response at increments between 4 Hz and 8 Hz with roughly a 0.05 Hz frequency resolution. Although the experimental measurements were taken with a 0.025 Hz frequency domain resolution, the FE steady state response functions generally do not require that fine a resolution, particularly because the computed modal frequencies were also included as frequency increments to ensure the peak response was captured (a luxury not afforded during experimental testing).

Steady state analysis was performed twice for each of the driving point locations. For the two analyses at each point, damping was specified as a constant value for all frequencies and was

input as either the estimated damping at the dominant frequency from experimental measurements of the bay under investigation or using the proposed damping values for a bare floor based on general bay location (1%, 1.5%, 2%). The results using the measured damping values are presented first in this section, followed by an overall summary of how well the response using an assumed level of damping was in agreement with measured response, which would be the only option for a designer modeling this floor prior to construction. The points of excitation and each of the two damping ratios used for analysis are shown in Figure 4.19.

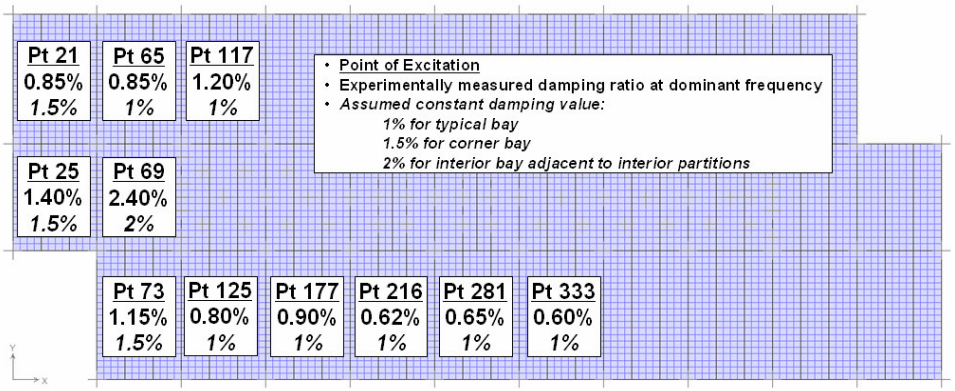

Figure 4.19: NOC VII – Constant Damping Ratios Used in Steady State Analysis

The computed driving point accelerance FRFs for each of the eleven bays are presented in Figures 4.20 and 4.21. As expected from the computed mode shapes, the FE accelerance FRFs are in better agreement with the measured accelerance FRFs for Points 21, 25, 69, and 73 as shown in the Figure 4.20. As shown in these four plots, using the measured estimates of damping did not always result in better agreement, which is particularly apparent for Point 21 where the computed response is nearly one and a half times larger than measured. This is likely a result of the dominant mode shape for Point 21 not being accurately represented by the computed shape of Mode 1. The shape for this mode is localized to a small area around the bay containing Point 21, which essentially translates into a small participating (effective) mass. An underestimation of the effective mass of that mode will result in excessively high computed acceleration response because the modal mass term is in the denominator. The same effect can be seen by the overestimated response for Point 25. It is encouraging to know, however, that an extremely localized mode results in an excessively large computed response and to recognize that it is likely a conservative estimate of response when the localized mode shape is observed from the modal analysis. The computed accelerance FRFs for Points 69 and 73 are in good agreement with the experimental FRFs.

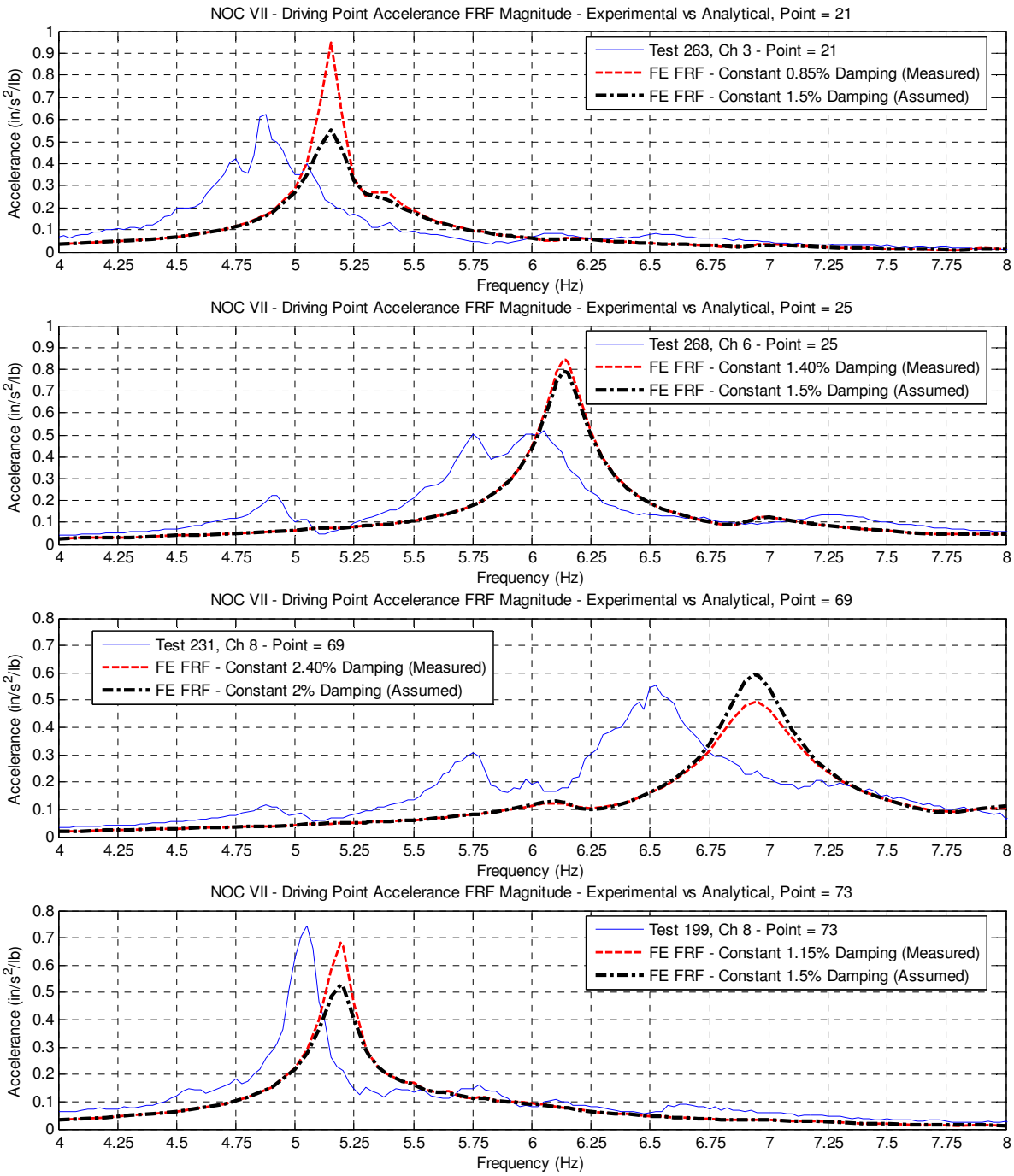

Figure 4.20: NOC VII – Full Floor Accelerance FRFs (Points 21, 25, 69, 73)

The computed accelerance FRFs for the remaining seven tested/analyzed locations were not in agreement with the measured FRFs for either magnitude or shape, as shown in Figure 4.21. The inability to match response at Points 65 and 281 with this model, which both have clearly dominant single peaks, is disappointing because they have the largest magnitudes of any of the measured locations on the floor and thus represent vulnerabilities of the floor that a

designer would strive to identify in the design phase. Again, the inability for the model to correctly represent the mode shapes of the entire strip of bays, namely a single dominant shape of alternating concavity, is the reason for the poor correlation.

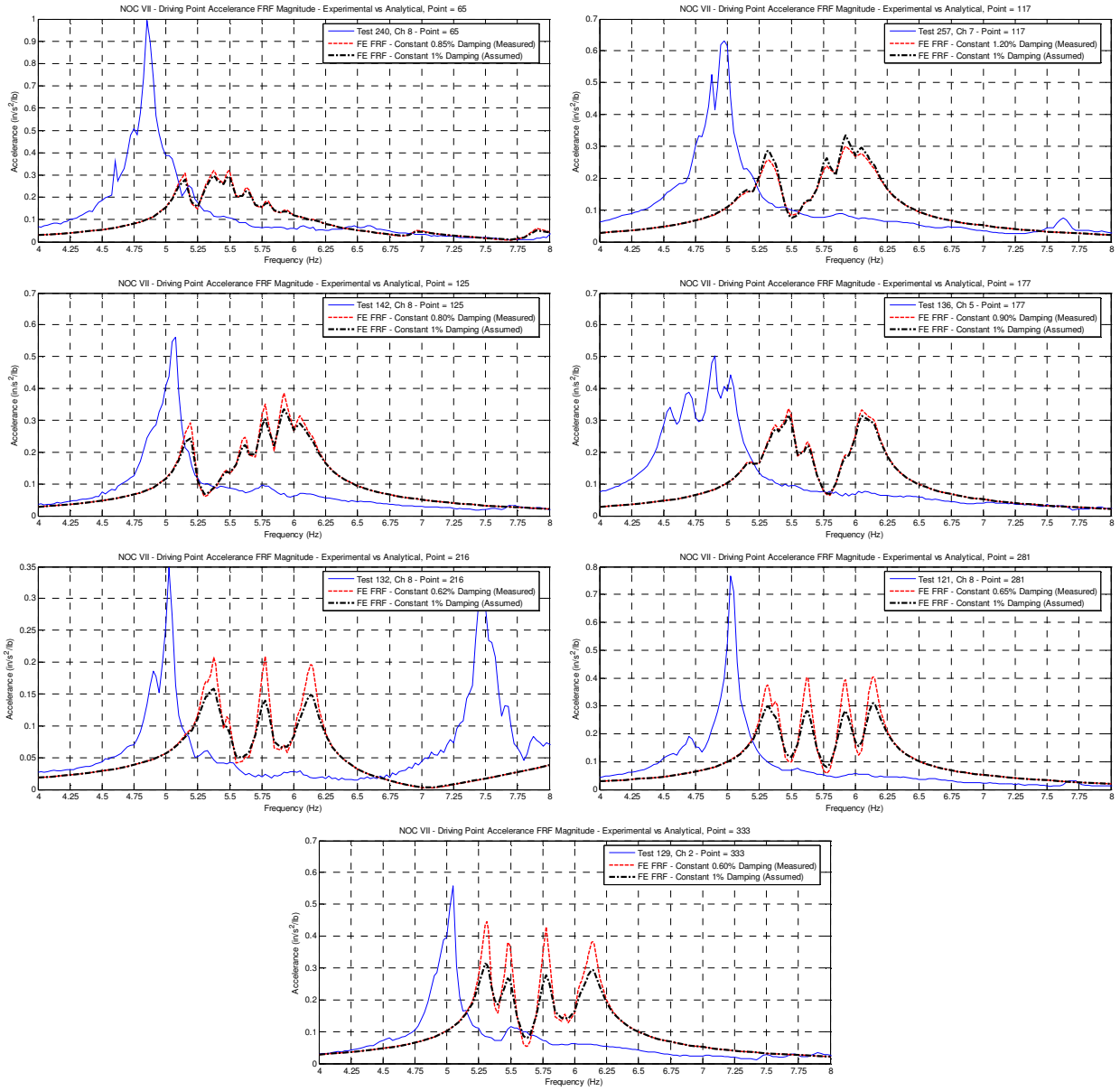

Figure 4.21: NOC VII – Full Floor Accelerance FRFs (Pts 65,117,125,177,216,281, & 333)

While the computed accelerance FRFs in Figure 4.21 did not match the measured FRFs for any level of damping, the assumed levels of damping used in the four plots of Figure 4.20 actually provided a reasonable approximation of the measured response. While notably high for Point 25 (which was true for both measured and assumed) and about 25% low for Point 73, the response was within 12% for Points 21 and 69. Overall, there seemed to be about the same

number of locations in agreement using either measured or assumed damping values. Although the computed traces are not overwhelmingly in agreement with measured values for this model, the frequencies were predicted within 6% of measured and the general shape of the accelerance FRF peaks from the different participating frequencies are represented well, including magnitude. Despite the discrepancies, this is an encouraging result for the recommended modeling techniques.

NOC VII 10-Bay Strip Model – To further investigate the bays along the length of the floor that did not agree well with measured values, a reduced model including just the 10-bay strip along the floor's length was generated using the same recommended techniques and analyzed using the same methods as presented above. The 10-bay coverage area of the reduced FE model is shown in Figure 4.22 along with the 3-D views of the model's framing and slab. All floor beams spanning between girders retained their end moment releases and partial fixity values, although due to the absence of members framing into the beam-to-girder joints on the other side of the girders, the effect of the partial fixity on frequencies and mode shapes was negligible.

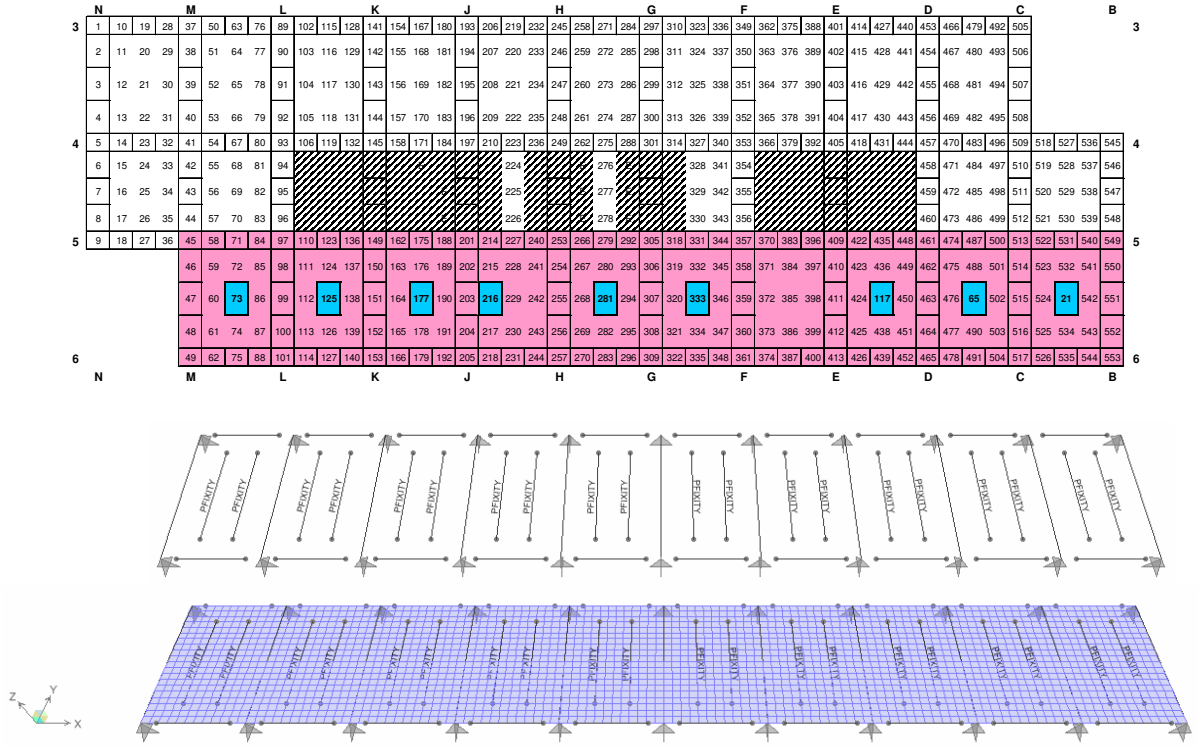

Figure 4.22: NOC VII – 10-Bay Strip FE Model

To account for the missing portions of the slab on the end bays that were adjacent to open areas of the floor (bays containing Points 73, 65, and 21 in Figure 4.22), a modeling technique

recommended by Perry (2003) was used. He recommended applying a mass property modifier of 0.5 to the girder and a strong axis moment of inertia property modifier of 0.5 times the baseline value (i.e. half mass and half composite stiffness), resulting in a member that has the same static deflection as if the adjacent bay were present. This technique was applied without any refinement to attempt to improve the results. All spandrel members (bottom, right, and left edges) retained their originally applied property modifiers, which were 2.5 times the computed baseline values. The girders that bound interior bays (i.e. girders beneath full height partition walls) also retained their respective 2.5-times-baseline stiffness property modifiers. No adjustments were made to the stiffness or mass of these interior girders to account for the missing interior bays.

The main difference of this 10-bay strip model compared to the full floor model is the absence of the highly restrained interior bays, which is probably the main contributor to the discrepancy. As expected, the computed frequencies of the 10-bay strip model were lower than their full floor model counterparts. Modal analysis of the 10-bay strip model for NOC VII computed the 16 frequencies listed in Table 4.3. It is interesting to note the first 10 computed frequencies are within 0.4 Hz of one another; however there is a 1.5 Hz gap in frequency between the 10^{th} and 11^{th} modes, which represents the delineation between modes with single curvature within a bay and those with double curvature. This is readily apparent in floor models with the same or very similar bay dimensions and framing members but may be less obvious in floor models that have smaller interior bays. These small interior bays tend to have higher frequencies that may be close to the double curvature modes of the larger exterior bays. The first 12 mode shapes are presented in Figure 4.23.

Table 4.3: NOC VII – Computed Modes for 10-Bay Strip Model

Mode:	Frequency (Hz)	Mode:	Frequency (Hz)
1	4.823	9	5.219
2	4.845	10	5.235
3	5.009	11	6.790
4	5.057	12	6.888
5	5.087	13	7.055
6	5.124	14	7.292
7	5.161	15	7.597
8	5.194	16	7.969

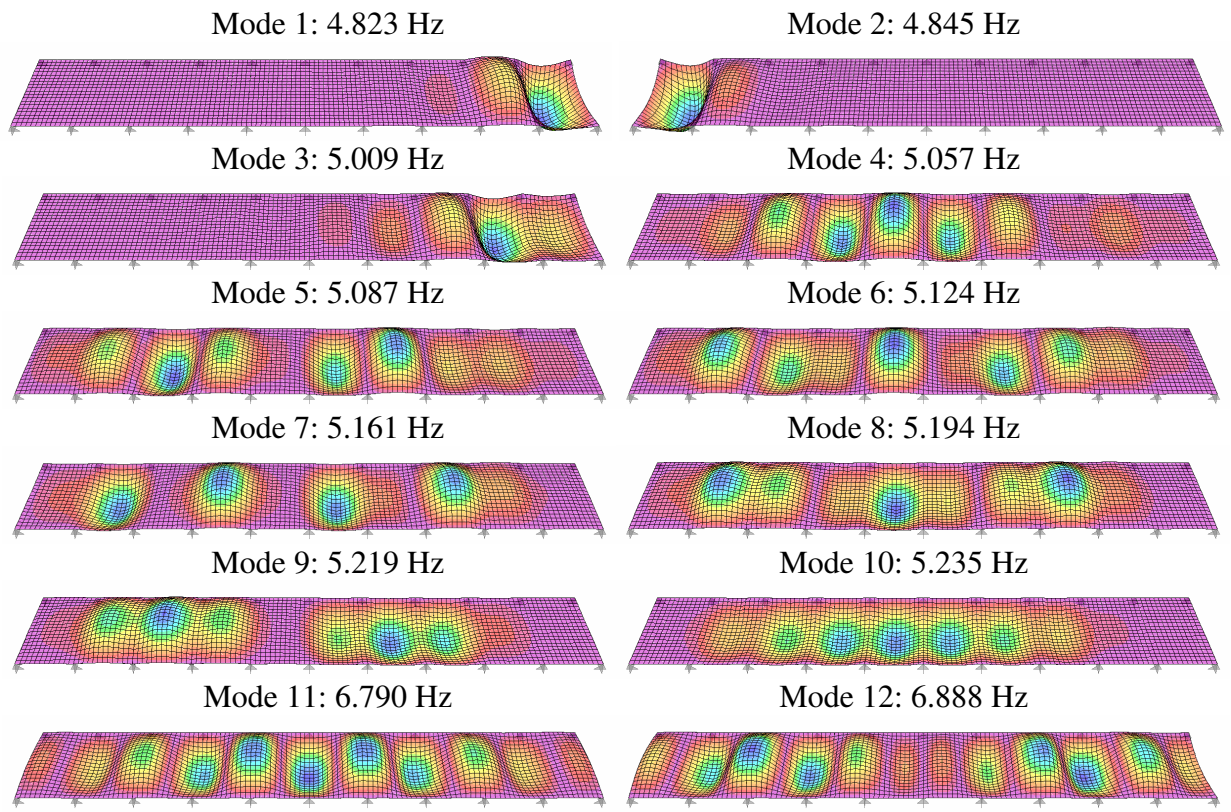

Figure 4.23: NOC VII – 10-Bay Strip Model Computed Mode Shapes

As anticipated, the lower modes show the greatest response in the "softer" areas of the floor, which are the end bays with the girders assigned lower stiffness property modifiers. As with the full floor model, the lower modes are also represented by localized response in a few adjacent bays, which would indicate large forced response values for excitations in these locations at their dominant frequencies. Unlike the full floor model, however, the frequency of the first mode shape with significant response along the middle portion of the model (Mode 4: 5.057 Hz) is very close to the measured frequencies in these bays (5.025 Hz to 5.075 Hz) and the mode shape is very similar to the measured dominant shape, as shown in Figure 4.24.

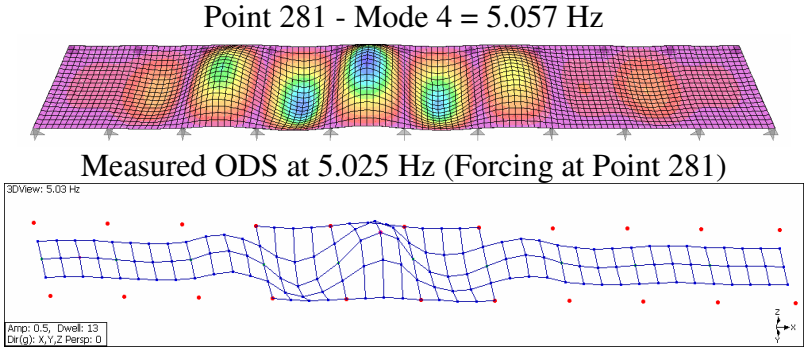

Figure 4.24: NOC VII – 10-Bay Strip Model Mode Shape and ODS Comparison (Point 281)

It should be noted that due to the point symmetric nature of the floor geometry, the mid-bay locations on the end three bays of the right side (Points 533, 489, and 437) should demonstrate the same response as the corresponding locations on the opposite corner of the building, which are Points 21, 65, and 117, respectively. Thus, unit point loads were applied to the 10-bay strip FE model and analyzed to represent these respective locations. The mode shapes with responses in these locations can also be compared with measured shapes. Figure 4.25 shows the comparison of Mode 3 with the measured ODS at the dominant frequency of Point 65. Note that the FE model was rotated to reflect its representation of Point 65 and for comparison with the ODS at the 4.875 Hz dominant frequency. Although the ODS used in the comparison was obtained by driving at Point 73, the similarity in shape is apparent by the two corresponding upper bays that are in phase (concave up). This is a promising result because this dominant response shape in the bay containing Point 65 could not be achieved in the full floor model.

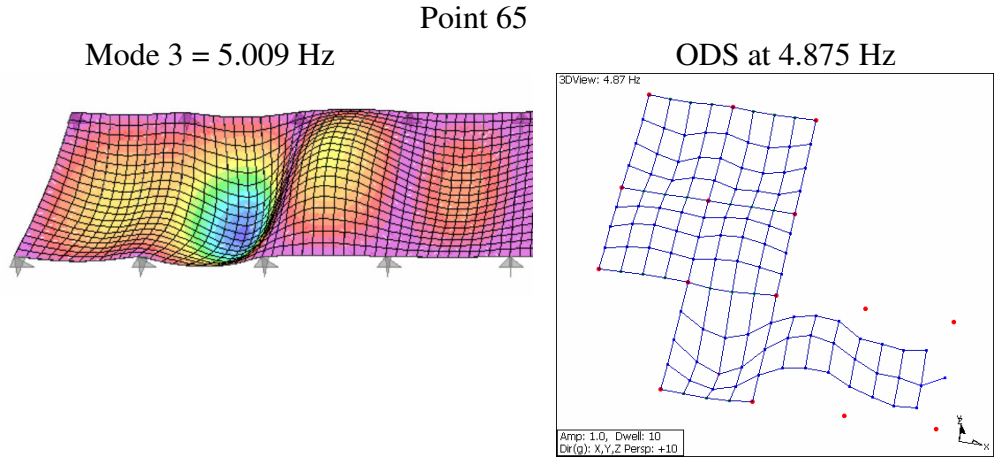

Figure 4.25: NOC VII – 10-Bay Strip Model Mode Shape and ODS Comparison (Point 65)

The computed driving point accelerance FRFs from steady state analysis of the tested bays are presented in Figure 4.26. While the strip model was expected to better represent the response of the bays in the middle of the strip, all of the analyzed bays' computed accelerance FRFs are in better agreement with the measured accelerance FRFs than the corresponding analyses of the full floor model. While the computed peak response magnitude for Point 65 was nearly 25% low using the measured value of damping (37% low for assumed level of damping), the shape of the FRF was much improved in this model. For Point 21, the computed response was essentially the same for the strip model as it was for the full floor model, which is consistent

with the observation that the mode shape is localized to the immediately adjacent bays and thus the bulk of the participating (effective) mass was not removed with the other portion of the floor.

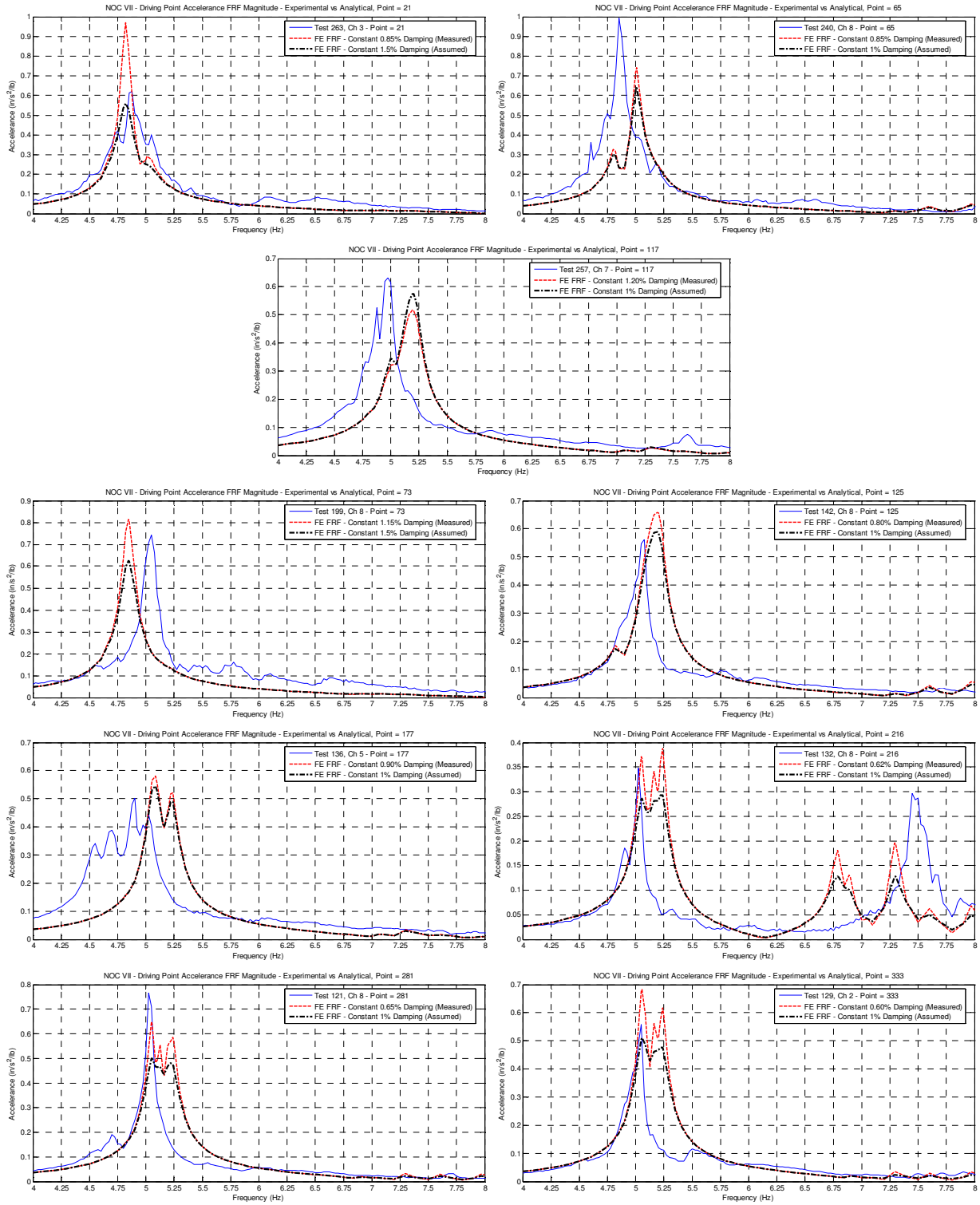

Figure 4.26: NOC VII – 10-Bay Strip Model Accelerance FRFs

The remaining analyzed locations predicted dominant frequencies within 10% of measured dominant frequencies and response magnitudes at the peaks using measured damping values to within 25%. Using an assumed level of damping, the computed peak response values were generally 10-20% low, but not unreasonable considering the smaller values of damping estimated from measurements of the bays along the interior of the strip (0.6-0.9%). It is interesting to note the ability of the model to predict the general shape of the odd multi-mode response for Point 177 and the double curvature mode measured at the higher frequencies in the FRF for Point 216, the only driving point not located at mid-bay. Overall, the reduced strip model provided some very encouraging results for both the recommended modeling techniques as well as the implication that reduced floor models can be effective in adequately predicting the response.

4.2.2 VT KnowledgeWorks 2 Building, VTK2

For the FE model of VTK2, the floor framing geometry was laid out with the steel framing members specified in the design drawings and pinned supports were applied at the column locations. Like NOC VII, a user-defined material (VTK2-VIBCON) and area plate element (VTK2-SLAB) were created to represent the composite slab in the floor model. The input values of these user-defined parameters, and the composite slab properties used in their development, are presented in Table 4.4.

Table 4.4: VTK2 – Composite Slab Parameters and Slab Area Element/Material Properties

Overall Slab/Deck Height:	5.25 in.	Unit weight of concrete, w_c:	115 pcf
Slab height above ribs, d:	3.25 in.	Concrete compressive strength, f'_c:	3000 psi
Deck rib height, d_r:	2.00 in.	Dynamic modulus of elasticity, $1.35*E_c$	2884 ksi
Area weight of steel deck, w_{deck}:	2.4 psf	Superimposed loads, $w_d + w_l + w_{coll}$:	0 psf

User-Defined Material Name:	**VTK2-VIBCON**	User-Defined Area Section Name:	**VTK2-SLAB**
Type of Material:	Isotropic	Type of Area Section:	Plate-Thin
Mass per unit Volume:	2.3869×10^{-7} k-s^2/in^4	Assigned Material:	VTK2-VIBCON
Weight per unit Volume:	9.2156×10^{-5} k/in^3	Thickness (Membrane/Bending)	3.25 in.
Poisson's Ratio	0.2	Stiffness Modifiers:	Bending m11 = 2.88
Additional Material Damping:	None		

A notable difference in the VTK2 floor from the NOC VII floor is the irregular framing in portions of the building. For both the experimentally derived mode shapes and the computed mode shapes it was found that the irregular locations of various columns and offset bays tended to localize the participation of the floor in a given mode to just a few adjacent bays. Slab details and the framing plan of the specified steel sections for VTK2 are found in Appendix A. Plan and 3-D views of the floor model's slab and framing layout are presented in Figure 4.27, including the twelve locations of forced response analysis presented later in this section for comparison with experimental measurements.

Using a slab area element size that was similar to the one used for the NOC VII model gave convergent results. This corresponded to a mesh size of 12x12 elements for interior bays (30 in. x 30 in.) and 12x16 elements (30 in. x 26.25 in.) for exterior bays. Because of the irregular geometry in some areas of the floor and the offset end bays, a few smaller rectangular elements were used in the transition areas. With this configuration, the full floor model contains nearly 3,400 mass degrees of freedom (UZ) (slightly less than half the size of the NOC VII full floor model). The joints corresponding to test locations were renumbered to the pattern shown in Figure 3.52 to ease analysis of results.

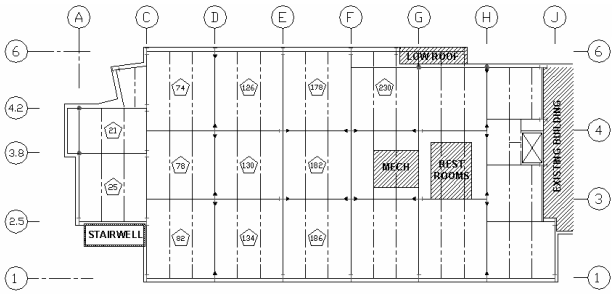

(a) VTK2 Floor Framing Layout (b) FE Model Plan View of Framing & Slab

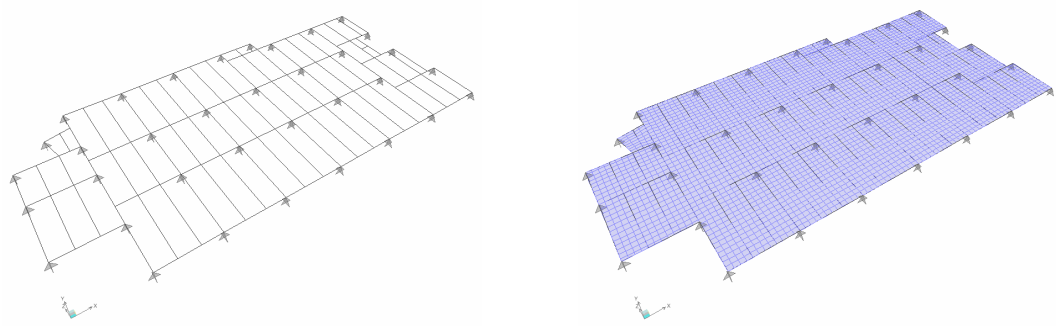

(b) FE Model 3-D View – Framing Only (c) FE Model 3-D View – Framing and Slab

Figure 4.27: VTK2 – Floor Layout and FE Model

The transformed composite moments of inertia were computed for each framing member to determine the baseline stiffness property modifiers, which ranged from 2.5 to 3.8 for the main framing members of VTK2. A full listing of the calculated transformed moments of inertia and their respective baseline (and final) PMs is found in Appendix N. The baseline values were applied as PMs to the strong axis moment of inertia for all framing members, and 2.5 times the baseline values were applied as PMs to all spandrel beams and girders with the exception of the two spandrel members of bay A/C-2.5/3.8. This bay contained Point 25 and was in a stage of construction that essentially left it with two free edges. For this same reason, a smaller assumed damping value of 1% was used for analysis rather than the recommended 1.5% for a corner bay.

Strong axis bending moment releases without any partial fixity were applied to all members framing into the webs of columns, and no moment releases were applied to the beam members that framed into the flanges of columns. For beams framing into the webs of girders, strong axis moment releases with partial fixity values of $6EI/L$ were applied at both ends. No partial fixity values were assigned to beams framing into the webs of girders if there was not a corresponding beam framing into the other side of the beam-to-girder web connection (i.e. representing a loss of continuity and the flexibility of the unsupported girder web). Because of the irregular framing, this condition existed for several joints in the interior of the floor other

than at spandrel beams/girders. The framing layout of VTK2 showing end releases and members with assigned partial fixities is presented in Figure 4.28.

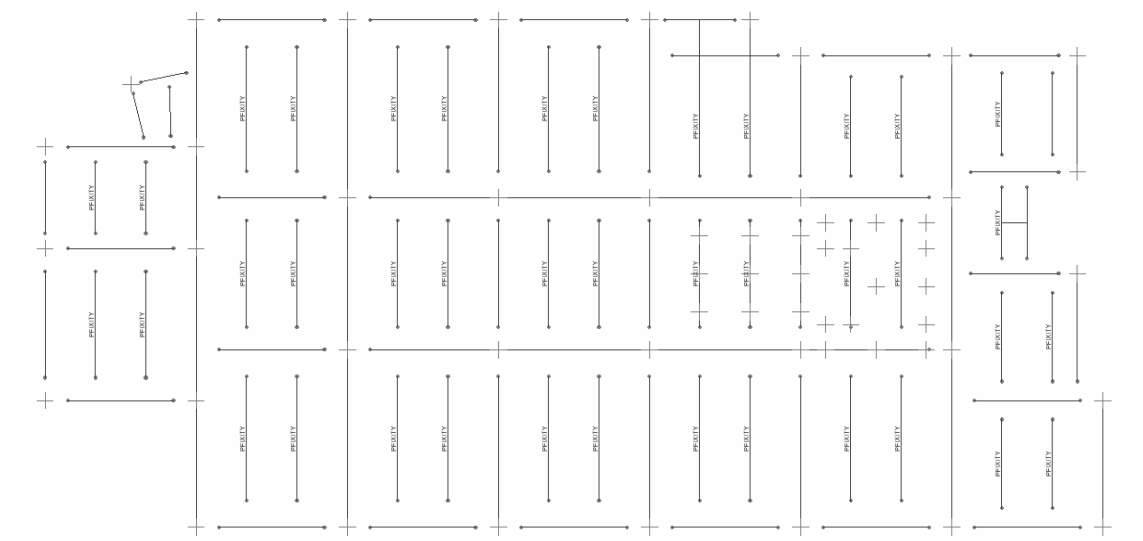

Figure 4.28: VTK2 – Moment End Releases and Partial Fixities

Additional pinned restraints were applied to two interior bays (bays F/G-3/4 and G/H-3/4 in Figure 3.45) to represent the full-height light gage steel stud framing in place above and below the floor at the time of testing (Figure 3.51). The locations of the interior pinned restraints are shown in Figure 4.29. Although the metal stud framing was connected to the underside of the floor using a clip designed to allow vertical movement, the bays with this framing were considerably stiffer. Like the stiffened behavior of the spandrel members that also had similar vertical clips at the slab edges, it is likely that the amplitudes of vibration were not enough to overcome friction at all locations and cause the increased stiffness.

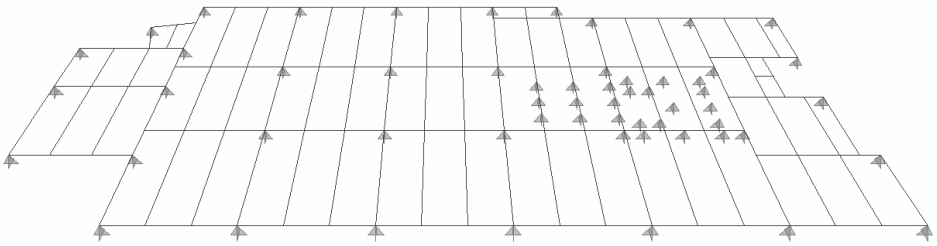

Figure 4.29: VTK2 – Interior Pinned Restraints

It should be noted that pinned supports at the interior locations shown in Figure 4.29 are likely to be much stiffer than the in-situ framing; however they were used in lieu of vertical springs, which more truly reflect the restraint condition in these areas. The use of pinned restraints was justified because formulating a vertical spring value for the light gage framing

would be impractical (and more likely inaccurate) due to variability in construction at that stage of installation and the contribution of friction at the vertical clips. The locations of these interior pins were based on judgment and the layout of the framing. It is likely they provide some degree of over-restraint in those areas that may be reflected in inaccuracies of the mode shapes and frequencies of the adjacent bays. While there is no comparison of accuracy for the untested far end of the floor, the bays most likely to be affected include Points 182 and 230.

The frequencies of the first 20 modes are presented in Table 4.5. It was determined only 20 modes were necessary to capture the dominant shapes of all bays; modes beyond this demonstrated double curvature within a bay. The 13 mode shapes that have a preponderance of participation (say that 10 times fast!) in the tested areas of the floor are presented in Figures 4.30 and 4.31.

Table 4.5: VTK2 – Computed Modes

Mode:	Frequency (Hz)	Mode:	Frequency (Hz)
1	6.535	11	7.725
2	6.689	12	7.795
3	6.772	13	8.024
4	6.867	14	8.129
5	6.870	15	8.399
6	7.055	16	8.509
7	7.200	17	8.659
8	7.295	18	8.828
9	7.307	19	8.936
10	7.387	20	9.152

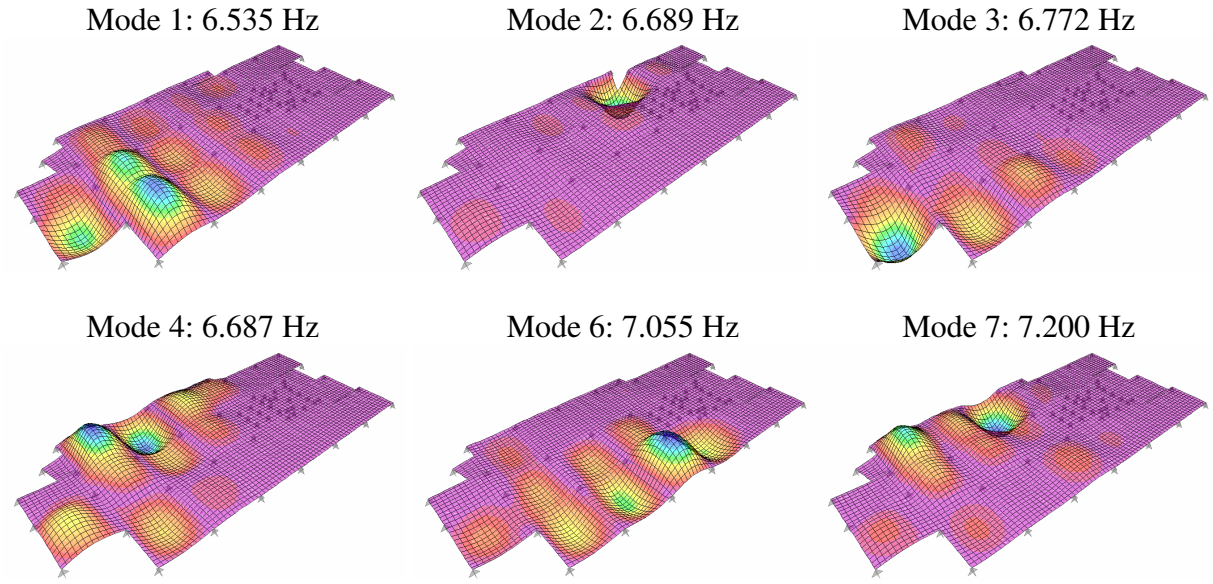

Figure 4.30: VTK2 – Computed Mode Shapes 1-7 (Tested Area of Floor)

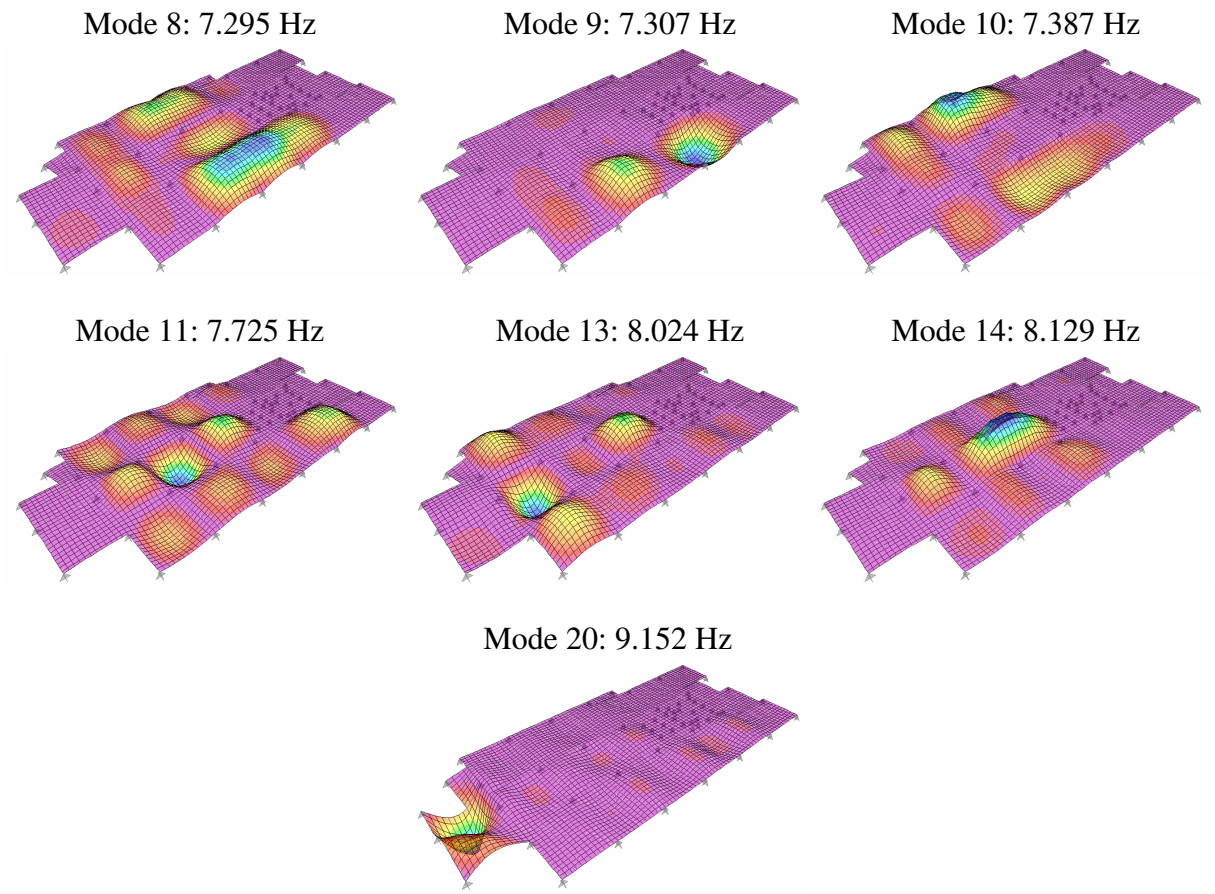

Figure 4.31: VTK2 – Computed Mode Shapes 8-20 (Tested Area of Floor)

In contrast to all but a handful of computed modes for NOC VII, it is interesting to note the localization of response within many of the modes. As previously observed in the NOC VII models, almost every mode has one or two bays with dominant participation, highlighting the dominant or significantly participating frequencies of that location of the floor. These frequencies will be significant or dominant peaks in the computed accelerance FRFs, just as they would from testing an in-situ floor. It is also evident that the irregularity of the framing and the column locations causes what could be considered "complicated" mode shapes, or mode shapes that are not necessarily intuitive or expected. However, when comparing the computed mode shapes to those measured during testing, the validity of many difficult-to-anticipate shapes was confirmed, making a strong argument for additional case studies with high quality modal testing of in-situ floors (or mid-bay testing, at the very least). Because a large area of VTK2 was tested using multiple references, the experimental data was more conducive to curve fitting and extracting quality mode shapes of multiple modes. Access to reliable extracted mode shapes (or high quality ODSs that closely resemble the mode shape near resonance) eases the comparison of

experimental data and computed mode shapes. Seven of the extracted mode shapes from in-situ testing are presented in Figure 4.32 for comparison with the respective computed mode shapes of the FE model. For reference, the area of the floor represented in the presented experimental mode shapes is shown at the top of Figure 4.32.

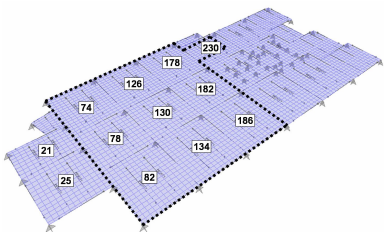

Mode 1: 6.53 Hz | Curve Fit: 6.56 Hz | Mode 4: 6.87 Hz | Curve Fit: 6.98 Hz

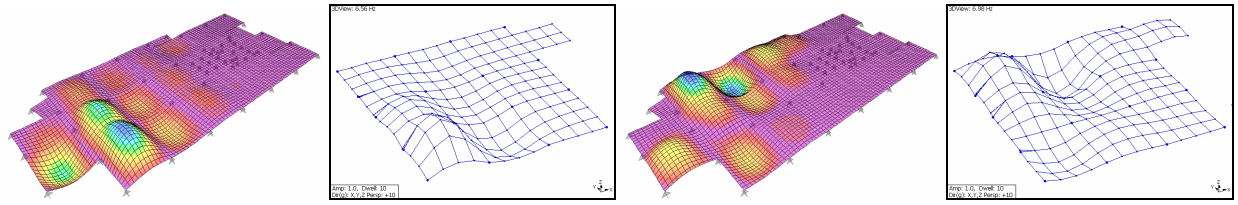

Mode 6: 7.05 Hz | Curve Fit: 7.19 Hz | Mode 7: 7.20 Hz | Curve Fit: 7.30 Hz

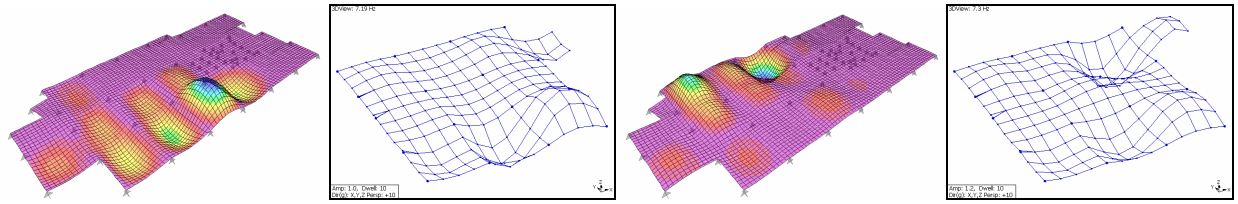

Mode 8: 7.29 Hz | Curve Fit: 7.58 Hz | Mode 11: 7.73 Hz | Curve Fit: 7.97 Hz

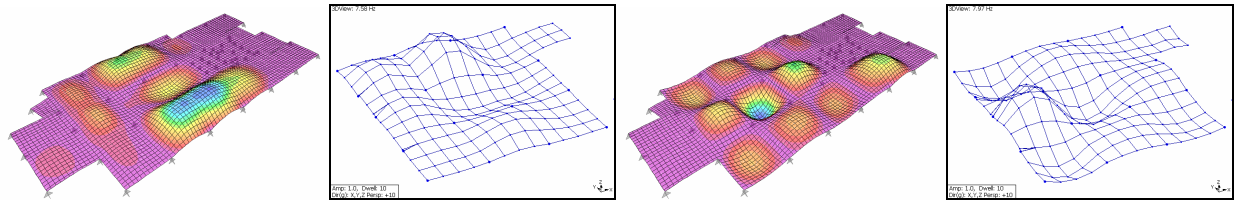

Mode 13: 8.02 Hz | Curve Fit: 8.21

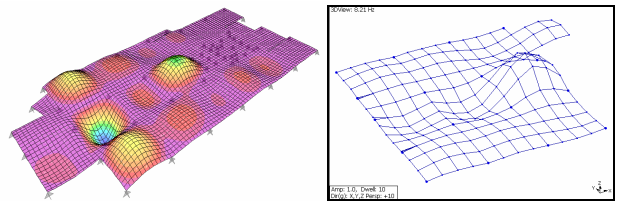

Figure 4.32: VTK2 – FE Mode Shape and Curve Fit Mode Shape Comparison

Although a numerical comparison between the computed and experimental mode shapes was not accomplished, there is exceptional agreement from visual inspection of the seven modes

compared in Figure 4.32. This is a very encouraging result given the simplified approach of many of the applied modeling techniques. Several modes were likely present in the in-situ structure but were not captured from modal testing due to either the lack of adequately exciting the mode at the forcing location or not measuring the area during the modal sweep. The three mode shapes in Figure 4.33 are the computed dominant modes at Points 25, 230, and 21. The computed modes that cannot be remarked upon due to lack of measurement of the far areas of the floor are presented in Figure 4.34.

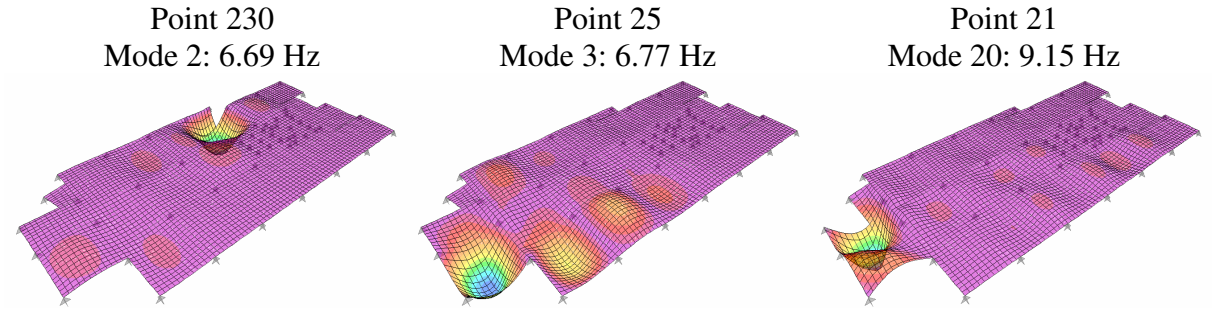

Figure 4.33: VTK2 – Dominant Mode Shapes (Points 25, 230, 21)

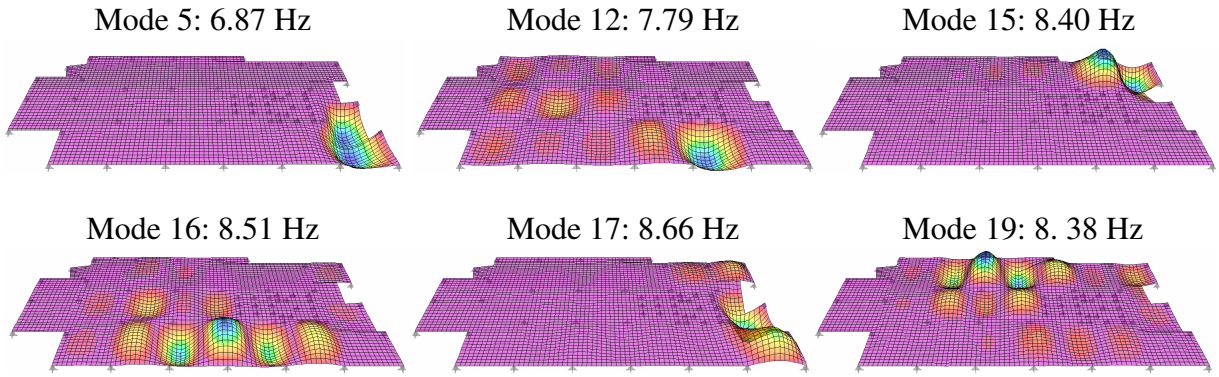

Figure 4.34: VTK2 – Computed Modes (Non-Tested Area of Floor and Double Curvature)

Steady state analysis was performed on the modeled floor for the twelve different unit load locations shown in Figure 4.27(b), each corresponding to a mid-bay driving point location on the floor during modal testing. To correspond with the burst chirp frequency range of the experimental driving point accelerance FRFs, the steady state analyses evaluated response at increments between 4 Hz and 12 Hz with roughly a 0.05 Hz frequency resolution. Steady state analysis was performed twice for each of the driving point locations. In he first analysis, constant damping was specified for all frequencies using measured estimates of damping (estimated at the dominant frequency of the tested bay) and a second analysis using the proposed

damping values for a bare floor based on general bay location (1%, 1.5%, 2%). The points of excitation and each of the two damping ratios used for analysis are shown in Figure 4.35. Note that 1% damping was used for the assumed damping analysis of Point 25. As a corner bay, 1.5% would follow the recommendations; however this bay had two sides that were essentially free edges. This is a good example of how engineering judgment must be applied at several steps in the modeling process to maximize the chances of adequately representing the in-situ behavior.

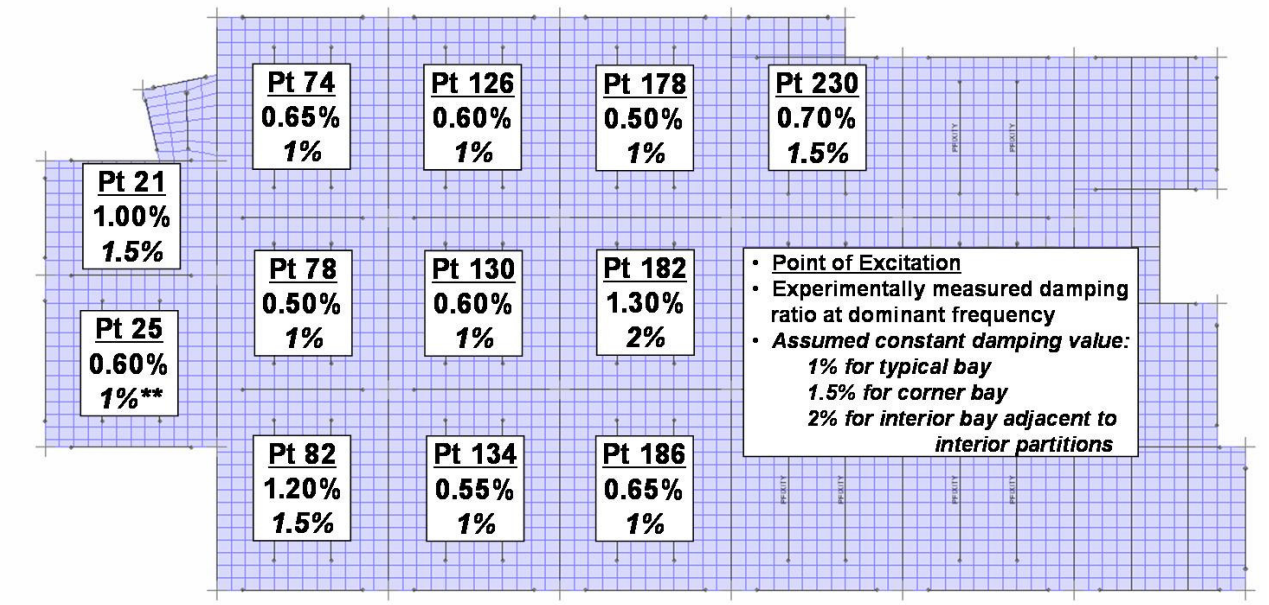

Figure 4.35: VTK2 – Constant Damping Ratios Used in Steady State Analysis

The computed driving point accelerance FRFs for each of the twelve bays analyzed are presented in Figures 4.36, 4.37, 4.38, and 4.39. The accelerance FRFs in these four figures are presented in sets of three to correspond with a three-bay strip along the short direction of the building. Although the computed FRFs are not ideal representations of the measured driving point FRFs, they provide very encouraging results for this floor model and the recommended modeling techniques. The dominant and participating frequencies of nearly all analysis locations are in good agreement with the measured frequencies, which was anticipated from the visual comparison of the computed mode shapes with the experimentally extracted modes shapes. The predicted dominant frequencies of the analyzed bays were all within 5% of the measured dominant frequencies, and half of the analyzed bays were within 1% of measured. For predicted accelerance, however, it was observed that using the measured estimates of damping did not always result in better agreement in the magnitude of the peaks of the accelerance FRFs.

Point 21:

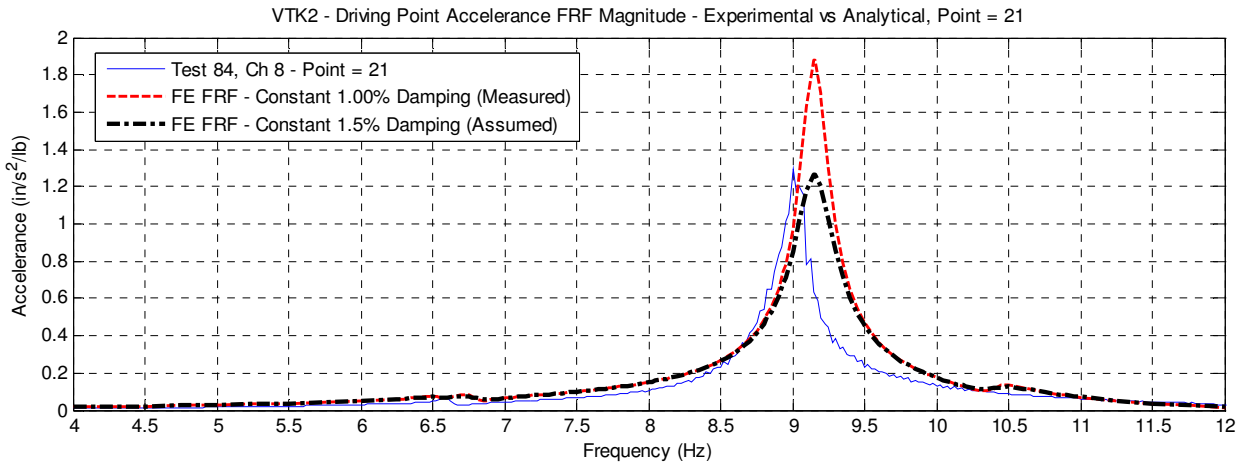

Point 25:

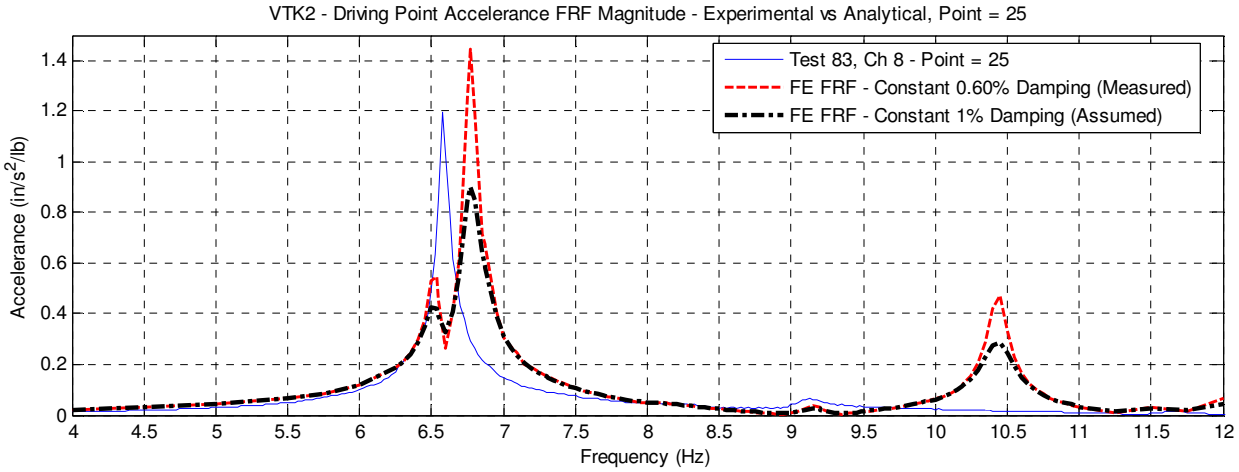

Point 230:

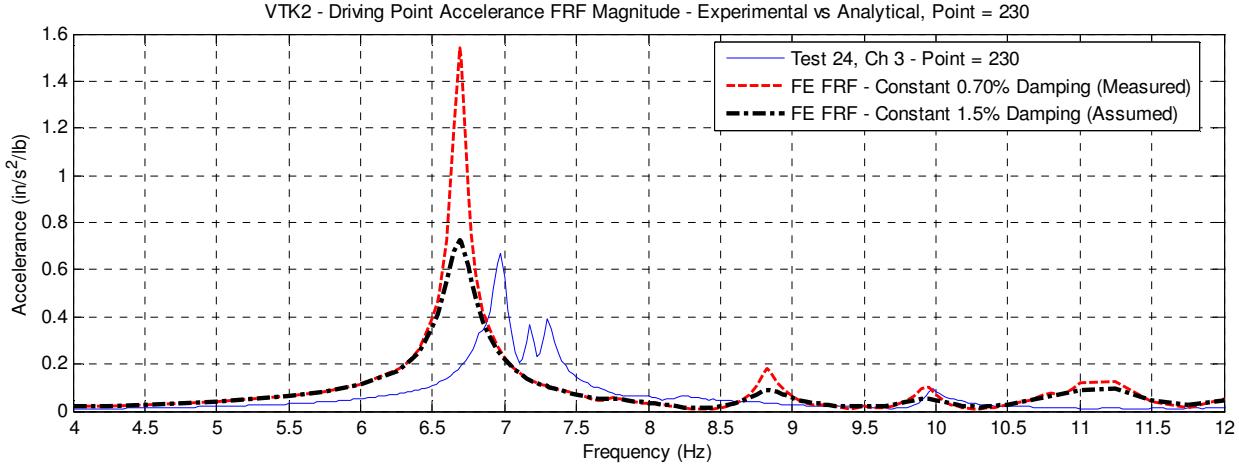

Figure 4.36: VTK2 – Accelerance FRFs (Points 21, 25, 230)

Point 74:

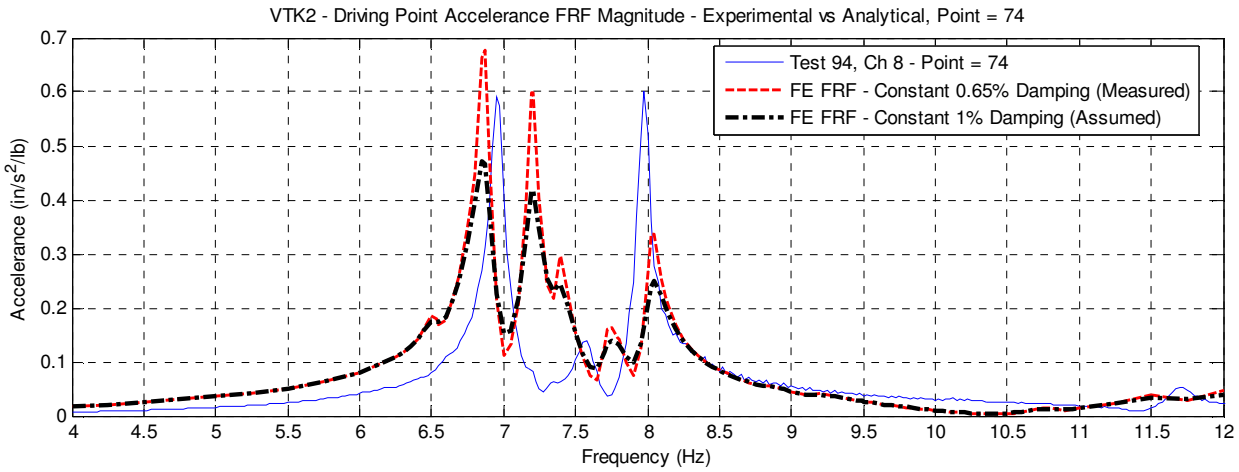

Point 78:

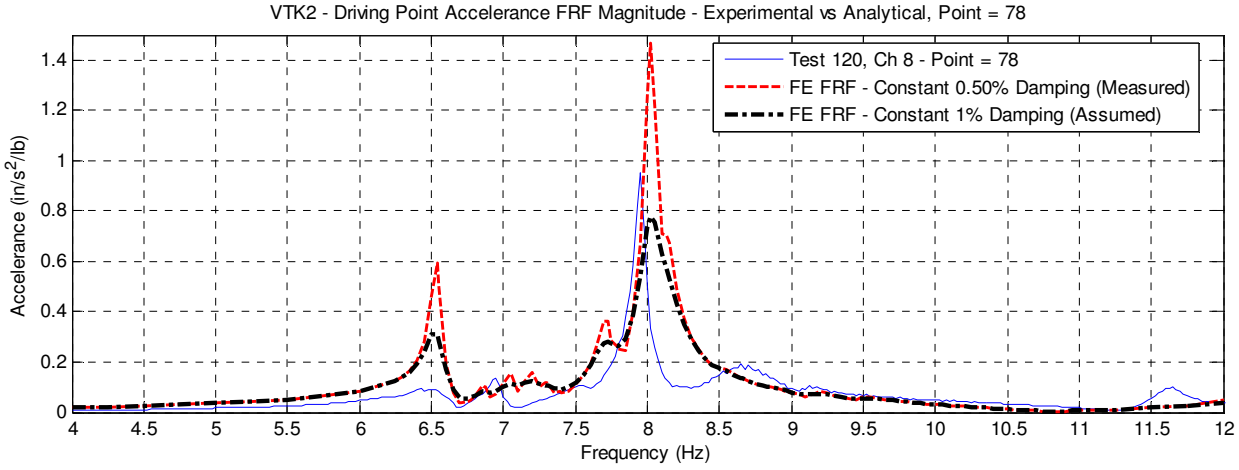

Point 82:

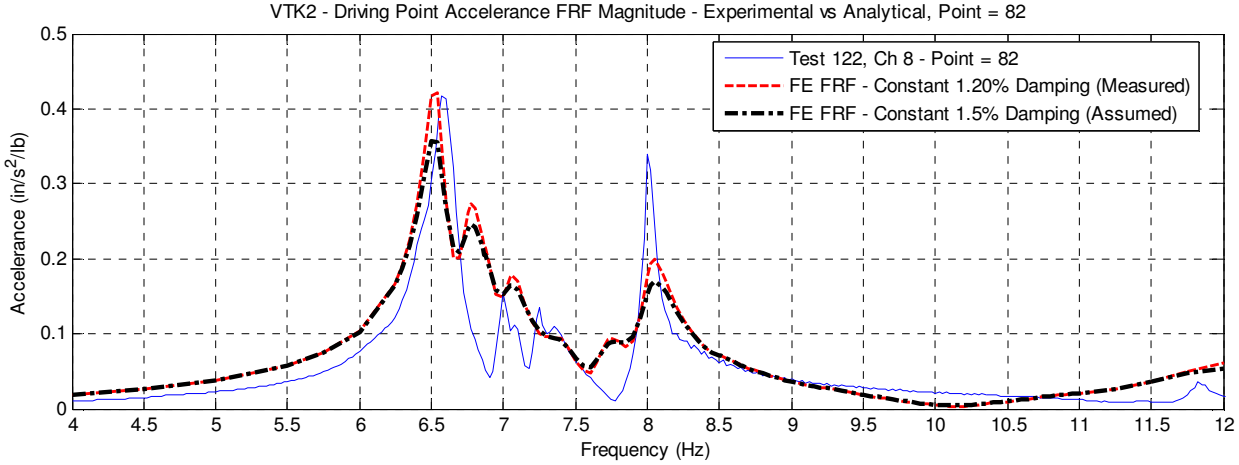

Figure 4.37: VTK2 – Accelerance FRFs (Points 74, 78, 82)

Point 126:

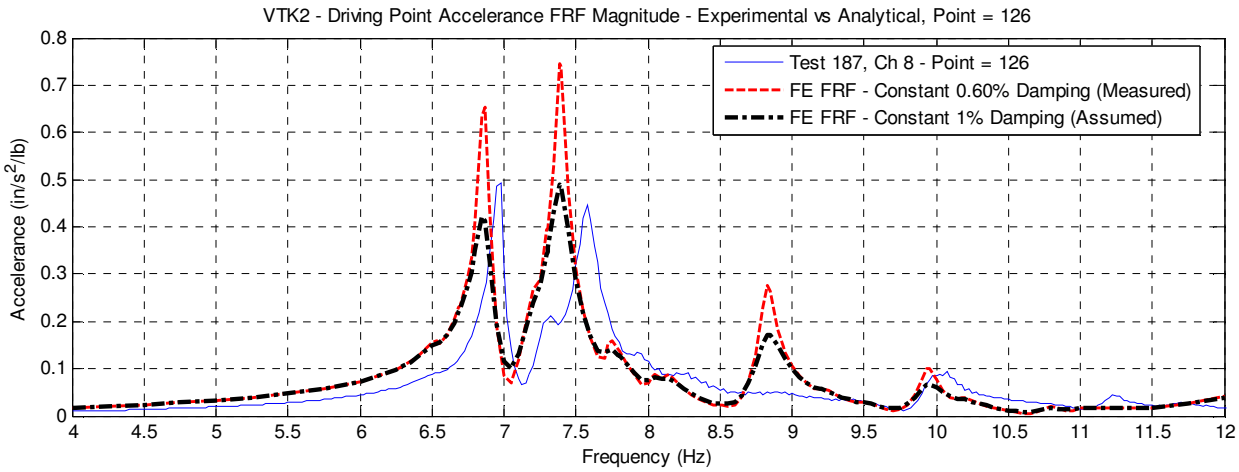

Point 130:

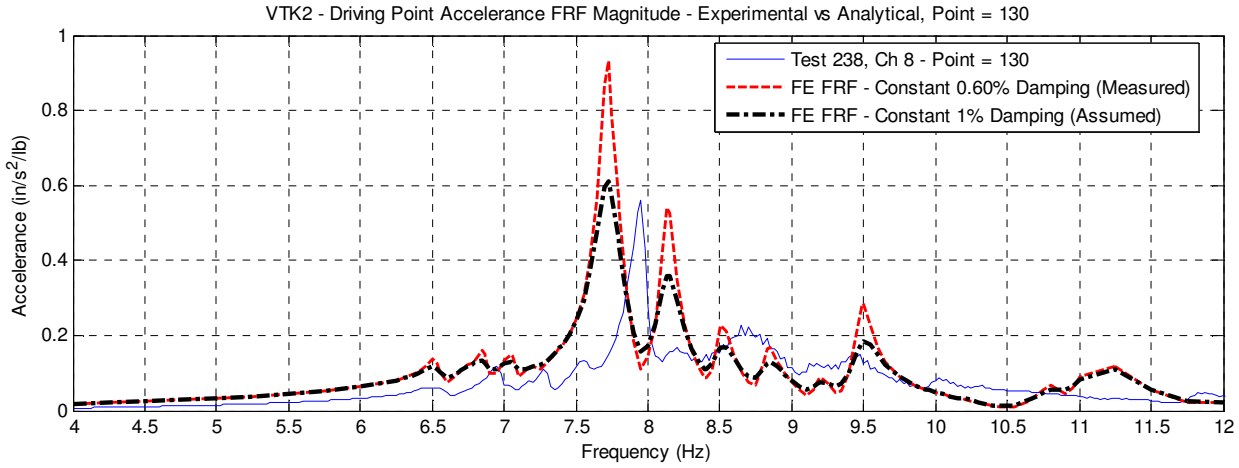

Point 134:

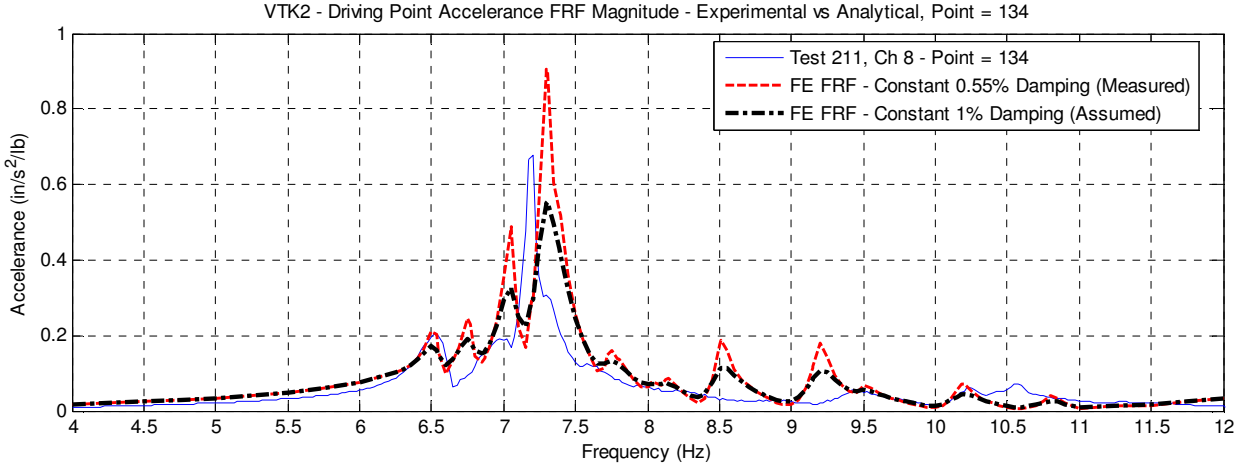

Figure 4.38: VTK2 – Accelerance FRFs (Points 126, 130, 134)

Point 178:

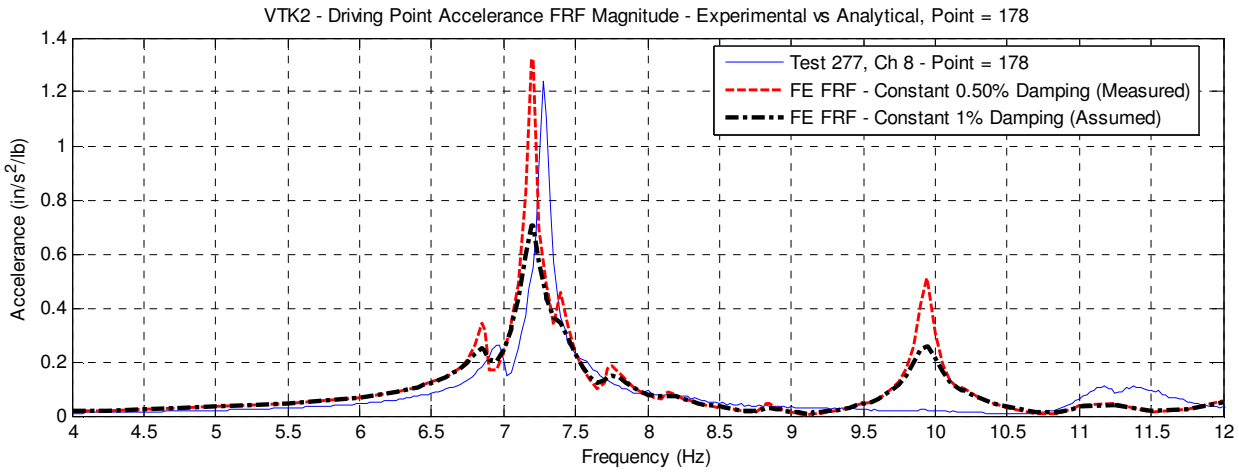

Point 182:

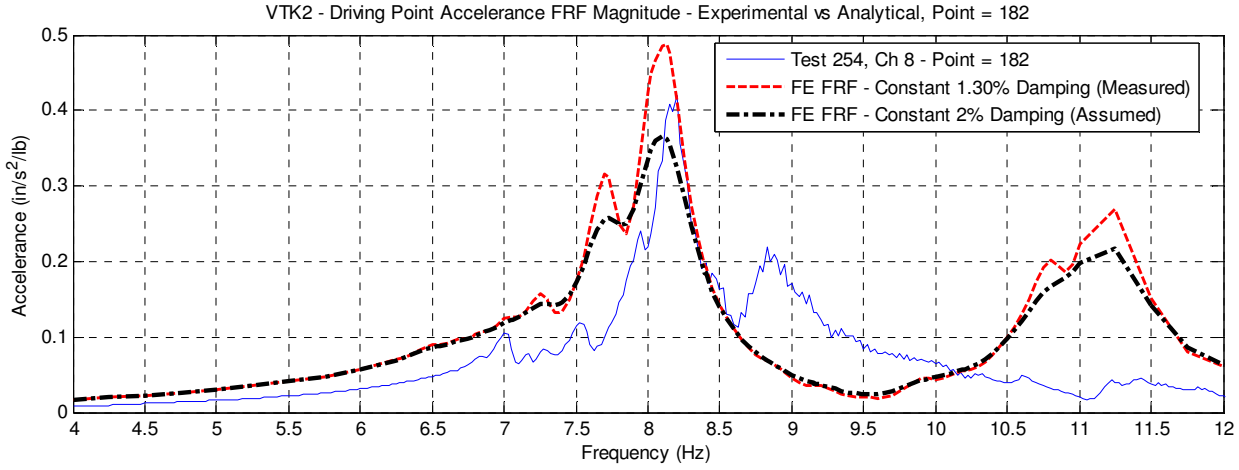

Point 186:

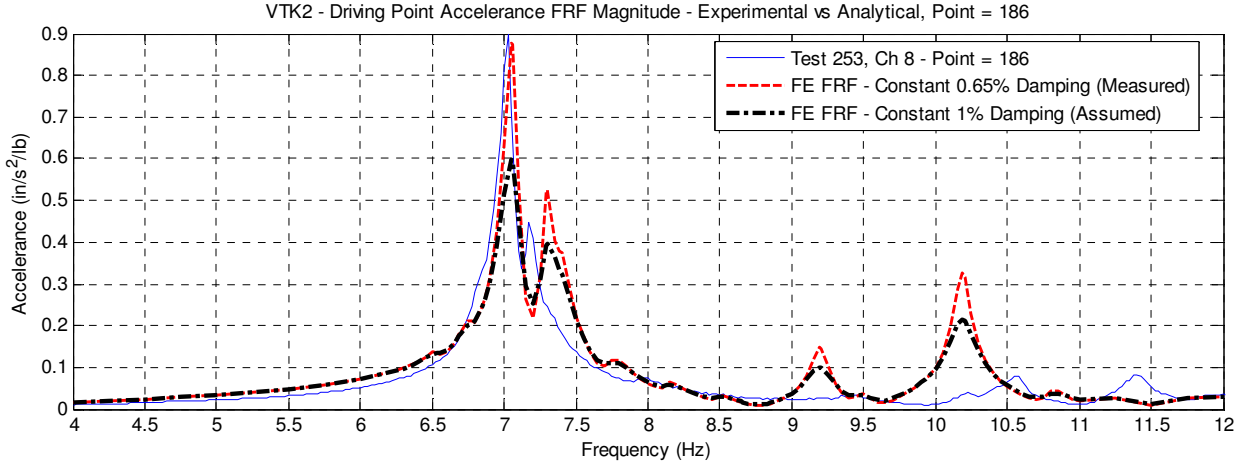

Figure 4.39: VTK2 – Accelerance FRFs (Points 178, 182, 186)

Using the measured estimates of damping, the FE steady state analyses predicted peak accelerance values (at the dominant frequency) higher than measured values in all but one of the twelve analyzed bays. Additionally, six out of the twelve bay analyzes predicted a peak accelerance within 25% of measured, although the computed accelerance for three of the bay analyses exceeded the measured value by over 50%. The substantial disagreements in magnitude for these three dominant peaks are likely attributed to an overly localized response, which translates into a smaller effective mass for that mode. The effective mass of a mode is inversely proportional to the acceleration response at resonance, hence the overestimation of the peak. Using assumed values of damping in the analyses, all but one of the twelve bay analyzes underestimated the peak accelerance value at the dominant frequency; however, ten of the twelve bay analyses predicted values within 25% of measured while the other two were within 50%.

Although there is admittedly room for refinement to the proposed modeling techniques, the encouraging results presented in this section demonstrate that steel composite floor systems can be modeled using a set of fundamental techniques where the resulting dynamic analyses adequately represent the behavior of an in-situ floor. Other encouraging results demonstrated that partial floor models developed with the recommended techniques can also provide a good representation of in-situ behavior. This is beneficial because creating a detailed finite element model of an entire floor system can be excessive and costly, especially if only a portion of the floor requires modeling for purposes of an adequate evaluation. The computed mid-bay accelerance FRF is the cornerstone of analysis using the FE method because of its ability to represent all important dynamic characteristics of the most vulnerable portion of a floor. It also remains an invaluable tool for validating an FE model because of its ability for direct comparison to mid-bay driving point measurements of in-situ structures.

4.3 Summary of Recommended FE Modeling Techniques for Composite Floors

This section serves as a consolidated summary of the recommended modeling techniques presented in Section 4.1 and applied to the two tested in-situ floor models in Section 4.2. The recommended techniques are presented in bullet format and follow the same order as the six *general* steps of creating an FE model of a floor system for evaluation of vibration serviceability that were presented in Section 4.1; that is,

1) Lay out the floor geometry using the design specified steel framing members for the beams and girders and apply vertical restraints at the location of the columns.
2) Define area elements and materials to represent the composite slab and apply the slab area elements to the model.
3) Adjust model to adequately reflect mass and stiffness (releases, restraints, PMs, etc.).
4) Perform modal analysis on the FE model to compute the frequencies and mode shapes.
5) Specify damping in the model.
6) Apply dynamic loads and perform forced response analysis for use in evaluation of vibration serviceability.

Mass & Materials

- Lay out the geometry of the steel floor framing in the XY-plane using the predefined frame elements in the FE program that correspond to the steel sections of the design drawings. Use centerline dimensions.
- Apply translational (vertical) restraints at all column locations.
- Create a user-defined isotropic material, and specify the modulus of elasticity to reflect the dynamic modulus of elasticity of concrete ($1.35*E_c$ as computed by Equation (1.6)). Specify weight and mass densities of the material as computed using Equations (4.1) and (4.2) to account for the composite slab and superimposed loads, and specify a Poisson's ratio of 0.2.
- Create a user-defined thin-plate area element to represent the composite slab. Assign the user-defined concrete material to the element and input a plate thickness equal to the depth of the slab above the deck ribs. Determine the bending stiffness property modifier (PM) to represent the orthotropic stiffness of the corrugated slab by computing the ratio of strong-to-weak direction moments of inertia of the slab. Assign this PM to the appropriate plate bending moment direction (this will be based on the element's local axis).

- Apply the slab area elements to the model in the same plane as the steel framing members. Mesh the slab area elements over the floor system attempting to keep the element aspect ratio close to unity. Use at least twelve elements along the length of a bay, but slab area element sizes of 26 in. to 30 in. along each side will generally give convergent results. Using a finer mesh is acceptable but will be computationally more expensive.
- Ensure framing members are auto-subdivided along their lengths corresponding with the slab mesh size to ensure connectivity to the slab and adequate distribution of mass.

Stiffness and Boundary Conditions

- Compute the transformed composite moments of inertia for all framing members using DG11 fundamentals. Using the computed moments of inertia, calculate the respective *baseline* PMs for the framing members. When computing the PMs for members parallel to the deck ribs, account for the orthotropic bending stiffness PM assigned to the slab area elements.
- Apply the computed baseline PMs to all interior framing members and 2.5 times the baseline PMs to all spandrel members that are not free edges. Use the baseline PMs for free-edge spandrel members. Exercise engineering judgment on other members of the floor that may justify an increased stiffness PM, such as members adjacent to full-height interior partition walls or elevator cores.
- Release the strong-axis end-moment of all beams and girders framing into a column web.
- Do not assign a moment end release for any beam or girder connected to a column flange, regardless of whether it is part of a moment frame or not.
- Release the strong-axis moment in all beam-to-girder web connections that are not restrained on the other side by another member (e.g. framing into spandrel girders).
- Release the strong-axis moment and assign a partial fixity for all continuous beam-to-girder connections. Use a partial fixity rotational spring value equal to $6EI/L$, where EI/L is determined using the connecting members properties.
- Using engineering judgment, apply pinned restraints where appropriate to simulate unknown contributions of stiffness from interior partitions or interior/boundary conditions.
- In general, over-restraint of the floor using excessive numbers of interior pinned restraints, rotationally restrained degrees of freedom, or very high stiffness property modifiers does not produce good results. When in doubt, leave the model flexible in areas of unknown restraint.

Modal Analysis and Steady State Analysis

- Ensure all dynamic analysis is performed with the structure analyzed as a plane grid (UZ, RX, and RY are the available DOFs), with UZ the only translational mass DOF.
- Perform an eigenvector modal analysis to compute the frequencies and mode shapes. To determine the range of the frequencies of interest for the modeled floor, adjust the number of modes to be computed to account for all modes with single curvature within a bay.
- Apply mid-bay unit loads at all bays of interest (separate load cases for each).
- Generate separate steady state analysis cases for each bay to be evaluated and assign the respective mid-bay load case.
- Determine the frequency range of interest and the frequency increments for the steady state analysis. A frequency resolution of 0.05 Hz or finer is recommended. Include the frequencies from the modal analysis case to ensure the peak response is computed.
- Determine the assumed level of damping for each steady state analysis case based on the bay's location. Recommended levels of damping for bare floors are 1% for typical bays, 1.5% for corner bays (two exterior boundaries), and 2% for interior bays that are adjacent to interior framing. For occupied floors, assume 3% for all bays.
- For each steady state analysis case, input the assumed (or measured) level of damping as constant hysteretic damping for all frequencies. Constant modal damping is approximated by specifying the mass proportional coefficient as zero and the stiffness proportional coefficient as twice the modal damping ratio (i.e. for the assumed levels of damping for bare floors, the ratios would be 0.02, 0.03, and 0.04).
- Perform the steady state analysis and interpret the results. The most informative results are the computed driving point accelerance FRFs. Other available evaluation tools include the floor's computed operating deflection shape at resonance (very close to the computed mode shape only in actual displacement units) and envelope contour plots showing the maximum computed response at any frequency across the area of the floor.

4.4 Floor Vibration Serviceability Evaluation Using the Finite Element Method

The following section proposes a method for evaluation of vibration serviceability using the mid-bay driving point accelerance FRFs of a floor. In its most basic form, the method proposes using a *design accelerance curve* to represent a limit of vibration serviceability, and thus the peaks of an accelerance FRF for a floor must fall below the design accelerance curve to be considered acceptable. While the focus of the proposed method in this section uses the *computed* mid-bay accelerance FRFs from forced response analyses of a floor's FE model, the method is also applicable to evaluation of existing floors using *measured* mid-bay accelerance FRFs, allowing instant evaluation with field measurements. It should be noted that only the fundamental premise of the method is presented in this research, and it is neither in a final form nor validated by any case studies of floors with known serviceability problems. Efforts to identify a final form are left for future research endeavors; however the strength of the proposed method of evaluation lies in its ability to be verified with field measurements and its potential for automation within an FE program. Ideally, the form of a design accelerance threshold would be based on a database of high-quality accelerance FRFs measured from both acceptable floors and problem floors, allowing researchers to hone in on a form that is statistically significant. Unfortunately, as mentioned in Chapter 1, there is currently a very limited database of these types of measurements in the published literature, with this document possibly representing the most comprehensive listing of mid-bay driving point accelerance measurements for in-situ floors. In the absence of a significant database of measured accelerance FRFs and their corresponding subjective serviceability evaluations (human surveys of whether the floor is acceptable or unacceptable), a suggested form should be based on current practice of floor vibration evaluation. A source for this practice is the current design guidance used for serviceability evaluation. In the following section, a proposed design accelerance curve is presented based on DG11 fundamentals, although other design/evaluation methodologies are briefly discussed for reference on how their fundamentals could be adapted to develop similar design accelerance curve(s).

As mentioned in Section 1.1, the various design guidance and codes currently in use around the world address vibration serviceability in the same general manner:

1) Estimate the dynamic properties of the floor.
2) Estimate a dynamic loading to simulate the forces applied from human activities.

3) Compute the acceleration response of the floor for comparison with an established level of acceptability.

The two leading publications presently used for evaluation of vibration serviceability for walking excitation are the *AISC/CISC Steel Design Guide Series 11: Floor Vibrations Due to Human Activitie*s (Murray et al. 1997), which is used extensively in North America, and the Steel Construction Institute (SCI) *Design Guide for Vibrations of Long Span Composite Floors* (Hicks et al. 2000), which is often followed in the United Kingdom. Both publications offer simplified methods for manually computing the dynamic properties of fundamental frequency and effective mass/weight of the floor and provide recommended values of damping. Both publications recognize the complexity of representing the forces from human activities such as walking and take the approach of representing this complex loading as a Fourier series of the harmonics of footfall frequency. Lastly, using the computed properties of the floor and assumed loading, the publications compute an acceleration response to compare to acceptability criteria. For office floors, the acceptability criteria suggested by DG11 is a constant 0.005g for frequencies between 4 Hz and 8 Hz, whereas SCI allows for three different tolerance thresholds depending on a busy/general/special office occupancy condition. As discussed in Section 1.3.2, a notable difference in the two evaluation methods is in the recommended Fourier coefficients for the harmonics of step frequency. While each method recognizes a stepped nature of the dynamic load coefficients within certain frequency ranges (corresponding to the various harmonics of step frequency) DG11 offers a simplified exponentially decreasing term, $0.83exp^{-0.35f}$, and the SCI method remains as stepped values. Young (2001) analyzed extensive footfall data and developed linear functions within each harmonic, which are still stepped in nature but with a slight upward slope. This form of the dynamic load coefficients was incorporated into more recent methods of evaluation that have been presented by Arup (Willford et al. 2006). The Arup method includes a more complex computation of acceleration response that includes the mode shape and off-resonant response in its formulation. Willford presents a reduction factor to be applied to the computed acceleration to account for not achieving full steady state response. This reduction accounts for two phenomena: an individual walks *across* the bay rather than exciting it sinusoidally at its anti-node, and a floor with a low level of damping may not undergo enough loading cycles to achieve steady state. While a similar reduction factor is included in the DG11 method of evaluation (R=0.5), the Arup method directly includes the bay dimensions, stride

length of an individual, and damping ratio. The computed acceleration using DG11 or SCI applies for a single fundamental frequency used in analysis and no other consideration is given for the response at (or contribution from) other frequencies. In this respect, using the accelerance FRF differs because it describes the response (and allows evaluation) over a range of frequencies and includes the contribution of other modes.

The fundamental premise of the proposed evaluation method, and its ability to represent the computed acceleration response of a floor and a level of serviceability over a range of frequencies, is the accelerance frequency response. The value of accelerance is best described by its definition as a *measured* quantity:

$$\frac{\underline{Measured}\ \text{Accelerance}}{\text{FRF Magnitude}} = \frac{measured\ \text{steady state acceleration response}}{measured\ \text{input force}} \tag{4.5}$$

Equation (4.5) states the magnitude of the measured accelerance at a given frequency is equal to the magnitude of the measured steady state response divided by the magnitude of the input force. Because current design guidance defines a steady state acceleration limit for human comfort and estimates the applied loading from walking excitation as a steady state harmonic force, a *design* accelerance magnitude is defined:

$$\frac{\underline{Design}\ \text{Accelerance}}{\text{FRF Magnitude}} = \frac{design\ \text{acceleration limit for human comfort}}{design\ \text{input force}} \tag{4.6}$$

Although the design acceleration limit is typically taken as a constant value over the frequency range of interest, the accelerance FRF is a function of frequency and does not require a constant acceleration threshold for all frequencies. The input force from walking excitation is generally considered a function of frequency and the magnitude of the simulated sinusoidal force is based on the harmonic of walking that will likely correspond with frequency of the floor. Thus, the design accelerance curve, $A_o(f)$, is defined in general terms as

$$A_o(f) = \frac{design\ \text{steady state acceleration limit}}{design\ \text{sinusoidal input force due to walking}} = \frac{a_o(f)}{F(f)} \quad \text{(acceleration units)} \Big/ \text{(force units)} \tag{4.7}$$

Using this form, the design accelerance curve can easily accommodate the suggested acceleration limits and effective harmonic force representation of walking excitation from DG11:

$$A_o(f) = \frac{a_o}{R\alpha_i P} = \frac{a_o}{P_o e^{-0.35f}} = \left(\frac{a_o}{P_o}\right) e^{0.35f} \tag{4.8}$$

where

$A_o(f)$ = design accelerance limit in units of acceleration per unit of input force

a_o = acceleration limit for human comfort, $0.005g$ $(1.93\ in/s^2)$ for office floors

$\alpha_i = 0.83e^{-0.35f}$ (DG11 simplified dynamic load coefficient)

P = person's weight (taken as 157 lbs for DG11)

R = reduction factor (taken as 0.5 for office floors in DG11)

$P_o = 0.83RP = (0.83)(0.5)(157\ lbs) = 65\ lbs$ when R=0.5 is used, otherwise $130R\ lbs$

Although the variables a_o, R, and $\alpha_i P$ in the basic expression of Equation (4.8) are from DG11, they represent the general terms used in all of the evaluation methods (acceleration limit, reduction factor, and effective forcing amplitude, respectively). Using DG11 values to evaluate the expression, a final form of the design accelerance curve for a reduction factor $R = 0.5$ is:

$$A_{o,R=0.5}(f) = \frac{a_o}{R\alpha_i P} = \frac{0.005g(386\ in/s^2/g)}{(0.5)(0.83e^{-0.35f})(157\ lbs)} = \left(\frac{1.93\ in/s^2}{65\ lbs}\right)e^{0.35f} = 0.02969e^{0.35f}$$

or

$$A_{o,R=0.5}(f) \cong 0.03e^{0.35f} \quad \Big/_{lb\text{ of input force}}^{\left(in/s^2\right)} \tag{4.9}$$

The acceleration limit a_o and forcing terms $\alpha_i P$ are based on established theories of human tolerance to vibration and the effective harmonic force due to walking, however R represents a catch-all reduction factor used to account for less-than-full steady state resonant response and because the individual walking and the individual subject to vibration are not located at the point of maximum response within a bay. The subjective nature of its suggested value means that other values of R may be considered in determining a final form of a design accelerance curve. The design accelerance curve of Equation (4.9) for R=0.5 is plotted in Figure 4.40 along with other values of R to illustrate the effect on using a different reduction factor.

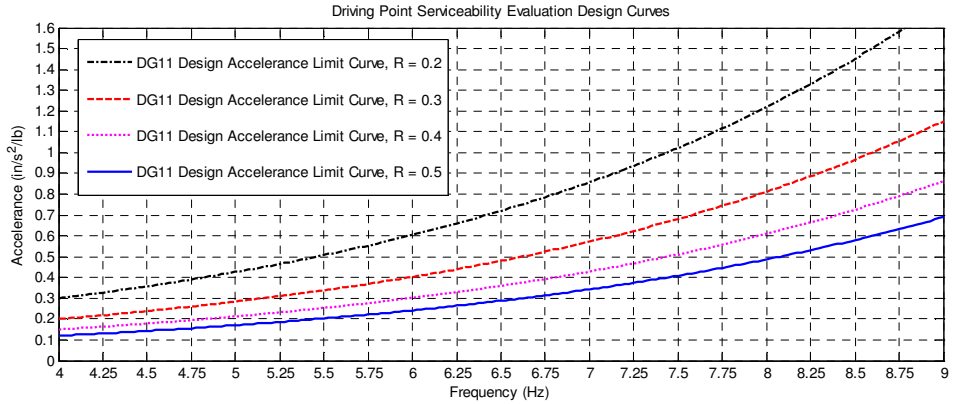

Figure 4.40: Proposed DG11 Design Accelerance Curves for Different Reduction Factors

Note that the design accelerance curves in Figure 4.40 are plotted from 4 Hz to 9 Hz, which corresponds with the lower 0.005g plateau in Figure 1.1, the figure illustrating the recommended peak accelerations for human comfort for vibrations due to human activities. The simplified dynamic load coefficient term used by DG11 makes each design accelerance curve a smooth increasing exponential. The other methods of evaluation offered by SCI and Arup use a stepped dynamic load coefficient (or stepped function with slight slope), and thus the form of the design accelerance "curve" would also be stepped. The reduction factor included in the Arup method would be computed for each analyzed bay because it is based on damping and the bay dimensions. Thus, the Arup design curves for each analyzed bay would shift up or down depending on the computed reduction factor. Although specific terms of the other methods differ from DG11, they are only highlighted to demonstrate that they are not insurmountable for developing a design accelerance curve based on the evaluation method fundamentals.

A demonstration of the proposed method for evaluation is made using the design accelerance curve for R=0.5 shown in Figure 4.40 and the VTK2 FE model presented in Section 4.2.2. The development and analysis of the FE model presented in that section comprise the first step in the proposed evaluation process, simply modeling the floor assuming bare conditions. This floor was modeled assuming a bare floor condition with no superimposed loads and was analyzed using the recommended damping values for a bare floor (1%, 1.5%, and 2% depending on bay type). Although the acceleration response is the critical parameter for evaluation, there are other modeling results that provide insight on the predicted performance of the floor. Modal analysis of the bare floor system indicates both frequency content of the floor as well as the general shapes of expected modes. For the bare condition VTK2 FE model, the lowest computed frequencies were 6.5-7.0 Hz, a bit high for floors that historically have shown serviceability problems. The frequencies of a floor will decrease with superimposed load, thus if the computed bare floor frequencies are initially low (4-5 Hz), this may indicate a potential problem floor early in the design process. Additionally, examining the mode shapes of the bare floor model also provides preliminary evaluation, as certain mode shapes may indicate problem areas of the floors at certain frequencies. These "soft spots" (very localized mode shapes) may result in large accelerance values at resonant frequencies due to the smaller effective mass of the mode. Performing a forced response steady state analysis of the floor at each mid-bay location will give an overall idea of the performance of that area of the floor. Analysis of the bare floor does not

have much relevance for comparison to recommended design accelerance values because it is unlikely that the floor is occupied in such a condition. The performance of the occupied condition is of the most interest for evaluation, however the computed accelerance FRFs of the bare floor (with the smaller assumed damping values) are important because they highlight dominant and significantly participating frequencies/modes. At higher levels of damping, many of these peaks will be smoothed out and difficult to distinguish. (However, on the usefulness of bare floor FE models, a bare floor is a much more likely condition for the acquisition of field measurements for validation of an FE model).

The second step in the evaluation process is to adjust the bare floor model to reflect the occupied condition. To simulate the increased load of an occupied condition, superimposed loads of 4 pounds per square foot (psf) of dead load and 6-11 psf of live load are assumed (Murray et al. 1997). This superimposed load is applied to the model by re-computing the weight and mass densities of the slab user-defined material using Equations (4.1) and (4.2). The mass density, assuming a live load of 11 psf, and the first 10 computed frequencies of the occupied floor model are listed in Table 4.6 for comparison with the mass density and frequencies of the bare floor model.

Table 4.6: FE Serviceability Evaluation Example – Change in Computed Frequencies

VTK2 Bare Floor		VTK2 Occupied	
Mass Density:		Mass Density:	
2.3869x10-7 k-s2/in4		3.2171x10-7 k-s2/in4	
Mode:	Frequency (Hz)	Mode:	Frequency (Hz)
1	6.535	1	5.699
2	6.689	2	5.828
3	6.772	3	5.901
4	6.867	4	5.983
5	6.870	5	5.991
6	7.055	6	6.155
7	7.200	7	6.281
8	7.295	8	6.358
9	7.307	9	6.371
10	7.387	10	6.442

A superimposed load is assumed to add mass to the system and not stiffness. For a typical steel composite floor, the slab will be 80-90% of a floor's mass, with the remainder belonging to the steel framing members (for the bare VTK2 model in this example, the slab elements were 86% of the floor's total mass). Thus, any increase in the mass density of the slab material to account for superimposed load will effectively be a uniform increase in the total

system mass. As a result, the shape and order of all mode shapes will not change but their respective frequencies will decrease, as will the acceleration response due to an increase in effective mass. Note this only holds true for the addition of a superimposed load. An increase in slab thickness must be accounted for in the mass *and* stiffness of the slab as well as a corresponding increase in composite stiffness of the steel framing members.

For the provided example, a forced response steady state analysis was conducted on the mass density-adjusted model at the mid-bay location of Point 82 assuming an occupied condition damping value of 3%. This location was originally analyzed with an assumed bare floor damping value of 1.5% (corner bay). A comparison of the two computed accelerance FRFs is presented in Figure 4.41. As expected, the peaks of the accelerance FRF shift to reflect the decrease in frequencies due to the applied superimposed load. The increased level of damping smoothes out all but two dominant peaks, and the peak accelerance values decrease due to both the higher damping and the increase in mass. Using DG11 as a basis for evaluation, the design accelerance curve for an office floor (R=0.5) is plotted along with the two computed accelerance traces. The most important comparison in Figure 4.41 is the peak magnitude of the occupied floor model's computed accelerance FRF in relation to the design accelerance curve. For this example, the peak at 5.70 Hz dominant peak is 0.17 in/s^2/lb of input force, below the 0.22 in/s^2/lb design curve value. Because the computed peak accelerance was less than the design accelerance curve, this bay would be considered acceptable for vibration serviceability using the proposed method of evaluation.

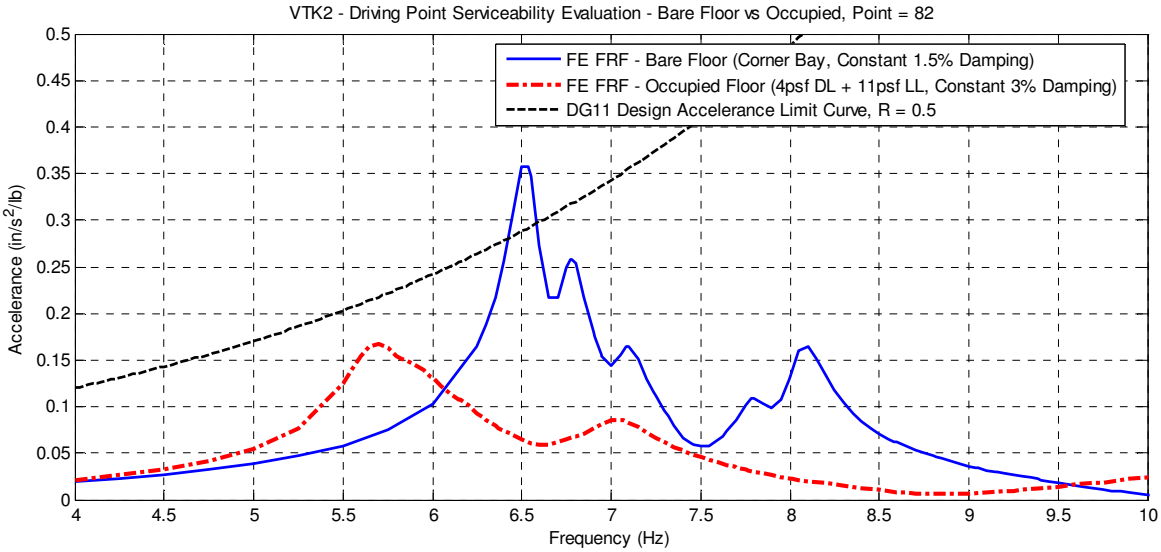

Figure 4.41: FE Serviceability Evaluation Example – Accelerance FRFs and Design Curve

Note that the comparison of this single peak accelerance value to the design accelerance curve is equivalent to the single frequency response computation of DG11 with one exception: the bay's dominant frequency and effective weight were calculated within the FE model rather than using DG11's simplified methods. The availability of the peak response of all participating modes over the frequency spectrum is advantageous, particularly if an analyzed location has multiple significant peaks, which was observed for some locations of the tested in-situ floors. Additional advantages of using the finite element method for evaluation of vibration serviceability are that the predicted frequencies of simplified methods often do not account for the effect of non-standard conditions such as different beam sizes between columns, increased stiffness at boundaries, or irregular framing that may affect the mode shapes. The effective mass estimated using these simplified procedures is also based on gross generalizations, a necessity for their broad application, whereas the FE models determine effective mass based on mode shapes that account for irregular framing or the non-standard conditions, provided they are included in the model.

Continuing the previous evaluation example, the remaining bays of the floor were analyzed in a similar manner with steady state analyses at all mid-bay locations for comparison with the design accelerance curve. The computed accelerance FRFs for the bare floor and occupied floor FE models are presented below in Figures 4.42(b) and (c) for comparison. According to the serviceability evaluation of the occupied floor model in Figure 4.42(c), all but two bays on the floor satisfy the 0.005g serviceability limit at their respective dominant peaks. If all bays had exceeded the design curve, then a major change in the design may be warranted, however the slight overage in only a few bays may only call for some minor adjustments or may even be considered acceptable given the assumptions built into the FE model. To demonstrate the reasonableness of this example to represent in-situ floor behavior, the measured accelerance FRFs from each of the twelve analyzed bays in VTK2 are also included in Figure 4.42(a).

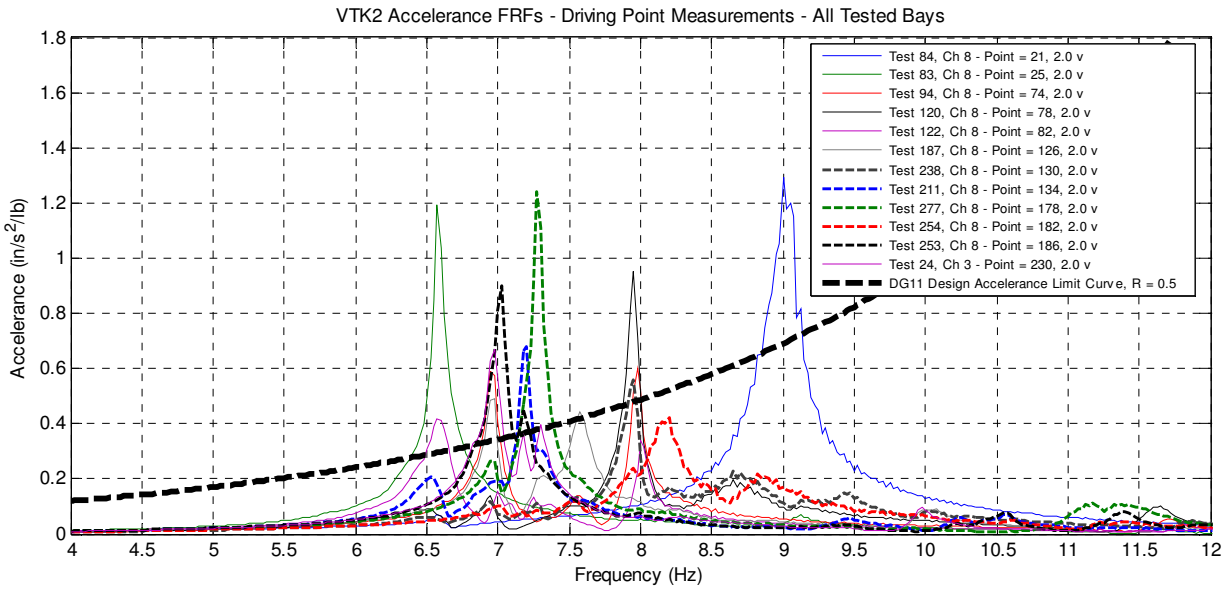

(a) VTK2 - Measured Mid-Bay Driving Point Accelerance FRFs (All Bays)

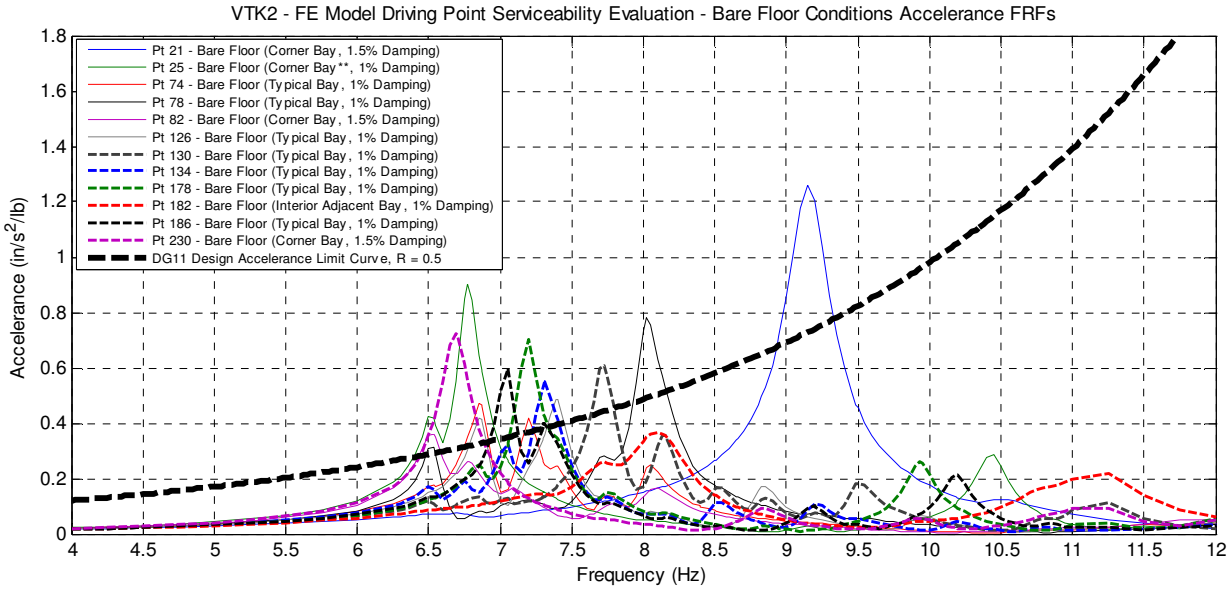

(b) Bare Floor FE Model Accelerance FRFs – 1%, 1.5%, 2% Damping

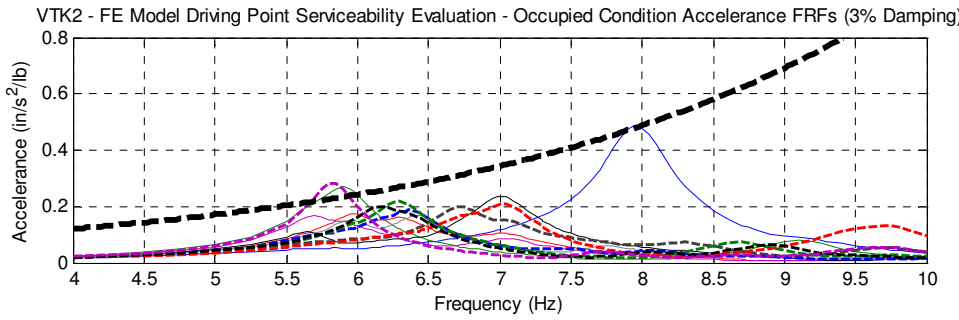

(c) Occupied Floor FE Model Accelerance FRFs – 3% Damping (All Bays)

Figure 4.42: FE Serviceability Evaluation Example – All Bays

Another valuable observation can be made from Figures 4.41 and 4.42 in the example. The simple comparison of the computed accelerance FRFs of an adjusted FE model is a good tool to help designers visualize the effect of design or occupancy changes on vibration performance. Using a lower damping value and decreasing the superimposed load of an existing floor system may simulate a change to a more open and lightly furnished office floor plan. Some design changes may be more tedious to address than simple occupancy-change adjustments to superimposed load and damping, adjustments to member sizes, slab thicknesses, strength or unit weight of concrete, or even the depth of steel deck can be investigated to determine their effect on vibration performance. All of the above listed items have the potential to change the frequencies and mode shapes of a floor, but sifting through a list of frequencies and looking at displayed mode shapes can easily obscure the important performance parameter, acceleration response. The computed accelerance FRF allows instant and intuitive feedback on how the design change affects vibration performance across a range of frequencies. If the computed accelerance FRFs are compared to a design accelerance curve representing a level of vibration serviceability, then the designer can make informed decisions early in the design process.

The ease of computing a design accelerance curve and the simplicity of the proposed modeling techniques and mid-bay steady state analysis presented in Sections 4.1 and 4.2 make the proposed method of evaluation for vibration serviceability a viable candidate for automation within an FE program. *It should be stressed, however, that the final form of the proposed evaluation process is not calibrated against any known problem floor case studies and should not be viewed as a replacement for current design guidance at this point.* Although the recommended FE modeling techniques demonstrated a modest ability to adequately represent measured behavior, future refinement of the modeling techniques using further testing of in-situ structures will strengthen both the accuracy of the models and the method of evaluation. DG11 seems to be a good starting point for the form of the design accelerance curve; however the final form should be based on a survey of tested in-situ floors with known subjective serviceability evaluations. Although the database of floors with high-quality accelerance measurements is very limited, an extensive database of problem floors does exist with response-only measurements and subjective evaluations. This is where a refined and accurate method for modeling floors would help define the form of the design curve, because FE models of the database of surveyed floors could be generated in lieu of high quality accelerance FRF measurements.

A final note on the proposed method is that it also serves as a simplified method of evaluating existing floors in the field. Current methods of on-site serviceability evaluation typically involve a series of heel drop or walking tests to record peak acceleration response, generally as response-only single channel measurements. A general understanding of the floor response is achieved by looking at the acceleration traces and autospectra from these excitations. Using an instrumented heel drop (Class-III Testing per Section 2.5) instantly provides a high-quality accelerance FRF that can immediately be compared to a predefined design accelerance curve.